Protease-Activated Receptor 2 and α-Crystallin: Interactions and Functional Implications

Dissertation

zur Erlangung des akademischen Grades
(To the acquisition of the academic degree)

doctor rerum naturalium
(Dr. rer. nat.)

genehmigt durch

die Fakultät für Naturwissenschaften

der Otto-von-Guericke-Universität Magdeburg

von **M. Sc. Rongyu Li**
geb. am 24.06.1973 in Liaoning, China

Gutachter: Prof. Dr. Georg Reiser

Prof. Dr. Uwe-Karsten Hanisch

eingereicht am: 25 February 2010

verteidigt am: 2 September 2010

Acknowledgements

The work presented in this dissertation was made possible due to help and support of several people. Firstly, I am grateful and indebted to Prof. Dr. G. Reiser for giving me the opportunity to join the Institute for Neurobiochemistry in September 2005 for doing my doctoral work under his guidance. His continuous support, encouragement, motivation and discussion enabled me to move forward in my work. I would also like to thank Prof. Dr. V. Höllt for assessing my project proposal and guidelines my work.

No words can truly describe the extent of my appreciation for Dr. Theodor Hanck, my practical supervisor during the tenure of this work. He has been a pillar of strength for me during all the ups and downs which I faced during the course of experiments. He infused in me the spirit of endless perseverance and motivation. He helped me in developing my scientific attitude through the countless discussions and suggestions.

I am thankful to Dr. Rolf Stricker for introducing me to the field of protein chemistry. His immense knowledge helped me in crossing many hurdles and learning a lot in the process.

I am grateful to Dr. Abidat Schneider, Mrs. Petra Hennig and Mrs. Evi Busse for their technical help.

My appreciation also goes to Mrs. M. Dullin-Viehweg, secretary of the Graduiertenkolleg, Mrs. I. Klaes, and Mr. P. Ehrbarth for their friendly support.

The time spent at the institute was made a pleasurable, eventful, learning and unforgettable experience due to the presence of colleagues, Dr. Mikhail Strokin, Ms. Ewa Ostrowska, Ms. Claudia Borrmann, Ms. Denise Ecke, Dr. Elena Sokolova, Mrs. Nastya Galvita, Mrs. Yingfei Wang, Mr. Weibo Lou, Dr. Stefan Kahlert and Dr. Gregor Zündorf.

Last but not the least this work was made possible due to love and encouragement of my family and all my friends. Their belief in me gave me the power to move on.

This study was supported financially by a stipend from Deutsche Forschungsgemeinschaft (Graduiertenkolleg GRK-1167) and the Medical Faculty, Magdeburg.

Table of Content

1. Introduction **7**

1.1 Proteases **7**
1.2 Protease-activated receptors (PARs) **8**
1.3 Protease-activated receptor 2 (PAR-2) **8**
1.4 α-Crystallin **12**
1.5 Astrocytes and neurodegeneration **14**
1.6 Aims and workflow **15**

2. Materials and Methods **18**

2.1 Materials **18**
2.1.1 Animals **18**
2.1.2 Cell lines **18**
2.1.3 Bacteria **18**
2.1.4 Plasmid vectors **18**
2.1.5 Enzymes **18**
2.1.6 Kits **19**
2.1.7 Laboratory instruments **19**
2.1.8 Chemicals and Reagents **20**
2.1.9 Antibodies. **21**
2.1.10 Buffers and solvents **22**
2.1.10.1 Cell culture medium and solutions 22
2.1.10.2 Buffer and solutions 23
2.1.10.3 Microbial media 24
2.1.11 Oligonucleotides **24**
2.1.11.1 PCR Primers 24
2.1.11.2 Cloning Primers 25
2.1.11.3 Sequencing Primers 27
2.1.11.4 siRNA of α-crystallin 27
2.1.12 Molecular weight markers **27**
2.1.12.1 Nucleic acid standard marker 27

2.1.12.2 Protein standard marker 28

2.2 Methods 28
2.2.1 Isolation of Nucleic acids 28
2.2.1.1 RNA isolation from Animal cells 28
2.2.1.2 Plasmid DNA isolation from bacteria (mini-preparation) 28
2.2.1.3 Plasmid DNA isolation from bacteria (Midi-preparation) 29
2.2.1.4 Isolation and purification of DNA fragment from agarose gel 29
2.2.1.5 Precipitation and Sequencing of DNA 29
2.2.1.6 Quantification of Nucleic acids 29
2.2.2 Biochemical analysis of Nucleic acids 29
2.2.2.1 Hydrolysis of DNA with restriction endonucleases 29
2.2.2.2 Gel electrophoresis 30
2.2.2.2.1 Agarose gel electrophoresis of DNA 30
2.2.2.2.2 Agarose gel electrophoresis of RNA 30
2.2.2.3 Polymerase Chain Reaction (PCR) 31
2.2.2.4 Reverse Transcription-Polymerase Chain Reaction (RT-PCR) 31
2.2.2.5 Real Time-Polymerase Chain Reaction (Real-Time-PCR) 32
2.2.3 Cloning 33
2.2.3.1 Generation of DNA insert by PCR 33
2.2.3.2 Dephosphorylation of digested plasmid 34
2.2.3.3 Ligation of plasmid and DNA insert 34
2.2.3.4 Mutation of target gene 35
2.2.4 Microbiological techniques 35
2.2.5 Cell culture 36
2.2.6 Cell transfection with plasmids 37
2.2.7 Subcloning 37
2.2.8 Protein chemistry 37
2.2.8.1 Cell lysate 37
2.2.8.2 SDS-PAGE and Western Blot (WB) 38
2.2.8.3 Coomassie stain 38
2.2.8.4 GST pull-down assays 38
2.2.8.5 Immunoprecipitation (IP) 39
2.2.9 Immunocytochemistry 39

2.2.10 Cell death induction and measurement 39
2.2.11 Expression of α-crystallin in bacteria and purification 40
2.2.12 Statistics and NCBI-Blast 40

3. Results 41

3.1 Expression of PAR-2 in astrocytes and transfected cells 41
3.2 Expression of α-crystallin in astrocytes and transfected cells 42
3.3 Identification of the interaction of PAR-2 with α-crystallin 44
3.3.1 Identification of the interaction of PAR-2 with α-crystallin by GST pull down 44
3.3.2 Identification of the interaction of PAR-2 with α-crystallin by co-immunoprecipitation 45
3.3.3 Identification of the interaction of PAR-2 with α-crystallin by immunostaining ... 46
3.3.4 Only PAR-2 interacts with α-crystallin in the PARs family 47
3.3.5 Identification of the interaction of C-tail of PAR-2 with α-crystallin 48
3.3.6 Interaction domains of αA-crystallin with PAR-2 50
3.4 The role of PAR-2 in astrocytes 52
3.5 The role of α-crystallin in astrocytes 53
3.5.1 Overexpression of α-crystallin rescues astrocytes from death induced by C2-ceramide and staurosporine 53
3.5.2 Downregulation of α-crystallin increases astrocytes death induced by C2-ceramide and staurosporine 56
3.6 The mechanism of cytoprotection by PAR-2 and α-crystallin 60
3.6.1 PAR-2 activation activates p38, ERK and JNK MAP kinases 60
3.6.2 Application of inhibitors of p38, ERK and JNK reduces cytoprotection by PAR-2 activation in astrocytes 61
3.6.3 Application of inhibitors of p38 and ERK reduces cytoprotection caused by overexpression of α-crystallin 62
3.7 The functional connection of PAR-2 with α-crystallin 63
3.7.1 PAR-2 activation regulates expression of α-crystallin 63
3.7.2 PAR-2 activation increases phosphorylated Ser59-αB-crystallin level 65
3.7.3 Phosphorylation of α-crystallin contributes to protective activity in astrocytes 66
3.7.3.1 Generation of α-crystallin mutants 66

3.7.3.2 Mimicking of phosphorylation/unphosphorylation of α-crystallin 66
3.8 Extracellular expression of α-crystallin and its function 69
3.8.1 Expression of α-crystallin in bacteria and purification 69
3.8.2 Extracellular application of α-crystallin protects astrocytes 73

4. Discussion 75

4.1 Interaction of α-crystallin with PAR-2 75
4.1.1 Interaction domains of α-crystallin with PAR-2 75
4.1.2 Specificity of the interaction of α-crystallin with PAR-2 75
4.2 PAR-2 activation and change in expression of α-crystallin 76
4.3 Mechanism of cytoprotection by PAR-2 and α-crystallin in astrocytes 77
4.4 Potential functions of α-crystallin in the extracellular medium 81
4.5 The role of PAR-2 and α-crystallin in the nervous system 83
4.5.1 Widespread expression and multiple roles of PAR-2 83
4.5.2 The role of PAR-2 in cell death 84
4.5.3 The role of α-crystallin in cell death 85
4.5.4 The role of PAR-2 and α-crystallin in neurodegenerative diseases 85
4.6 Further possible functional connections of PAR-2 and α-crystallin 87

5. Zusammenfassung 88

6. Abstract 90

7. References 91

8. Abbreviations 96

9. Publication during Ph. D studies 98

10. Curriculum Vitae 99

1. Introduction

1.1 Proteases

Proteases are enzymes that mediate proteolysis by hydrolysis of the peptide bonds in a protein molecule. Proteases exist naturally in all organisms and are involved in multiple physiological processes. Proteases can either break specific peptide bonds in a sequence-dependant manner, or break down proteins to single amino acids. On the basis of their catalytic mechanism, proteases are currently classified into six groups: aspartic, cysteine, glutamic, metalloproteinase, serine, and unclassified. Metalloproteinases and serine proteases comprise the largest classes. Examples for metalloproteinases include matrix metalloproteases (thermolysin), while serine proteases include thrombin, trypsin and chymotrypsin to name a few. Alternatively, proteases may be classified by the optimal pH in which they are active: acid, neutral and basic proteases.

Proteases have multiple biological roles (Coughlin, 1999, 2000; Yan and Blomme, 2003). They catabolize proteins in the lumen of the intestine and in the lysosomes, participate in cascades of coagulation and complement formation, and remodel the extracellular matrix when cells migrate. Certain proteases, exemplified by thrombin, possess biological activity that is receptor mediated. Thrombin, a critically important protease for blood clotting, directly regulates many cell types by cleaving specific receptors at the plasma membrane. Accumulating evidence indicates that the proteases act not only as simple degradative enzymes but their highly specific mode of action (hydrolysis) can regulate a wide variety of biological processes by activating a series of receptors, the protease-activated receptor (PAR) family (Dery et al., 1998; Hirade et al., 2002; Macfarlane et al., 2005; Ossovskaya and Bunnett, 2004; Pai et al., 2001). Identification of the family of PARs implies that tissue and systemic serine proteases play a key role, not only as protein-degrading enzymes, but also as potential G protein-coupled receptor activators (Wang and Reiser, 2003a; Wang and Reiser, 2003b; Wang et al., 2008). These proteases transmit extracellular stimuli into intracellular signalling events (Asokananthan et al., 2002; Berger et al., 2001; Cottrell et al., 2003) and regulate almost all biological processes, like inflammation, mitogenesis, proliferation, migration, apoptosis, wound healing and angiogenesis (Fan et al., 2005; Fiorucci et al., 2001; Hirota et al., 2005; Kanke et al., 2001; Kanke et al., 2005). Dysregulation of their expression and functional pattern can result in various pathologic conditions, such as neurodegenerative and cardiovascular diseases and cancer (Yan and Blomme, 2003). Thus, identification and functional characterization of proteases and their receptors through which proteases act and manifest their action can open the way for looking for

therapeutic targets and medical treatments to cure diseases. The ability of proteases to regulate neuronal functions has led to new insights about the potential involvement of PAR family receptors in brain inflammation, neurodegenerative processes and nociception.

1.2 Protease-activated receptors (PARs)

Protease activated receptors are G protein-coupled, seven-transmembrane domain receptors including PAR-1, PAR-2, PAR-3 and PAR-4 (Rohatgi et al., 2004; Sokolova and Reiser, 2007; Steinhoff et al., 2005; Wang and Reiser, 2003a). PARs are activated by a series of serine proteases and factors by cleavage of the receptor at a specific site within the extracellular amino terminus. The new N-terminus tethered interacts with the second extracellular loop and evokes transmembrane signalling. The cleavage of the receptor is irreversible. Once activated, the receptor rapidly uncouples from the transmembrane signalling and is internalised by phosphorylation-dependent mechanism which is mediated by extracellular signal regulated kinase (ERK) (Stalheim et al., 2005; Steinhoff et al., 2005). PARs are also distributed in large intracellular pools in the Golgi apparatus and in vesicles. Resensitization of the receptor involves mobilization of the intracellular pools (Coughlin, 1999, 2000; Dery et al., 1998).

1.3 Protease-activated receptor 2 (PAR-2)

PAR-2 is the second receptor of PARs family and was cloned in mouse (Nystedt et al., 1994). The human PAR-2 gene codes for a protein with 397 amino acids and shares 30% amino acid identity with the human PAR-1 protein. It has further been shown that the PAR-2 is ubiquitously expressed in every tissue and organ (Buddenkotte et al., 2005; Bushell et al., 2006; D'Andrea et al., 1998; Darmoul et al., 2004; Napoli et al., 2000; Wang et al., 2002).

The mechanism by which trypsin activates PAR-2 has been investigated. Trypsin cleaves human PAR-2 at $N^{30}RSSKGR^{36}\downarrow S^{37}LIGKV$ to expose the tethered ligand SLIGKV, which activates the cleaved receptor, resulting in signal transduction (Cottrell et al., 2003). Synthetic peptides corresponding to the tethered ligand domain (SLIGKV for human PAR-2; SLIGRL for rat PAR-2) activate PAR-2 without the need for receptor cleavage (Al-Ani et al., 1999; Wang et al., 2007a). Such synthetic agonists, referred to as activating peptides (AP), are useful tools for investigating PAR functions.

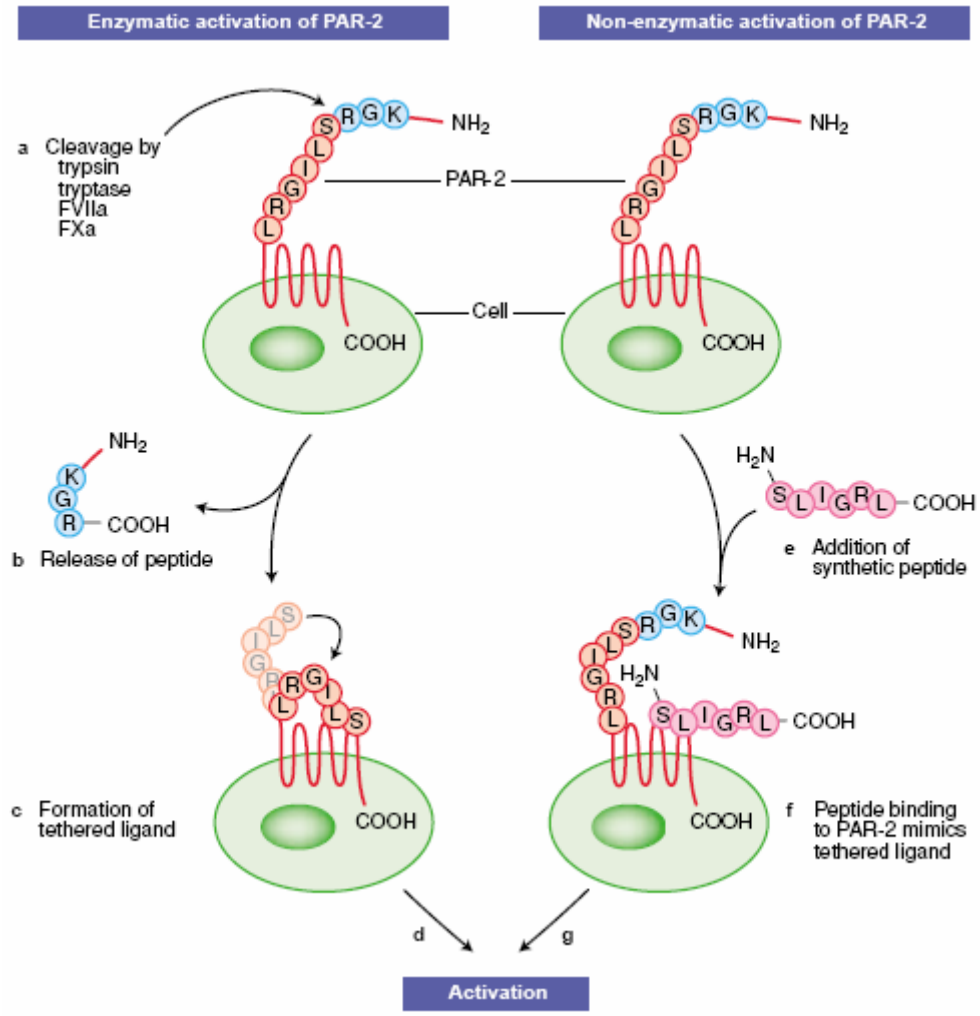

Figure 1.1 Model of rat PAR-2 activation (from Kawabata 2002)

(a) Endogenous proteases, such as trypsin, tryptase and coagulation factors VIIa (FVIIa) and Xa (FXa) enzymatically cleave the N-terminal peptide of PAR-2, a seven transmembrane-type receptor, at a specific site, (b) releasing a peptide. (c) The new N-terminal end of PAR-2 (NH_2-SLIGRL for rat PAR-2) then binds to the second loop of the PAR-2 molecule, and therefore constitutes an exposed tethered ligand. (d) This activates the receptor, triggering an intracellular G protein-coupled pathway that results in Ca^{2+} mobilisation and activation of protein kinase C (downstream pathway not shown). (e) A synthetic SLIGRL peptide, based on the amino acid sequence of the tethered ligand, (f) directly binds to the body of PAR-2 without cleaving the N-terminal peptide, thereby (g) mimicking the effect of the PAR-2-activating proteases.

PAR-2 is involved in the regulation of important biological effects such as inflammation, mitogenesis, proliferation, differentiation and apoptosis (Coelho et al., 2003; Steinhoff et al., 2005; Wang and Reiser, 2003b). Brain injury might also increase the tryptase levels in the brain parenchyma and cause activation of PAR-2 (Lozada et al., 2005; Wang et al., 2008). Depending on the physiological or pathophysiological environments, PAR-2 may be involved in different pro- or anti-inflammatory processes (Morozov and Wawrousek, 2006;

Sharma et al., 2005; Steinhoff et al., 2005). PAR-2 is expressed by sensory nerves in rat lumbar dorsal root ganglion neurones and mediates neurogenic inflammation through neuropeptides, calcitonin gene-related peptide and substance P (Steinhoff et al., 2005). Substance P interacts with the neurokinin 1 receptor on endothelial cells of post-capillary venules to cause plasma extravasation and granulocyte infiltration, and calcitonin gene-related peptide interact with its type 1 receptor (the calcitonin receptor like receptor and receptor activity modifying protein 1) on arteriolar smooth muscle to cause vasodilatation. On the other hand, PAR-2 agonists can also trigger processes that protect against inflammation (Cocks et al., 1999; Fiorucci et al., 2001). PAR-2 agonists improve cardiac function and reduce tissue damage after myocardial ischemia/reperfusion injury (Napoli et al., 2000).

Systemic injection of PAR-2 activating peptide to mice protects from colitis induced by intrarectal injection of the hapten trinitrobenzene sulfonic acid and decreases pro-inflammatory cytokine synthesis (IL-1β, IL-12 and interferon γ) and lethality (Fiorucci et al., 2001; Temkin et al., 2002). This anti-inflammatory effect depends on release of calcitonin gene-related peptide and a neurogenic mechanism (Steinhoff et al., 2000). Deficiency of PAR-2 gene increases acute focal ischemic brain injury (Jin et al., 2005). It has been reported that PAR-2 plays a protective role. For example, PAR-2 might prevent neural cell death during HIV infection and acute focal ischemic brain injury (Noorbakhsh et al., 2005). In our laboratory it was shown that both PAR-1 and PAR-2 activation caused rescue of cells from C2-ceramide (Cer)-induced apoptosis via regulating Growth related oncogene/Cytokine-induced neutrophil chemoattractant-1 (GRO/CINC-1) secretion in astrocytes (Wang et al., 2007b).

Compared with the large number of reports exploring the PAR-1 signalling pathway, little is known about the mechanism of PAR-2 intracellular signalling. Activation of PAR-2 elicits diverse cellular responses, including cell proliferation, differentiation, and production and release of proteins, such as interleukin-6, interleukin-8. In a number of different cell types, PAR-2 effectively couples to the Gq/11 to activate phospholipase C (PLC), protein kinase C (PKC) and mitogen-activated protein kinase (MAPK) pathways (Asokananthan et al., 2002; Steinhoff et al., 2005). The activation of PLC results in generation of the second messengers inositol 1,4,5-trisphosphate and diacylglycerol, which further trigger mobilization of Ca^{2+} and activation of PKC (Macfarlane et al., 2005). Activation of PAR-2-mediated extracellular signal regulated kinase activation in cells. PAR-2-mediated activation of other members of the MAPK family, c-Jun N-terminal kinase (JNK) and p38 MAPK were partially regulated by PKC. Similarly, activation of nuclear factor kappa B (NFκB) and its upstream regulating kinase, I kappa B kinase (IKK), was also found to be partially PKC-dependent (Coelho et al., 2003; Steinhoff et al., 2005).

These findings may imply that PAR-2 transmits important cellular responses through activation of multiple kinase pathways, ERK, JNK, p38 MAP kinase, and IKK in a cell-type specific manner (Steinhoff et al., 2005). Nevertheless, not enough is known about the mechanism of intracellular signaling of PAR-2 especially in the nervous system. An interesting question is how PAR-2 protects brain from insults.

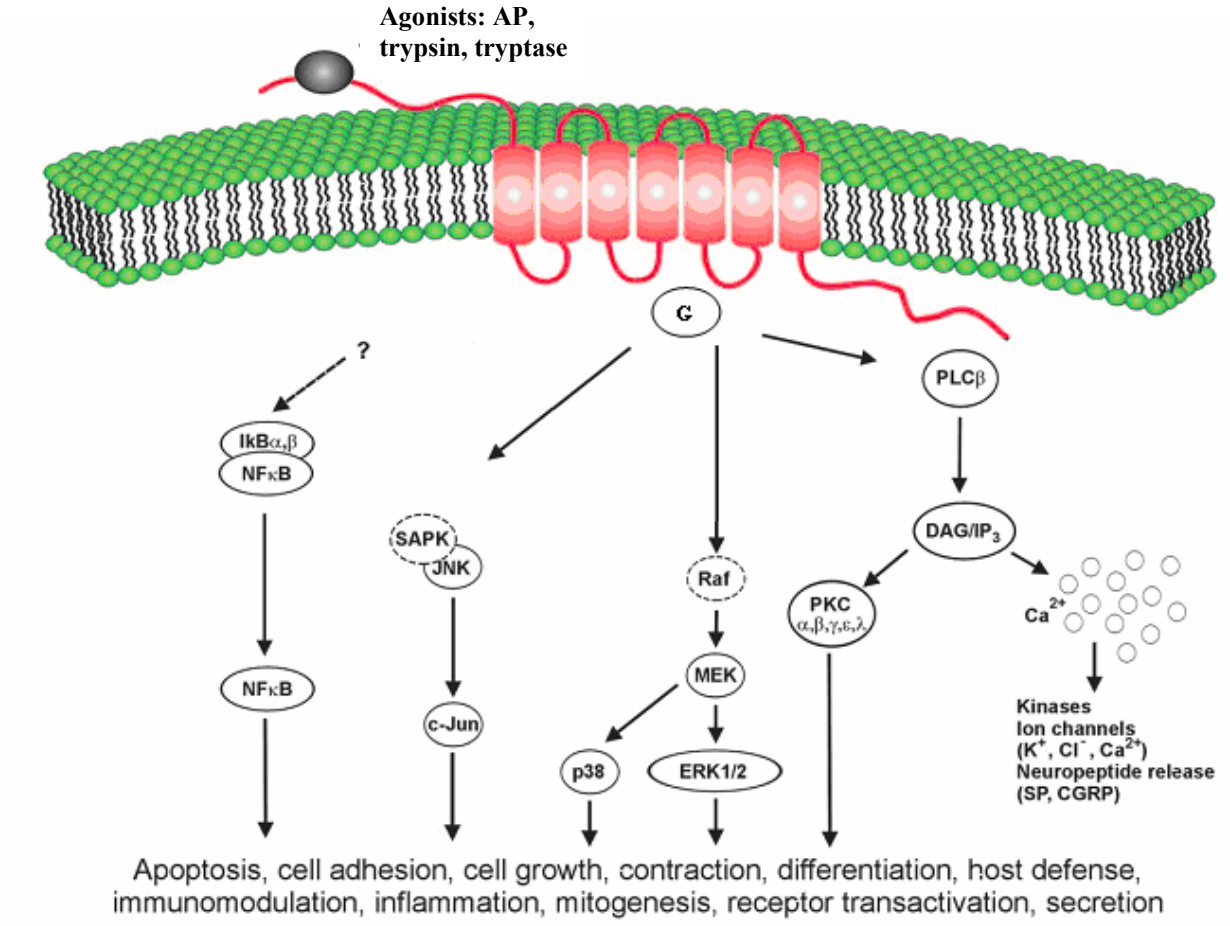

Figure 1.2 PAR-2 signalling (from Steinhoff 2005)

G protein-mediated PAR-2 signaling pathways can affect various cell activities including cell proliferation, morphological changes, motility and survival, gene transcription regulation, inflammation and so on. Stimulation by tryptase as well as PAR-2 activating peptid leads to subsequent activation of PLC and PKC, consequently activates intracellular Ca^{2+} influx, the release of cytokines, chemokines and neuropeptide, and modulates ion channels. PAR-2 agonists stimulate JNK, ERK1/2 and p38 MAP Kinases activation in different cells. It was shown that PAR-2 agonists stimulate NFκB-DNA binding activity and activation of upstream kinases IKKα and IKKβ.

1.4 α-Crystallin

α-Crystallin is the major structural protein of the mammalian lens, comprising of two primary gene products, the αA-crystallin (CRYAA) and αB-crystallin (CRYAB) polypeptides (Augusteyn, 2004). Functional expression of α-crystallin is also found in brain, spleen, lung, kidney, cornea and skin (Bajramovic et al., 1997; Iwaki et al., 1990; Kozawa et al., 2001; Maddala and Rao, 2005; Srinivasan et al., 1992). Like other small heat shock proteins, α-crystallin can act as molecular chaperones *in vitro*, preventing protein aggregation induced by stress (Horwitz, 1992). Functions of α-crystallin *in vivo* have been investigated. Numerous evidence suggests that α-crystallin can provide powerful anti-apoptotic protection against multiple stress situation (Ito et al., 1997; Ousman et al., 2007). The expression of α-crystallin is upregulated in response to different stress factors like chemicals and heat shock (Sun and MacRae, 2005). Increased α-crystallin acts on members of the Bcl-2 family and mediates anti-apoptotic response (Mao et al., 2004). Moreover, the alteration of phosphorylation state of α-crystallin takes place during the processes against stress, and phosphorylation of α-crystallin is required for protection against stress (Eaton et al., 2001; Golenhofen et al., 1998; Ito et al., 1997; Morrison et al., 2003; Webster, 2003). Accumulating evidence proves that α-crystallin is phosphorylated via MAPK pathway (Hoover et al., 2000; Piao et al., 2005).

There are several possible ways for α-crystallin to protect cells: 1) As chaperones, α-crystallin can bind to proteins to prevent their denaturation and stabilize them under the stress (Andley et al., 1998; Andley et al., 2000; Masilamoni et al., 2006). On the other hand, α-crystallin also binds to denatured proteins and facilitates the recovery of their activity (Andley et al., 2000). 2) α-Crystallin directly interacts with intracellular mediators of cell death and inhibits their apoptotic activity (Kamradt et al., 2001; Kamradt et al., 2002; Li et al., 2005; Liu et al., 2004; Mao et al., 2004). 3) α-Crystallin interacts with the cytoskeletal elements and keep the stability of cytoskeleton (Djabali et al., 1997; Morozov and Wawrousek, 2006; Nicholl and Quinlan, 1994; Tseng et al., 2006; Wang and Spector, 1996; Xi et al., 2006). 4) α-Crystallin acts on cytoplasmic membrane and keeps it from rupturing (Cobb and Petrash, 2000). 5) α-Crystallin translocates from cytosol to nucleus and regulates gene expression (den Engelsman et al., 2004; den Engelsman et al., 2005). 6) α-Crystallin acts on extracellular components and reduces their damage to cells (Sharma et al., 1987).

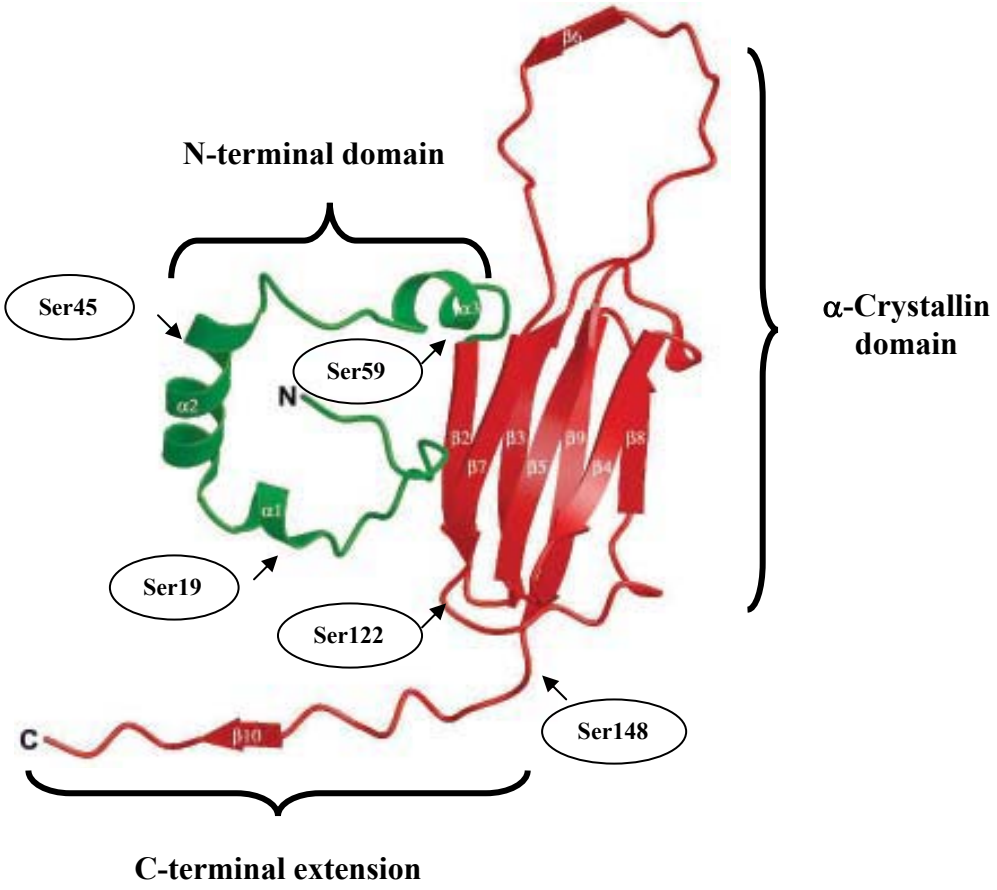

Figure 1.3 Model of structure of α-crystallin (from Augusteyn 2004)

The secondary structure of α-crystallin comprises of an ordered N-terminus, a conserved domain 'α-crystallin domain' and a C-terminal extension. The N-terminal domain (green) contains three helical segments. The α-crystallin domain (red) consists of a seven-stranded β-sandwich, an interdomain loop containing one β-strand (β 6 at the top). The C-terminal extension (at the bottom) is unstructured except for the short β-strand. Phosphorylation sites of αA-crystallin at Ser122 and Ser148 and αB-crystallin at Ser19, Ser45 and Ser59 are also indicated in the figure.

Mitogen-activated protein kinases are suggested to be involved in these protective processes (Hoover et al., 2000; Piao et al., 2005). Under the stress conditions, αB-crystallin is phosphorylated on three serine residues including Ser19, Ser45 and Ser59. αA-crystallin is phosphorylated on two serine residues including Ser122 and Ser148. Ser45 and Ser59 of αB-crystallin are substrates for the p42/44 ERK-MAPK and p38 MAPK pathways, respectively (Kato et al., 1998; Webster, 2003). Ser-59 phosphorylation of αB-crystallin is required to protect cells against ischemia (Morrison et al., 2003). Ser19 and Ser45 phosphorylation also contributes

to cell migrating under some circumstances (Maddala and Rao, 2005). In astrocytes, co-induction of αB-crystallin and MAPK-AP2 was found after transient focal cerebral ischemia (Piao et al., 2005). Oligomerization of α-crystallin contributes to their chaperone activity. Studies suggest that oligomerization of α-crystallin is regulated by alteration of phosphrylation state in different sites (Ito et al., 2001). The mechanism of dephosphorylation of α-crystallin is unknown, although evidence indicated that α-crystallin is dephosphorylated in a calcium dependent manner (Chiesa and Spector, 1989).

Multiple stress factors are associated with ischemic stress and a battery of intrinsic pathways work to attenuate damage. These include antioxidants, anti-apoptotic factors such as Bcl-2 families and endogenous caspase inhibitors. α-Crystallin is demonstrated to serve as a mediator of Bcl-Xs and inhibitor of caspases (Mao et al., 2004). More recently α-crystallin has been shown to prevent induced apoptosis by various factors including staurosporine (STS), TNF, UVA irradiation, okadaic acid and hydrogen peroxide (Andley et al., 1998; Ito et al., 1997). Regarding the anti-apoptotic mechanism, recent studies have demonstrated that α-crystallin can directly interact with precursors of caspase-3, Bax and Bcl-Xs to suppress their activity (Liu et al., 2004; Mao et al., 2004). As a result of these interactions, α-crystallin preserves the integrity of mitochondria and turn off downstream apoptotic events.

1.5 Astrocytes and neurodegeneration

Astrocytes were believed to be structural cells in the brain, and function in maintenance of the extracellular environment and stablization of cell-cell communication in the central nervous system (CNS) (Benarroch, 2005). Impairment in these astrocyte functions can critically influence neuronal survival. The neurodegeneration is the term for the progressive loss of structure or function of neurons, even the death of neurons. As the result of neurodegeneration, neurodegenerative diseases including amyotrophic lateral sclerosis, Alzheimer's disease and Parkinson's disease occur. Studies suggest that reactive astrocytes at the early stage of CNS injury have a beneficial effect on neurons by regulating several biological processes such as control of the blood-CNS interface, repair of extracellular matrix and the regulation of extracellular ions and neurotransmitter levels. Researches indicate that astrocyte apoptosis may contribute to pathogenesis of many acute and chronic neurodegenerative disorders. Significant astrocyte death was found after reactive astrocytosis, and dying astrocytes kill neighboring cells in brain injury. Thus, the regulation of astrocytes apoptosis is essential in neurodegeneration. Understanding the molecular mechanism of astrocytes apoptosis will help to develop therapies for neurodegenerative diseases.

1.6 Aims and workflow

There is increasing evidence for physiological and pathophysiological roles of PAR-2 in multiple tissues. PAR-2 could be a target for the development of drugs for treating diseases such as neurodegenerative diseases and inflammatory diseases. Identifying the mechanisms of PAR-2-mediated signalling in the nervous system will facilitate the development of therapeutic strategies for neuroinflammatory/degenerative diseases. Recently, we have described the neuroprotective function of activated PAR-2 in astrocytes. Little is known about the mechanisms involved in this effect. Interestingly, we for the first time observed the interaction of PAR-2 with αA-crystallin by yeast-two hybrid assays. It is the first issue to clarify whether and how PAR-2 interacts with αA-crystallin in the current research. In the progress of this work it became clear that it is important to find out what the role of αA-crystallin in PAR-2-mediated signalling is. Whether α-crystallin is neuroprotective in the brain has not yet been reported, but highly expressed α-crystallin is observed in pathological conditions in the brain. We propose that α-crystallin could be protective in the brain. If both PAR-2 and α-crystallin are involved in protective processes in the brain, the question whether they are functionally connected becomes an even more interesting question. Figuring out the answers of these questions will be helpful in understanding the mechanisms of neurodegeneration and neuroregeneration, and therapy of neurodegenerative diseases. Similarly, it was important to understand whether also αB-crystallin interacts with PAR-2 and whether also αB-crystallin plays a similar role. Therefore, the main focus of the present project was to identify the interaction of PAR-2 with α-crystallin and find out the functional connection of PAR-2 and α-crystallin in the nervous system.

Aim 1: explore the interaction of PAR-2 with α-crystallin.

The results from yeast-two hybrid assays suggest the interaction of PAR-2 with αA-crystallin. More evidence is needed to elucidate the interaction of PAR-2 with αA-crystallin. Moreover, further experiments should be performed to explore the mechanism of interaction to see how the interaction of PAR-2 with αA-crystallin takes place. In parallel, it should be investigated whether PAR-2 interacts with αB-crystallin. We also wanted to know whether only PAR-2 interacts with αB-crystallin in the PARs family. The following questions will be studied in this part:

1. Does PAR-2 really interact with αA-crystallin ?
2. Does PAR-2 really interact with αB-crystallin ?
3. Do PAR-1, PAR-3 and PAR-4 interact with αA-crystallin and αB-crystallin ?

4. Which domains are required for the interaction of PAR-2 with αA-crystallin and αB-crystallin ?

Aim 2: investigate the functional roles of PAR-2 together with α-crystallin in the nervous system and explore the mechanism.

Our previous work indicated that PAR-2 activation is protective in astrocytes treated with C2-ceramide. Since α-crystallin has powerful protective activity in lens and heart cells, we propose that α-crystallin is also protective in astrocytes under C2-ceramide treatment. To confirm the protective role of α-crystallin and PAR-2, we applied staurosporine to induce astrocytes death to observe the effect of PAR-2 activation and upregulation or downregulation of α-crystallin on astrocytes death. Furthermore, we try to explore the possible mechanism of cytoprotection by α-crystallin and PAR-2. It will be investigated whether different types of MAP kinases are involved in protective process. Phosphorylation of α-crystallin is an important issue in the function of α-crystallin. We will figure out whether phosphorylation of α-crystallin is required and which phosphorylation sites are important for protection. Since other evidence suggests that stresses will increase expression of α-crystallin, we will find out whether PAR-2 activation will regulate the expression of α-crystallin. The following questions will be studied in this part:

1. Is PAR-2 activation protective in astrocytes under staurosporine treatment ?
2. Is upregulation of α-crystallin protective in astrocytes under ceramde and staurosporine treatment ?
3. Does downregulation of α-crystallin result in enhanced astrocytes death under C2-ceramide and staurosporine treatment ?
4. Which MAP kinases are activated by PAR-2 activation in astrocytes ?
5. Are MAP kinases involved in protective processes in astrocytes ?
6. Is phosphorylation of α-crystallin required in protection in astrocytes ?
7. Which phosphorylation sites are important for protection ?
8. Will PAR-2 activation regulate the expression of α-crystallin ?

Workflow

Experiments in the project are performed as follows:

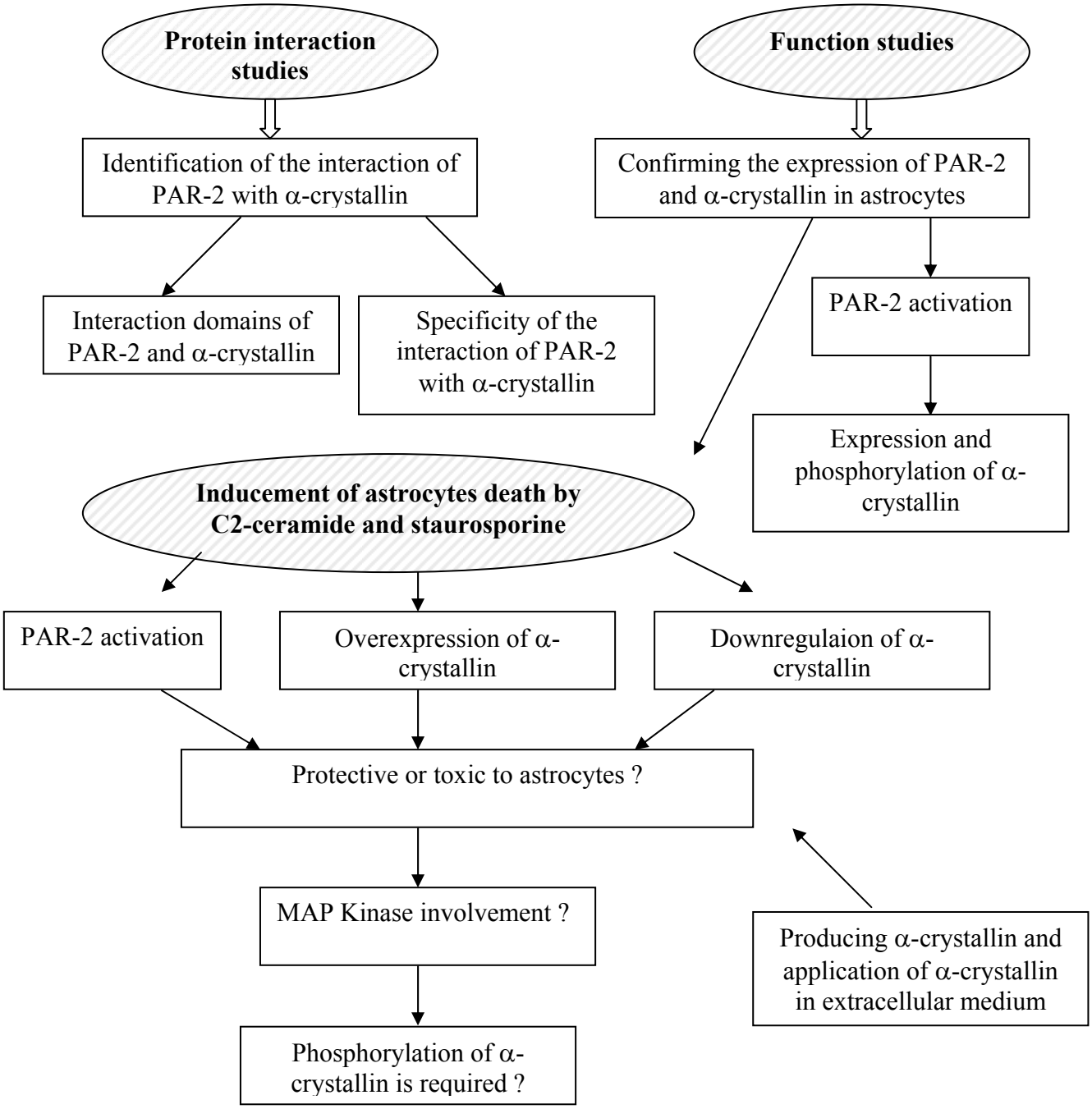

Figure 1.4 Workflow of the interaction study and functional implications of PAR-2 and α-crystallin

2. Materials and Methods

2.1 Materials

2.1.1 Animals

Male Sprague Dawley rats

2.1.2 Cell lines

a) Human embryonic kidney (HEK 293-epithelial)

b) Rat primary astrocytes (from whole brain)

c) *Spodoptera frugiperda* (sf.9)

2.1.3 Bacteria

E coli: XL1-Blue, ER2566 and DH 5α

2.1.4 Plasmid vectors

pcDNA3.1	Invitrogen, Karlsruhe,Germany
pEAK10	a gift from Dr. T. Koch, Institut für Pharmakologie und Toxikologie, Otto-von-Guericke-Universität Magdeburg
pEGFP-N1	Clontech, Heidelberg, Germany
pVL1392-GST	a gift from Dr. W. Luo, Institut für Neurobiochemie, Otto-von-Guericke-Universität Magdeburg

2.1.5 Enzymes

Bam HI	MBI Fermentas, St. Leon-Rot, Germany
Eco RI	MBI Fermentas, St. Leon-Rot, Germany
Hind III	MBI Fermentas, St. Leon-Rot, Germany
Pst I	MBI Fermentas, St. Leon-Rot, Germany
RNasin-Ribonuclease inhibitor	Promega, Mannheim, Germany
Shrimp Alkaline Phosphatase	Boeringer, Mannheim, Germany
T4 DNA Ligase	Invitrogen, Karlsruhe, Germany
Xho I	MBI Fermentas, St. Leon-Rot, Germany

2.1.6 Kits

Cytotoxicity detection kit (LDH)	Roche Diagnostics, Penzberg, Germany
ECL+Plus detection of western blot kit	Amersham Pharmacia Biotech, Buckinghamshire, UK
HiSpeed Plasmid Midi kit	Qiagen,Hilden,Germany
Hotstar Taq Master Mix kit	Qiagen, Hilden, Germany
Invisorb Spin Plasmid Mini kit	Invitek, Berlin,Germany
Magnet Assisted Transfection (MATra)	Promokine, Heidelberg, Germany
MinElute Gel Extraction kit	Qiagen, Hilden, Germany
MinElute PCR Purification kit	Qiagen, Hilden, Germany
Omniscript Reverse Transcription kit	Qiagen, Hilden, Germany
QuantiTect SYBR Green PCR Kits	Qiagen,Hilden,Germany
RNase-Free DNase Set	Qiagen, Hilden, Germany
RNeasy Midi and Mini kit	Qiagen, Hilden, Germany
Site-directed mutagenesis kit	Strategene, Amsterdam, Netherlands
Supersignal West Pico kit	Pierce, Rockford, IL, USA

2.1.7 Laboratory instruments

Biofuge A, 13 R, 3.2 RS (centrifuge)	Heraeus, Hamburg, Germany
Cell culture incubator	IBS, Fernwald, Germany
Eagle Eye Still video system	Stratagene, Heidelberg, Germany
Electrophoresis power supply Bio-Rad Laboratories	Bio-Rad Laboratories, München, Germany
Gel-blotting-papers	Schleicher & Schuell, Dassel, Germany
Gel electrophoresis system Mighty Small II	Amersham Pharmacia Biotech Buckinghamshire, UK
GENius Plus plate reader	Tecan, Crailsheim, Germany
GS-800 Calibrated Densitometer	Bio-Rad Laboratories, München, Germany
Icycler Opitical system	Bio-Rad Laboratories, München, Germany
Innova 4230 Refrigerated incubator shaker	New Brunswick Scientific, Nürtingen, Germany
LSM510 laser scanning confocal microscope Axiovert 135 fluorescence microscope	Carl Zeiss, Jena, Germany

Microplate reader	Molecular Devices
pH Meter (pH526) WTW	
Protran nitrocellulose transfer membrane (0.1 µm, 0.2 µm)	Whatman, Dassel, Germany
Semi-dry Transfer Cell	Bio-Rad Laboratories, München, Germany
Sorvall RC-5B Refrigerated Superspeed Centrifuge	Dupont Instruments, Hamburg,Germany
T3 Thermocycler Biometra	Biometra, Göttingen, Germany
Thermomixer comfort	Eppendof
UV/visible Spectrophotometer	Pharmacia Biotech

2.1.8 Chemicals and Reagents

Albumin Fraction V, protease free	Carl Roth, Karlsruhe, Germany
Ampicillin	
Bacto Agar	BD Bioscience (Clontech), Heidelberg, Germany
Bacto Tryptone	Applichem, Darmstadt, Germany
Bacto Yeast extract	BD Bioscience (Clontech), Heidelberg, Germany
ß-mercaptoethanol	Sigma, Deisenhofen, Germany
Bio-Rad protein assay dye reagent concentrate	Bio-Rad Laboratories, München, Germany
D-erythro-Sphingosine, N-Acetyl- (C2-ceramide)	Calbiochem, San Diego, CA, USA
Dimethyl sulfoxide (DMSO)	Sigma, Deisenhofen, Germany
DMEM + HAM'S F12 (1:1)	Biochrom, Berlin, Germany
DOTAP	Roche Diagnostic, Mannheim, Germany
Dulbecco's Modified Eagle's Medium (DMEM)	Biochrom, Berlin, Germany
ERK inhibitor (PD98059)	Calbiochem, La Jolla, CA, USA
Fetal calf serum (FCS)	Biochrom, Berlin, Germany
G418 Sulphate	Calbiochem, La Jolla, CA, USA
HBSS (w/o Ca^{2+} and Mg^{2+})	
Igepal CA630	Sigma, Deisenhofen, Germany

ImmersolTM 518N	Carl Zeiss, Oberkochen, Germany
IPTG	
JNK inhibitor II (SP600125)	Calbiochem, La Jolla, CA, USA
Kanamycin sulphate	
NDSB 256	Fluka, Buchs, Switzerland
p38 MAP kinase inhibitor (SB203580)	Calbiochem, La Jolla, CA, USA
PAR-2 activating peptide (SLIGRL)	NeoMPS SA, Strasbourg, France
Penicillin and Streptomycin	Biochrom, Berlin, Germany
Poly-L-lysine	Sigma, Deisenhofen, Germany
Ponceau S solution (0.2% in acetic acid)	Boehringer, Mannheim, Germany
Precision Plus Protein All Blue Standard	Bio-Rad Laboratories, München, Germany
Protein A sepherose beads	GE Healthcare, Freiburg, Germany
Protein G agarose beads	Sigma, Deisenhofen, Germany
Puromycin	
siRNA of α-crystallin	Qiagen, Hilden, Germany
TEMED	SERVA, Heidelberg, Germany
Template Suppression Reagent (TSR)	Applied Biosystems Division, Foster City, CA, USA
Triton-X-100	SERVA, Heidelberg, Germany
Trypsin	Roche Diagnostic, Mannheim, Germany
Tween 20	Sigma, Deisenhofen, Germany

2.1.9 Antibodies

Alexa488 anti-rabbit IgG	Molecular Probes, Eugene, OR, USA
Alexa488 anti-mouse IgG	Molecular Probes, Eugene, OR, USA
Alexa555 anti-mouse IgG	Molecular Probes, Eugene, OR, USA
Alexa 555goat anti-chicken IgG	Molecular Probes, Eugene, OR, USA
Mouse monoclonal antibody against αB-crystallin	Stressgen, Victoria, Canada
Mouse monoclonal antibody against β-tubulin I	Sigma, Saint Louis Missouri, USA
Mouse monoclonal antibody against glial fibrillary acidic protein (GFAP)	Boehringer, Mannheim, Germany
Mouse monoclonal antibody against phospho-	Cell Signaling Technology, Beverly, MA,

p42/44 MAPK	USA
Mouse monoclonal antibody against myc	Invitrogen, Carlsbad, CA, USA
Mouse monoclonal anti-PAR-2 (SAM11)	Santa Cruz Biotechnology, Heidelberg, Germany
Peroxidase-conjugated anti-mouse and anti-rabbit IgG	Dianova, Hamburg, Germany
Rabbit affinity isolated antibody against HA-tag	Sigma, St Louis, MO, USA
Rabbit p38 MAP kinase antibody	Cell Signaling Technology, Beverly, MA, USA
Rabbit p44/42 MAP kinase antibody	Cell Signaling Technology, Beverly, MA, USA
Rabbit phospho-p38 MAP kinase (Thr180/Tyr182) antibody	Cell Signaling Technology, Beverly, MA, USA
Rabbit phospho-SAPK/JNK (Thr183/Tyr185) antibody	Cell Signaling Technology, Beverly, MA, USA
Rabbit polyclonal antibody against αA-crystallin	Acris, Hiddenhausen, Germany
Rabbit polyclonal antibody against phospho-αB-crystallin (Ser59)	Stressgen, Victoria, Canada
Rabbit polyclonal anti-GFP	Sigma, St Louis, MO, USA
Rabbit SAPK/JNK antibody	Cell Signaling Technology, Beverly, MA, USA

2.1.10 Buffers and solvents

2.1.10.1 Cell culture medium and solutions

HEK-293 cells- DMEM/HAM'S F12 (1:1) with 10% FCS, 100U/ml Penicillin, 100 µg/ml Streptomycin

Rat primary astrocytes- DMEM with 10% FCS, 100U/ml Penicillin, 100 µg/ml Streptomycin

HBSS (Hanck's balanced salt solution) without Ca^{2+} and Mg^{2+}

G418 Sulphate- stock: 500 mg/ml, working concentration: 500 µg/ ml

Puromycin- stock: 1 mg/ml, working concentration: 1 µg/ ml

2.1.10.2 Buffer and solutions

• 1x PBS: 137 mM NaCl, 2.6 mM KCl, 8.1 mM Na_2PHO_4, 1.4 mM KH_2PO_4, pH 7.4

• 1xTBE: 89 mM Tris, 89 mM Boric acid, 2 mM EDTA, pH 8.0

• 1xTE: 10 mM Tris/HCl, pH 7.4, 1 mM EDTA, pH 8.0

• Ethidium bromide solution: 10 mg/ml

• TCM: 10 mM Tris/HCl, pH 7.5, 10 mM $CaCl_2$, 10 mM $MgCl_2$

• 4% PFA (Paraformaldehyde) solution: 4% PFA, 120 mM sodium phosphate, pH 7.4,
4% Saccharose

• FTP: Blocking and Washing buffer (immunostaining)-100 ml
10% FCS 10 ml
0.25% Triton-X100 0.25 ml
10X PBS 10 ml

• 4x Lysis buffer (cell lysate): 200 mM Tris/HCl, pH 7.4, 4 mM EDTA, 4 mM ß-Mercaptoethanol, 600 mM NaCl, 4% Igepal and one tablet of Protease Inhibitor Cocktail (Roche Molecular Biochemicals, Mannheim, Germany) per 50 ml

• 1x Lysis buffer (cell lysate)

• 40% Acrylamid/Bis

• Resolving buffer (SDS-PAGE-Laemmli): 750 mM Tris/HCl, pH 8.8

• Stacking buffer: 250 mM Tris/HCl, pH 6.8

• SDS solution: 10% (w/v) SDS in H_2O

• PER solution: 10% (w/v) Ammoniumperoxodisulfat in H_2O

• 4x Laemmli Sample buffer: 500 mM Tris/HCl, pH6.8, 8% SDS, 40% Glycerol

• 5x Laemmli Running buffer: 125 mM Tris, 960 mM Glycine, 0.5% SDS, pH 8.5

• 1x Transfer buffer (for Laemmli gels with NC membrane): 25 mM Tris, 192 mM Glycine, 20% (v/v) Methanol

• 100 mM CAPS [3-(Cyclohexylamino)-1-propansulfonic acid] /NaOH, pH 11

• 1x Transfer buffer (for Laemmli gels with PVDF membrane): 10% (v/v) Methanol, 10mM CAPS/NaOH

• Membrane stripping buffer: 62.5 mM Tris, pH 6.8, 100 mM ß-Mercaptoethanol, 2% SDS

• 20% Protein A slurry: 1 ml 1x PBS and 4 µl 10% sodium azide

• 5x KCM buffer (0.5 M KCl, 0.15 M $CaCl_2$, 0.25 M $MgCl_2$)

• Column buffer (20 mM Tris/HCl pH 8.5, 500 mM NaCl, 1 mM EDTA)

• Cleavage buffer (20 mM Tris/HCl pH 8.5, 500 mM NaCl, 1 mM EDTA, 50 mM DTT)

2.1.10.3 Microbial media

• Luria bertini (LB)

• SOC –250 ml

Bacto tryptone 5 g

Yeast extracts 1.25 g

NaCl 0.15 g

KCl 0.125 g

1M Glucose 5 ml (final 20 mM)

1M $MgCl_2$ 2.5 ml (final 10 mM)

1M $MgSO_4$ 2.5 ml (final 10 mM)

• TSB buffer-150 ml

		final concentration
2x LB-media	75 ml	1x LB
DMSO	7.5 ml	5%
1 M $MgCl_2$	1.5 ml	10 mM
1 M $MgSO_4$	1.5 ml	10 mM
PEG 4000	15 g	10%

2.1.11 Oligonucleotides

(Primers were synthesized by Invitrogen, Karlsruhe, Germany. siRNAs of α-crystallin were synthesized by Qiagen, Hilden, Germany.)

2.1.11.1 PCR Primers (s, sense strand; a, anti-sense strand)

Gene	Accession No.	Sequence (5'→3')	Position	Tm (°C)	PCR product (bp)
αA-crystallin	NM_012345	(s) CCGACTGTTCGACCAGTTCTTC	72	58	304
		(a) AGGCAGACGGTAGCGACGGTGA	375		
αB-crystallin	NM_012935	(s) TCCCTTCTTTCCTTTCCACTCC	318	58	420
		(a) GCCTGTTTCCTTGGTCCATTCA	1037		
Rat GAPDH	M17701	(s) GTGAAGGTCGGTGTCAAC	34	58	835
		(a) CAACCTGGTCCTCAGTGTAGC	868		

2.1.11.2 Cloning Primers (s, sense strand; a, anti-sense strand)

Gene	Accession No.	Sequence (5'→3')	Position	Tm (°C)	PCR product (bp)
αA-crystallin	NM_012345	(s) CCGGAAGCTTGCCACCATGGAC GT CACCATC	1	55	542
		(a) GCTCAGAATTCGGACGAGGGTG CCGAGCT	531		
αB-crystallin	NM_012935	(s) CATCAAGCTTGCCACCATGGAC ATA GCC ATC CAC CA	582	55	552
		(a) GCTCAGAA TTC CTT CTT AGG GGC TGC AGT G	1107		
Del 49 of αA-crystallin	NM_012345	(s) TCCACCATCAGCCCCTACTACC GGGACAAGTTTGTCATCTTC	136	52	
		(a) GAAGATGACAAACTTGTCCCGG TAGTAGGGGCTGATGGTGGA	216		
Del 95 of αA-crystallin	NM_012345	(s) AAGGTACTGGAAGATTTCGTGA TTTCCCGTGAATTTCACCGT	274	52	
		(a) ACGGTGAAATTCACGGGAAATC ACGAAATCTTCCAGTACCTT	319		
Del 120 of αA-crystallin	NM_012345	(s) GAATTTCACCGTCGCTACCGTT GCTCCTTGTCTGCGGATGGC	349	52	
		(a) GCCATCCGCAGACAAGGAGCA ACGGTAGCGACGGTGAAATTC	382		
Del 136 of αA-crystallin	NM_012345	(s) CTCTCCTGCTCCTTGTCTGCGA GCGAGAGGGCCATTCCCGTG	397	52	
		(a) CACGGGAATGGCCCTCTCGCTC GCAGACAAGGAGCAGGAGAG	454		

Rat PAR-1	NM_012950	(s) GGATGAATTCGCCACCATGGG GCCCCGGCGCT	66	55	1321
		(a) GAATGGATCCGCTAGTAGCTT TTTG	1360		
Rat C-tail PAR-2	U61373	(s)TTTGTTGAATTCATGTCGAA AGATTTCAGG	1036	58	186
		(a) CTCAGACCCGGATCCAGCTC AGTAGGAGGT	1206		
Rat PAR-2	U61373	(s) CCACGTCTCGAGCCGGGGAT GCGAAGTCTCAGC	1	58	1224
		(a)CCCAGCTCAAAGCTTGTAG GAGGTTTTAACACT	1200		
Rat PAR-3	NM-053313	(s) GGATCTGCAGGCCACCATGGA GATGAAAGTCCTTATC	62	55	1129
		(a) GAATGGATCCGAGGTCAGCTG ATCTAC	1166		
Rat PAR-4	AF269246	(s) GGATGAATTCGCCACCATGCT CGGGTTCAGCATC	1	55	1183
		(a) GAATGGATCCAGAAGTGTAG AGGAGCA	1158		

2.1.11.3 Sequencing Primers (s, sense strand; a, anti-sense strand)

Gene/Vector	Accession No.	Sequence (5'→3')	Position	Comment
pEGFP-N1	Clontech	(s) GGTCTATATAAGCAGAGCTG	550	
		(a) CCATGGTGGCGACCGGTGGAT	582	
pVL1392	Invitrogen (Modified)	(s)TATTCCGGATTATTCATACCGTC	4092	
		(a) CAACGACAAGCTTCATCGTGTCG	4265	
Rat PAR-1	NM_012950	(s) CAACATCACCACCTGCCACGAC	833	
Rat PAR-2	U61373	(s) GGTCACCATCCCTCTGTA	612	
Rat PAR-3	NM-053313	(s) CTACTTCGTCTCCTTGGCCTTCT	840	
Rat PAR-4	AF269246	(s) GCTGTCCTGGGCTGCTTTGTG	753	
T7 promoter	Invitrogen	(s) GTAATACGACTCACTATAGGGC		Published (for pcDNA 3.1)

2.1.11.4 siRNA of α-crystallin (s, sense strand)

Gene	Accession No.	Target Sequence (5'→3')	Position	Comment
CRYAA-1	NM_012345	(s) TTCGTGGAGATCCATGGCAAA	289	
CRYAA-2	NM_012345	(s) ATGATGGCATTGAACTCTTAA	758	
CRYAB-2	NM_012935	(s) AGGGCTGGCCCAGATTATTAA	1201	
CRYAB-3	NM_012935	(s) CTCTGTGAACCTGGACGTGAA	807	

2.1.12 Molecular mass markers

2.1.12.1 Nucleic acid standard marker

GeneRuler 100bp DNA Ladder (1 kb) MBI Fermentas, Germany

GeneRuler DNA Ladder Mix (10 kb)

2.1.12.2 Protein standard marker

Precision Plus (All Blue) (250-10 kDa) Bio-Rad, München, Germany

LWM-SDS marker GE Healthcare, München, Germany

2.2 Methods

2.2.1. Isolation of Nucleic acids

2.2.1.1 RNA isolation from Animal cells

Total RNA was isolated from cultured cells (wild type and transfected) using the RNeasy Mini kit (Qiagen, Hilden). The medium was aspirated from the culture dish (6 cm) and cells were lysed with 600 µl Buffer RLT. Cells were homogenised completely by pipetting with 1 ml tip, and to this homogenised suspension 700 µl of 70% ethanol added and mixed well by pipetting. Rest of the procedure was done as described above for total RNA isolation from animal tissue.

2.2.1.2 Plasmid DNA isolation from bacteria (mini-preparation)

Plasmid DNA from transformed bacteria was harvested using the Invisorb Spin Plasmid Mini Kit (Invitek, Berlin). E.coli culture (single colony) was grown under appropriate antibiotic selection pressure in 3 ml LB media overnight at 37°C with shaking at 250 rpm. 2 ml of overnight grown culture was transferred to microcentrifuge tube and centrifuged for 1 min at maximum speed to pellet the cells down. Supernatant was removed completely and pellet was resuspended in 200 µl of Solution I by vortexing. Added 250 µl of Solution II, closed the tube and mixed carefully by inverting the tube only 5 times (no vortexing since it can lead to shearing of chromosomal DNA which contaminates the plasmid DNA). Added 250 µl of Solution III and mixed gently, but thoroughly, by shaking the tube 4-6 times. Centrifuged for 3 min at maximum speed. Decanted the clarified supernatant into the Spin Filter placed in a 2.0 ml Receiver tube. Added 200 µl of Binding Solution to the filled Spin Filter and closed the tube. Inverted the tube one time and centrifuged for 1 min at 10,000 rpm. Discarded the filtrate and added 750 µl of Wash Buffer PL.

Centrifuged for 1 min at 10,000 rpm and discarded the filtrate. Then centrifuged for 2 min at maximum speed for complete removal of residual Wash Buffer PL. Placed the Spin Filter into a new 1.5 ml Receiver Tube and allowed the Spin Filter to air dry for 1 min for complete removal of ethanol in Wash Buffer. Then 30 µl of Elution Buffer added directly onto the membrane of Spin Filter and incubated at room temperature for 10 min. Finally, centrifuged for 2 min at 10,000 rpm to recover the plasmid DNA. Stored DNA at -20°C.

2.2.1.3 Plasmid DNA isolation from bacteria (midi-preparation)

Plasmid DNA from transformed bacteria was harvested using the HiSpeed Plasmid Midi Kit (Qiagen, Hilden). 50-200 ml of overnight grown transformed bacteria culture was applied for DNA isolation. The DNA was stored at -20°C.

2.2.1.4 Isolation and purification of DNA fragment from agarose gel

To isolate and purify DNA fragment (PCR or cDNA-insert in plasmid) from agarose gel, Concert Rapid Gel Extraction Kit (Gibco BRL) and Concert Rapid PCR Purification kit (Gibco BRL) were used. The purified DNA was stored at -20°C.

2.2.1.5 Precipitation and Sequencing of DNA

Sequencing PCR product was precipitated with sodium acetate and 100% ethanol. Briefly, to 80 µl H_2O added 10 µl of 3M Sodium Acetate. To this 20 µl of sequencing PCR reaction mixture was added and mixed thoroughly. Then added 250 µl of chilled 100% ethanol and incubated on ice for 5 min. Centrifuged for 15 min at 14,000 rpm. Supernatant discarded and pellet resuspended in 300 µl of 70% ethanol. Centrifuged again for 15 min at 14,000 rpm. Discarded the supernatant carefully and allowed the pellet to air-dry or at 37°C. DNA samples were sequenced by SEQLAB Göttingen, Germany.

2.2.1.6 Quantification of Nucleic acids

Quantity of Isolated DNA and RNA was measured by the UV absorption ratio 260 nm /280 nm using an Ultrospec 2000 UV/visible spectrophotometer (Pharmacia Biotech, Freiburg, Germany). Quality of the nucleic acid was checked on a 1% agarose/TBE gel pre-stained with ethidium bromide (10 mg/ml).

2.2.2 Biochemical analysis of Nucleic acids

2.2.2.1 Hydrolysis of DNA with restriction endonucleases

Restriction digestion of DNA was done with restriction enzyme and its appropriate 10x reaction buffer. Recombinant plasmids were cut either with one or two enzymes simultaneously. For single digestion appropriate reaction buffer (10x) was used at a final concentration of 1x, while for double digestion Y+/Tango buffer (10x) used at a final concentration of 2x.

	Single digestion	Double digestion
DNA	1-2 µg	5 µg
Enzyme 1 (10 u/µl)	1 µl	2 µl
Enzyme 2 (10 u/µl)	-	2 µl
Buffer (10x)	1x	2x
H_2O	variable	variable
	---	---
	30 µl	30 µl
Incubation time	3-4 h at 37°C	10-18 h at 37°C

After digestion, reaction mix was cleaned using Concert Rapid PCR Extraction kit (Gibco BRL), DNA quantified as described previously and 100 ng DNA checked on 1% agarose/TBE gel pre-stained with ethidium bromide in case of PCR DNA or plasmid vector digestion for cloning. To check for the presence of DNA insert in the recombinant plasmid whole of digestion mix was loaded on the gel. For subcloning purpose, after digestion of recombinant plasmid whole of digestion mixture was loaded on the gel and then the desired DNA fragment was cut from the gel and purified for further processing.

2.2.2.2 Gel electrophoresis

2.2.2.2.1 Agarose gel electrophoresis of DNA

To check the quality of DNA (PCR product, recombinant plasmid DNA, restriction analysis) 1% agarose (SIGMA) gel in 0.5x TBE buffer made.

2.2.2.2.2 Agarose gel electrophoresis of RNA

Quality of isolated RNA was checked in a 1% agarose / MOPS (NMorpholino-3-propansulphonic acid) gel. 0.1% DEPC-H_2O was used for making all the solutions required for RNA gel including the sample preparation. 3% Hydrogen peroxide (H_2O_2) used for decontaminating the gel assembly. RNase-free agarose (SIGMA) gel made in 1x MOPS buffer (SERVA, Heidelberg). Gel pre-stained with ethidium bromide (10 mg/ml). 200 ng of RNA used with 6x Loading buffer. Gel was run in 1x MOPS buffer for 1 h at 80 V. 18S and 28S RNA bands were visualised under UV-transilluminator in an Eagle Eye II video system (Stratagene, Heidelberg, Germany).

2.2.2.3 Polymerase Chain Reaction (PCR)

To check for the presence of the gene of interest either in the animal tissue or cell line (wild type and transfected), PCR was performed. PCR signal was amplified using the gene-specific primers (PAR-1, PAR-2, PAR-3, PAR-4, GAPDH, αA-crystallin and αB-crystallin) designed from the sequence available in the Genbank. PCR reaction was done in 0.2 ml thin wall tubes in T3 Thermocycler (Biometra) using the Hotstar Taq Master Mix kit (Qiagen, Hilden). The reaction mixture was pipetted as follows:

Template DNA 1-2 µl (50-100ng)
Hotstar Taq Master Mix 25 µl
5‘ primer (10 pmol/µl) 2 µl
3‘ primer (10 pmol/µl) 2 µl
H_2O variable
---
50 µl

The PCR reaction was done using the following programme (for Hotstar Taq polymerase):

Lid temperature = 110°C
Preheating = On
Initial denaturation = 95°C 15 min
35 cycles: Denaturation 94°C 30 sec
Annealing variable 1 min 30 sec
Extension 72°C 1 min
Final extension = 72°C 10 min
4°C pause

10 µl of reaction was used for gel electrophoresis to check for the presence of the desired gene product.

2.2.2.4 Reverse Transcription-Polymerase Chain Reaction (RT-PCR)

To reverse transcribe the isolated total RNA from either animal tissue or cells Omniscript Reverse Transcription kit (Qiagen, Hilden) was used. 1 µg of total RNA was used to make cDNA in a 0.5 µl tube. RT reaction was set as follows:

RNA 1 µg
RT Buffer (10x) 2 µl
dNTP mix (5 mM each) 2 µl
Oligo-dT primer (0.5 µg/µl) (Gibco BRL) 2 µl
Omniscript Reverse Transcriptase (4 u/µl) 1 µl
RNasin (10 u/µl) (Promega) 1 µl
H_2O variable
---
20 µl

RT was done in T3 Thermocycler (Biometra). The reaction was incubated for 1 h at 37°C, followed by 5 min at 95°C and then rapidly cooled at 4°C. cDNA was stored at -20°C.

PCR reaction was done with the cDNA generated from the RT step using the Hotstar Taq Master Mix kit (Qiagen, Hilden). The reaction mixture was pipetted as follows:
cDNA 1-2 µl
Hotstar Taq Master Mix 25 µl
5‘ primer (10 pmol/µl) 2 µl
3‘ primer (10 pmol/µl) 2 µl
H_2O variable
---
50 µl

The PCR reaction was done using the programme described previously. 10 µl of reaction was used for gel electrophoresis to check for the presence of the desired gene product.

2.2.2.5 Real Time-Polymerase Chain Reaction (Real-Time-PCR)

To detect the mRNA level of desired gene, Real-Time-PCR was performed with SYBR green dye. Reverse transcription is carried out according to the procedure mentioned above. The reaction mixture was pipetted as follows:
cDNA 1-2 µl (50-100 ng)
SYBR Green solution 12.5 µl
5‘ primer (10 pmol/µl) 1 µl
3‘ primer (10 pmol/µl) 1 µl
H_2O variable

---

25 µl

The PCR reaction was done using the following programme:
Lid temperature = 110°C
Preheating = On
Initial denaturation = 95°C 15 sec
45 cycles: 95ºC 15 sec, 60ºC 30 sec, 72ºC 30 sec
60°C 15 min, 95°C 15 min

PCR Base Line Subtracted Data is analyzed for Ct (cross threshold) calculation.

2.2.3 Cloning

2.2.3.1 Generation of DNA insert by PCR

To clone a particular DNA fragment into plasmid vector for generating a recombinant plasmid, PCR was done to amplify either the full coding sequence or particular region of interest from the gene. Cloning primers were designed from the sequences available in the Genbank. 30-33 bp long primers were designed flanking the 5‘ and 3‘ region of interest. Care was taken to have similar annealing temperature for the primer pair. Suitable restriction enzyme sites were included in the primer based on the multiple cloning site of the plasmid vector into which the fragment was to be cloned. DNA fragment to be cloned was checked for the presence of sequence matching the restriction site. Primers were designed in a way to ensure that the right amino acid codon frame remained intact in the recombinant plasmid. For cloning the full cDNA, stop codon was mutated in the 3‘primer when cloned into a vector with a 3‘ detection tag. 1 µl of cDNA used for generating the required cDNA fragment with 2 µl of each primer (10 pmol/µl) using the Hotstar Taq Master Mix kit (Qiagen, Hilden).

PCR cycling conditions were similar to described above for normal PCR with appropriate annealing temperature. 5 µl of amplified fragment was loaded on the agarose gel to check for the correct fragment size. PCR reaction mix cleaned using Concert Rapid PCR purification kit (Gibco BRL), quantified, restriction digested, again cleaned to remove digestion buffer, quantified and checked on the gel for correct size.

2.2.3.2 Dephosphorylation of digested plasmid

The restriction enzyme treated plasmid was dephosphorylated with Shrimp Alkaline Phosphatase (Boeringer Mannheim) to remove the phosphate groups from the linear plasmid and avoid self-ligation during the ligation process.

Restriction digested DNA	1-2 µg
Shrimp Alkaline Phosphatase (1 u/µl)	1 µl
Dephosphorylation buffer (10x)	1x
H_2O	variable
	20 µl

Incubated for 1 h at 37°C followed by 10 min at 65°C for denaturing the enzyme. After phosphatase reaction, plasmid vector was cleaned again to remove the reaction buffer.

2.2.3.3 Ligation of plasmid and DNA insert

To generate recombinant plasmid, dephosphorylated restriction digested plasmid was ligated with the DNA insert having the same restriction sites at their 5‘ and 3‘ end using the T4 DNA Ligase (Gibco BRL). All the restriction enzymes used in the present study generate sticky ends.

Plasmid vector	1x
DNA insert	3x
T4 DNA Ligase (1 u/µl)	1 µl
Ligase buffer (5x)	4 µl
H_2O	variable
	20 µl

Ligation was done in (T3) Thermocycler (Biometra) using following reaction

Conditions:
16°C 8 h
22°C 4 h
37°C 2 h
Pause 4°C

Ligation mixture was then used to transform bacteria to generate recombinant plasmid.

2.2.3.4 Mutation of target gene

To generate mutants of target genes, site-directed mutagenesis kit was used. Two complimentary oligonucleotides containing the desired mutation for each gene were synthesized. The reactions were prepared as indicated below:

5 µl of 10× reaction buffer
3 µl (10 ng/µl) of DNA
1 µl (10 µM) of primer-s
1 µl (10 µM) of primer -a
1 µl of dNTP mix
39 µl of H_2O
---
50 µl

Conditions:
95 °C 30 s
95 °C 30 s
55 °C 1 min
72 °C x min (2 min/kb)
} 18 x cycles
Pause 4°C

Then, add 1 µl of the *Dpn* I restriction enzyme (10 U/µl) to each amplification reaction, mix reaction mixture and immediately incubate each reaction at 37°C for 1 hour for digestion. 10 µl of the reaction are used for transformation of XL1-Blue supercompetent cells. Positive clones were selected using Kan^r or Amp^r LB agar plates.

2.2.4 Microbiological techniques

Transformation of bacteria with plasmid DNA E.coli by heat-shock method ($CaCl_2$ based)

For transformation of E.coli, XL1-Blue, ER2566 or DH 5α strain was used. To make competent cells single colony of XL1-Blue was grown in 5 ml LB media overnight at 37°C with shaking at 250 rpm. 1 ml of overnight bacterial culture was then transferred to 100 ml of fresh

LB media and continued to grow at 37°C with shaking till the cells reached their logarithmic phase i.e., OD_{600} = 0.3-0.4. Then the bacterial suspension was centrifuged at 6000 rpm in SS 34 Rotor in Sorvall centrifuge (pre-cooled) for 5 min at 4°C. Supernatant was discarded and cell pellet was resuspended in 10 ml of ice-cold 100 mM $CaCl_2$ solution. The cell suspension was then incubated on ice in cold room (4°C) for 1 h. Centrifuged for 5 min at 6000 rpm at 4 °C. Supernatant discarded carefully and pellet resuspended in 1 ml of ice-cold 100 mM $CaCl_2$ containing 30% glycerine (1 ml solution= 700 µl 100 mM $CaCl_2$ + 300µl of 100% glycerine). From this competent cell suspension aliquots of 200 µl made, frozen in liquid nitrogen and stored at -80°C.

To transform bacteria, 200 µl of $CaCl_2$ competent cells for each reaction thawed on ice. To the cells added 100 µl of cold TCM buffer and either 10-20 ng of super-coiled plasmid DNA or 20 µl of ligation mix. Incubated on ice for 20 min and then heat–shock was given for 90 sec at 42°C. Transformation reaction mix immediately incubated on ice for 1 min. 700 µl of LB media (pre-warmed at 37°C and without any antibiotic) added to transformation mix and incubated for 30-60 min with shaking at 37°C. 100 µl of the transformation mixture in case of super-coiled DNA was plated on the LB-agar plate containing suitable antibiotic. For ligation transformation, reaction mix was centrifuged briefly, supernatant was discarded and pellet was resuspended in the residual volume and plated on LB-agar containing suitable antibiotic. LB-agar plates incubated up-side down at 37°C to facilitate growth of transformants under appropriate antibiotic selection pressure.

2.2.5 Cell culture

For culturing of HEK-293 cells, frozen cells were thawed in 37°C water bath. 1 ml of cryopreserved cell suspension and 9 ml of complete cell culture medium centrifuged at 1000 rpm for 3 min at room temperature. Pellet was resuspended in tissue culture dish (10 cm) (Nunc, Denmark) and incubated in cell culture incubator (Heraeus) in a humidified atmosphere of 95% air, 5% CO_2 at 37°C. HEK-293 (Human embryonic kidney, epithelial) cells were cultured in DMEM (Dulbecco minimum essential medium) / HAM'S F12 (1:1) with 2 mM Glutamine, 10% FCS (fetal calf serum), 100U/ml Penicillin and 100 µg/ml Streptomycin (Biochrom). For cell passage, HEK-293 cells were detached with HBSS without Ca^{2+} and Mg^{2+} (Biochrom) for 5 min at room temperature after the medium was aspirated out.

Rat primary astrocytes were obtained from whole rat brain and grown in the Dulbecco's modified Eagle's medium (Biochrom, Germany) supplemented with 10% heat-inactivated fetal

calf serum, 100 units/ml penicillin and 100 µg/ml streptomycin at 37ºC and 10% CO_2. Rat primary astrocyte cultures were used from 10 to 14 days after preparation.

2.2.6 Cell transfection with plasmids

To express the protein of interest as a fusion protein in mammalian expression system, recombinant plasmid was transfected into HEK293 cells and rat primary astrocytes. Cells (80% confluent) were transfected using DOTAP liposomal transfection reagent or magnetic transfection reagent, according to the manufacturer's protocol (Roche Diagnostics, Germany). To generate the stable clone, the cells were selected with 500 µg/ml of G418 (for plasmids with vetor pcDNA3.1 or pEGFP-N1), 1 µg/ml of puromycin (for plasmids with vetor PEAK10).

2.2.7 Subcloning

Cells were selected for 100% transfection by subcloning. In case of GFP construct transfected cells, cluster of cells exhibiting high fluorescence selected using a plastic ring and propagated as independent clones in culture under antibiotic pressure. Since it was not possible to visualise myc-his (MH) tag fusion protein, cluster of cells seemingly originating from a single cell were selected in a similar way as GFP-fusion protein and propagated as independent clones under antibiotic selection pressure. HA-tag fusion proteins clones were selected on the basis of carrier GFP fluorescence. Independent clones of myc-his fusion and HA-fusion proteins were verified at the transcription and translation level by RT-PCR and western blot or immunostaining, respectively.

2.2.8 Protein chemistry

2.2.8.1 Cell lysate

To make whole cell lysate for protein measurement and subsequent protein studies, confluent cells (10 cm dish) were washed 1x with ice-cold PBS (1x) and lysed in 1 ml of 1x lysis buffer. The cell lysate was gently mixed on a rotator for 15 min at 4°C. Lysate was then sonificated 3x10 sec (40% power) in Ultrasonificator on ice. Then centrifuged at 14,000 rpm in a pre-cooled centrifuge for 15 min. Supernatant was transferred into a fresh tube and pellet discarded. Protein concentration was determined by Bradford method using 1% bovine serum albumin as standard. Lysate was stored at -20°C.

2.2.8.2 SDS-PAGE and Western Blot (WB)

The proteins with Laemmli buffer were boiled for 5 min or incubated on ice for 1 h, electrophoresed on a 10% or 12.5% SDS-PAGE gel, and transferred to nitrocellulose membrane. The membrane was blocked and incubated overnight with the primary antibody (anti-myc, 1:5000, Invitrogen; anti-HA, 1:5000, Sigma; anti-GST, 1:80000, Santa Cruz) at 4ºC, followed by goat anti-rabbit or goat anti-mouse IgG conjugated to HRP for 1 h at room temperature. After washing, the immune complexes were detected by the SuperSignal West Pico Chemiluminescent Substrate (Pierce).

To reprobe the membrane with a second primary antibody this procedure was followed: Washed out enhanced chemiluminiscence solution from membrane by washing in PBS-Tween (0.1%). Incubated membrane in stripping buffer for 30 min at 50°C. Washed extensively in PBS-Tween to remove ß-mercaptoethanol from the membrane. Blocked membrane overnight in 5% non-fat dry milk at 4°C. Probed with another primary antibody as described above.

2.2.8.3 Coomassie stain

After electrophoresis, removed the gel from the plate and covered the gel with coomassie-brilliant blue stain solution (0.2% brilliant blue R250 in 50% (v/v) methanol in water with 10% (v/v) acetic acid) for 20 min. Removed coomassie-brilliant blue stain solution and added destained solution (30% (v/v) methanol in water with 10% (v/v) acetic acid) and incubated overnight. Removed, destained, and fixed gel using gel drying frames in the presence of storage solution (15% (v/v) glycerol in water with 10% (v/v) methanol).

2.2.8.4 GST pull-down assays

The different GST fusion protein constructs were transfected into *Spodoptera frugiperda* (sf.9) cells. The recombinant baculovirus was amplified and tested for the production of the fusion protein. Cells infected with recombinant baculovirus containing C-tail or full-length of PAR-2-GST gene were lysed on ice in membrane fraction buffer 1 (50 mM Hepes pH 8, 300 mM NaCl, 0.1 mM EDTA, 10 mM β-mercaptoethanol, and Protease Inhibitor Cocktail (Roche Diagnostics, Germany, one tablet per 50 ml)). After centrifugation for 10 min at 1000 g and 4ºC, pellets were resuspended in membrane fraction buffer 1, sonicated, and centrifuged for 1 h at 100000 g and 4ºC. Afterwards, pellets were resuspended in membrane fraction buffer 2 (50 mM Hepes pH 8, 300 mM NaCl, 10 mM β-mercaptoethanol, 1% Brij 58, and Protease Inhibitor Cocktail), stirred and centrifuged again for 1 h at 100000 g at 4ºC. The resulting supernatant contained the membrane fraction of the recombinant fusion proteins. The recombinant fusion

proteins were purified by using glutathione-Sepharose beads (Pharmacia). Equal amounts of GST, C-tail of PAR-2-GST and PAR-2-GST fusion proteins immobilized on glutathione-Sepharose beads were incubated overnight at 4ºC with the crude HEK293-α-crystallin-myc-his or HEK293-α-crystallin-deletion-myc-his cell extracts in HEK293 lysis buffer (50 mM Tris/HCl pH 7.5, 1 mM β-mercaptoethanal, 150 mM NaCl, 1% Igepal, and Protease Inhibitor Cocktail). After washing three times with the HEK293 lysis buffer without protease inhibitor and one time with the HEK293 lysis buffer containing 1 M NaCl and without protease inhibitor, the bound proteins were separated by SDS-PAGE, and immunoblotted with the anti-myc antibody (1:5000, Invitrogen).

2.2.8.5 Immunoprecipitation (IP)

Cells were detached, rinsed with cold phosphate buffered saline buffer (pH 7.4, 8.1 mM Na_2HPO_4, 1.45 mM $KHPO_4$, 137 mM NaCl, 2.68 mM KCl), and lysed in the HEK293 lysis buffer (50 mM Tris/HCl pH 7.5, 1 mM β-mercaptoethanal, 150 mM NaCl, 1% Igepal, and Protease Inhibitor Cocktail). Equal amounts of lysates were rotated with the anti-GFP antibody (1:200, Sigma) for 6 h, followed by incubating with protein A Sepharose beads (Pharmacia) delete or with protein G agarose beads (Sigma) overnight at 4ºC. After washing three times with HEK293 lysis buffer without protease inhibitor, the bound beads were incubated in Laemmli buffer for 60 min on ice, separated by SDS-PAGE, and immunoblotted with the anti-myc antibody (1:5000, Invitrogen) or with the anti-HA antibody (1:5000, Sigma).

2.2.9 Immunocytochemistry

Cells (wild-type or transfected) cultured on coverglass were fixed in 4% paraformaldehyde for 25 min at room temperature, then washed and stored in PBS. All the following steps were performed at room temperature. Fixed cells were blocked and permeabilised in FTP buffer for 1 h. Then they were incubated overnight with mouse anti-myc antibody (2 μg/ml, Invitrogen) and incubated with Alexa™ 555 goat anti-mouse IgG antibody (20 μg/ml, Molecular Probes) for 120 min at room temperature in the dark. Mounted slides were observed with a LSM510 confocal laser scanning microscope (Carl Zeiss, Germany).

2.2.10 Cell death induction and measurement

Rat primary astrocytes were seeded at a density of 40,000 cells per assay (48-well culture plate) and treated with 20 μM of C2-ceramide (Calbiochem) or 0.2 μM of staurosporine (Sigma) or different concentrations of trypsin for 18 h to induce cell death. Cell death was

measured by lactate dehydrogenase (LDH) assay, according to the manufacturer's protocol (Roche Diagnostics, Germany). 500 μM of PAR-2 activating peptide (NeoMPS SA) was applied to activate PAR-2.

2.2.11 Expression of α-crystallin in bacteria and purification

αA-crystallin and αB-crystallin genes were cloned into PTXB1 and PTYB11 vectors. E. coli ER2566 was transformed with recombinant plasmids of CRYAA-PTXB1, CRYAA-PTYB11, CRYAB-PTXB1 and CRYAB-PTYB11 as described in method 2.2.4. Incubated the culture in the shaker at 37°C until the OD_{600} reached 0.5. Then, IPTG was added to a final concentration of 0.4 mM for induction of protein expression. After 2 hours' incubation, the cells from the IPTG-induced culture were spun down at 5000 x g for 15 minutes at 4°C and the supernatant is discarded. The cell pellet was resuspended in 100 ml of the ice-cold Column buffer and sonificated 3x10 sec (40% power) in ultrasonificator on ice. Centrifuged the lysate at 15,000 x g for 15 minutes at 4°C. The supernatant was the clarified extract. Incubated the clarified extract with chitin beads for four hours. Spun down at 500 x g for 5 minutes at 4°C. Washed the beads three times with Column buffer (20 mM Tris/HCl pH 8.5, 500 mM NaCl, 1 mM EDTA). Added three bed volumes of the Cleavage buffer (20 mM Tris/HCl pH 8.5, 500 mM NaCl, 1 mM EDTA, 50 mM DTT) and incubated overnight. Spun down at 500 x g for 5 minutes at 4°C. Used twenty bed volumes of Column buffer to wash the beads. Eluted the target protein with Column buffer containing 4 M of urea or 1 M of NDSB 256. Dialyzed the target protein with Column buffer. The eluted fractions and the beads were analyzed by SDS-PAGE and coomassie stain.

2.2.12 Statistics and NCBI-Blast

Data were expressed as mean ± S.E.M. Differences were examined by Student's *t*-test between two groups or one-way analysis of variance (ANOVA) within multiple groups. $p<0.05$ was considered significant. The experiments are repeated at least three times with comparable results.

To search for mRNA, protein and primer homology, NCBI genbank program-BLAST was used.

3. Results

3.1 Expression of PAR-2 in astrocytes and transfected cells

The human PAR-2 as well as rat PAR-2 protein comprises 397 amino acids, and native PAR-2 appears as a smear band as a result of glycosylation. Accumulating evidence revealed that PAR-2 is expressed in a wide range of biological systems such as gastrointestinal tract (Darmoul et al., 2004), cardiovascular system (Coelho et al., 2003; D'Andrea et al., 1998), skin (Macfarlane et al., 2005), immune cells (Fiorucci et al., 2001; Steinhoff et al., 2005), airways (Asokananthan et al., 2002; Berger et al., 2001; Cocks et al., 1999), and nervous system (Park et al., 2006; Smith-Swintosky et al., 1997).

In the current research, we determined the expression of PAR-2 in primary astrocytes by immunostaining.

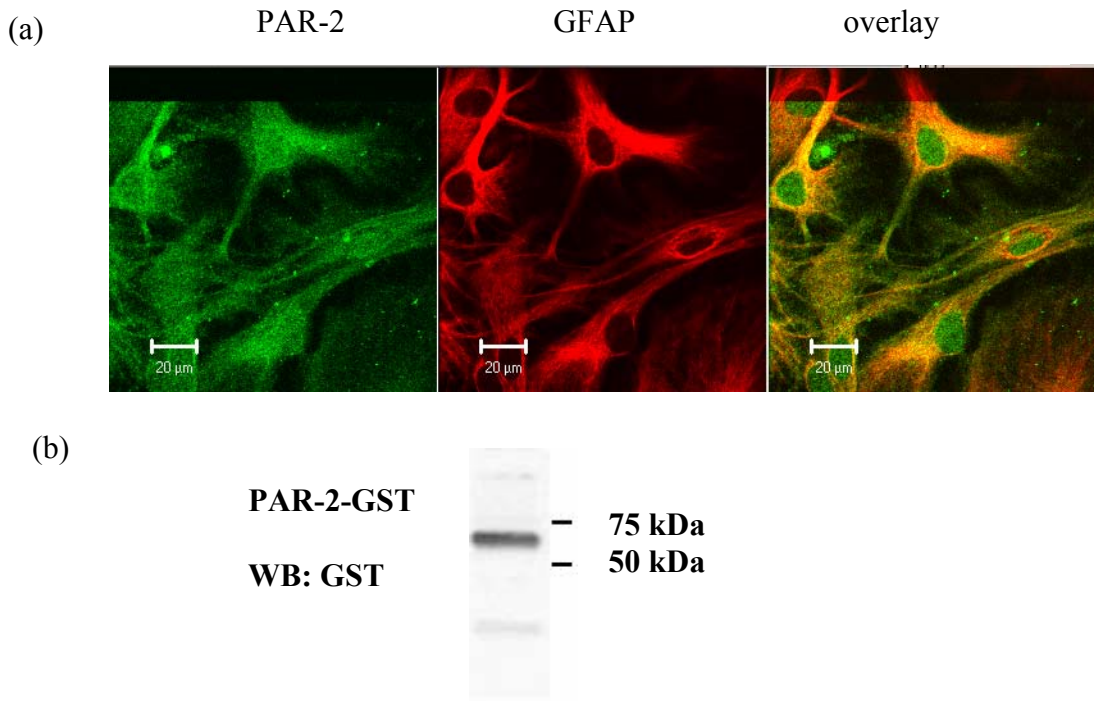

Figure 3.1 Expression of PAR-2 in astrocytes (a) and sf.9 cells (b)

(a). Expression of PAR-2 in astrocytes was determined by immunostaining. Astrocytes were cultured for 10-14 days and fixed with in 4% paraformaldehyde. Fixed cells were incubated overnight with PAR-2 antibody (1: 100, Santa Cruz Biotechnology) and GFAP antibody (1: 200, Boehringer). After washing, fixed cells were incubated with secondary antibodies Alexa488 anti-mouse IgG (20 µg/ml, Molecular Probes) and Alexa555 anti-mouse (1: 200, Molecular Probes) and detected by confocal laser scanning microscope (Carl Zeiss, Germany). (b). The membrane fraction with PAR-2-GST was extracted from infected sf.9 cells, analysed by western blot (WB) using a polyclonal anti-GST antibody (1: 80000, Santa Cruz). All the experiments were repeated three times with comparable results.

As shown in Fig. 3.1 (a), PAR-2 is detectable in astrocytes. Unfortunately, available PAR-2 antibody for western blot is not yet found. To figure out which proteins are PAR-2-interacting partners and how PAR-2 interacts with its partners, we generated a novel baculovirus GST expression vector in order to facilitate the expression of the transmembrane receptor protein tagged with GST in sf.9 cells. The PAR-2-GST fusion protein expressed in sf.9 cells was purified by glutathione-Sepharose beads. As shown in Fig. 3.1 (b), PAR-2-GST was strongly expressed with one major band (~60-70 kDa) in sf.9 cells. We also constructed a mammalian expression vector pEGFP-N1 containing an insert with the full-length PAR-2 cDNA fused with GFP at the N-terminus. This recombinant vector was used for stably transfecting HEK293 cells. As shown in Fig. 3.5, PAR-2 is strongly expressed at the membrane.

3.2 Expression of α-crystallin in astrocytes and transfected cells

α-Crystallins are the major lens structural proteins. The α-crystallin domain is a consensus sequence that is common to all the members of the small heat shock protein superfamily. αA-crystallin and αB-crystallin exhibit about 54% identity on amino acid level and have many properties in common. Like many other heat shock proteins, α-crystallin exhibits chaperone-like properties, including the ability to prevent the precipitation of denatured proteins and to increase cellular tolerance to stress. Expression of α-crystallin is not restricted to the lens (Bajramovic et al., 1997; Iwaki et al., 1990; Kozawa et al., 2001; Maddala and Rao, 2005; Srinivasan et al., 1992). Phosphorylation is a major post-translational modification of α-crystallin (Webster, 2003). It has been demonstrated that α-crystallin is phosphorylated via MAPK (Hoover et al., 2000). Phosphorylation of α-crystallin is observed in response to stress, like heat, arsenite, and phorbol ester, okadaic acid, tumor necrosis factor α, or interleukin-1α (Andley et al., 1998; Golenhofen et al., 1998; Ito et al., 1997). Phosphorylation of α-crystallin regulates their translocation, chaperone activity and the ability of binding to substrates. For example, phosphorylation of α-crystallin results in the dissociation of an aggregated form of α-crystallin to oligomers and translocation into special cellular compartments (Eaton et al., 2001). Phosphorylation of αB-crystallin on serine-59 is necessary and sufficient to provide maximal protection of cardiac myocytes from apoptosis (Morrison et al., 2003). Nuclear import and localisation of αB-crystallin is phosphorylation-dependent. The translocation and activities of binding to substrates may be related and both probably contribute to cytoprotection and suppression of apoptosis.

In the present study, we determined the expression of αA-crystallin and αB-crystallin in astrocytes. αA-crystallin and αB-crystallin are stably expressed in astrocytes (see Fig. 3.2 a and b). To study the interaction of PARs family with αA-crystallin and αB-crystallin, we also constructed a mammalian expression vector pcDNA3.1 containing an insert with the full-length α-crystallin cDNA fused with myc-his at the C-terminus. This recombinant vector was used for stably transfecting HEK293 cells for immunoprecipitation and immunostaining assays and studies on the functions of αA-crystallin and αB-crystallin. As shown in Fig. 3.2 (c) and (d), αA-crystallin and αB-crystallin with myc-his tag were nicely expressed in transfected HEK293 cells. In parallel, αA-crystallin and αB-crystallin are also cloned into pEAK10 vector for immunoprecipitation experiments.

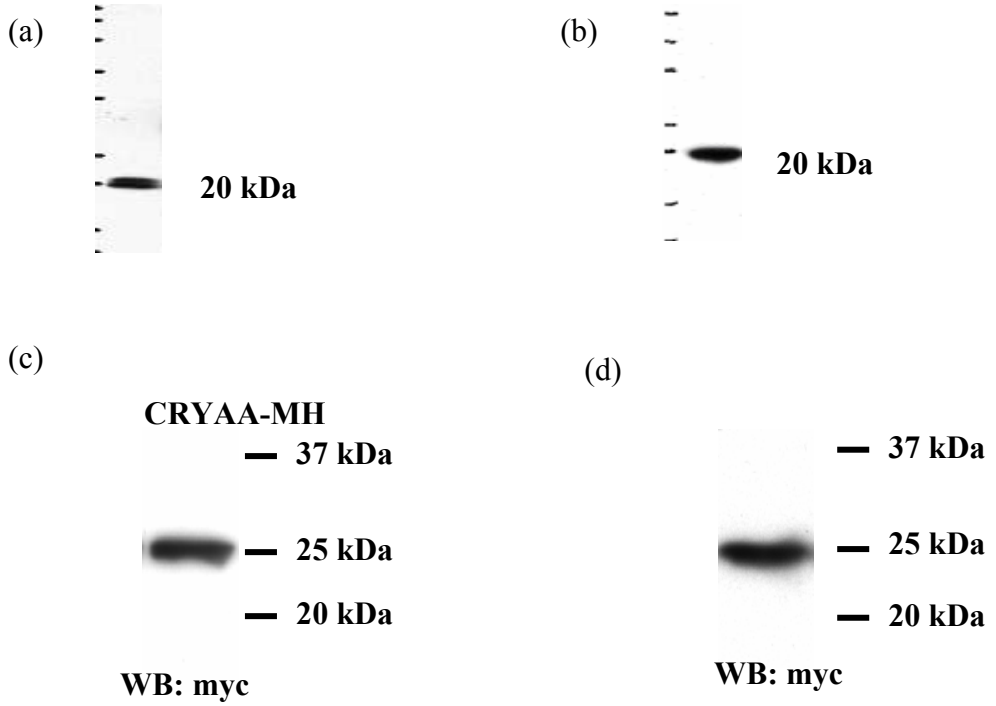

Figure 3.2 Expression of α-crystallin in astrocytes and transfected HEK293 cells

(a). Expression of αA-crystallin in astrocytes was determined by western blot. (b). Expression of αB-crystallin in astrocytes was determined by western blot. Astrocytes lysates were made by sonification and expression of α-crystallin was measured by western blot using anti-αA-crystallin antibody (1:5000, Acris) and anti-αB-crystallin antibody (1:10000, Stressgen). (c) and (d). HEK293 cells were transfected with αA-crystallin-myc-his (CRYAA-MH, in c) or αB-crystallin-myc-his (CRYAB-MH, in d). The expression of fusion proteins CRYAA-MH or CRYAB-MH were determined by western blot using myc antibody (1:5000, Invitrogen). All the experiments were repeated three times with comparable results.

3.3 Identification of the interaction of PAR-2 with α-crystallin

3.3.1 Identification of the interaction of PAR-2 with α-crystallin by GST pull down

To further clarify whether full-length PAR-2 interacts with αA-crystallin and αB-crystallin, we examined the *in vitro* interaction between full-length PAR-2 and α-crystallin by using GST pull down assays. We generated a novel baculovirus GST expression vector in order to facilitate the expression of the transmembrane receptor protein tagged with GST in sf.9 cells. PAR-2-GST expression was determined by western blot analysis using an anti-GST antibody. As shown in Fig. 3.1 (b), PAR-2-GST was strongly expressed with one major band of ~60-70 kDa in sf.9 cells. We also constructed a mammalian expression vector pcDNA3.1 containing an insert with the full-length α-crystallin cDNA fused with myc-his at the C-terminus. This recombinant vector was used for stably transfecting HEK293 cells. As shown in Fig. 3.2 (c) and (d), α-crystallin expression was detected in the lysates from HEK293-α-crystallin-myc-his cells by using an anti-myc antibody.

The PAR-2-GST fusion protein expressed in sf.9 cells was purified by glutathione-sepharose beads. These beads with immobilized PAR-2-GST fusion proteins were incubated overnight with the lysates from HEK293-α-crystallin-myc-his cells to examine the interaction of PAR-2-GST with α-crystallin-myc-his. The interaction was determined by western blot analysis using the anti-myc antibody. As shown in Fig. 3.3 (a) and (b), α-crystallin specifically interacted with the full-length PAR-2-GST fusion protein. To exclude the possible interaction of α-crystallin with the GST tag protein, we incubated the GST protein with the crude HEK293-α-crystallin-myc-his cell lysates. The western blot analysis showed that αA-crystallin did not interact with GST protein alone (Fig. 3.3 a, lane 4). Comparably, also αB-crystallin did not interact with GST protein alone (Fig. 3.3 b, lane 4). Similarly, no signal was detectable when PAR-2-GST proteins were incubated with wild-type lysate of HEK293 cells (Fig. 3.3 a, lane 3 and b, lane 3). This served as a negative control.

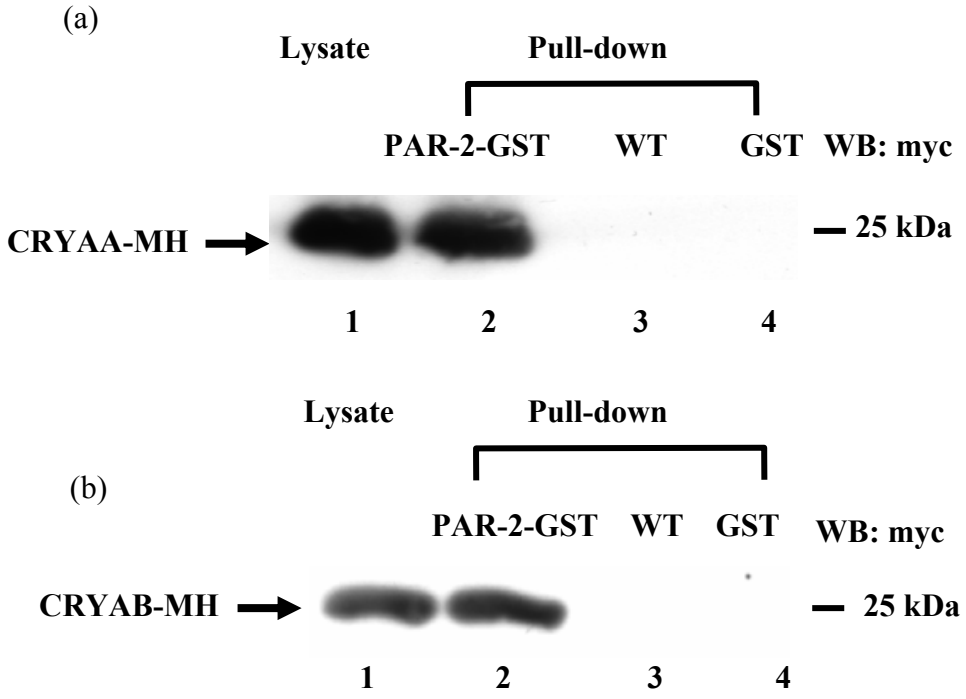

Figure 3.3 Identification of the interaction of PAR-2 with α-crystallin by GST pull down.

(a). Interaction of αA-crystallin with PAR-2 *in vitro*. (b). Interaction of αB-crystallin with PAR-2 *in vitro*. For the pull-down experiments, the whole cell lysates from HEK293 cells, HEK293-CRYAA-MH cells or HEK293-CRYAB-MH cells were incubated overnight with GST protein alone or full length PAR-2-GST fusion proteins immobilized on glutathione beads followed by western blot analysis with the anti-myc antibody. Lysate (lane 1) shows 2% of lysate used for the pull-down experiments, corresponding to the lysate from HEK293-CRYAA-MH (a) or HEK293-CRYAB-MH (b) cells. Lanes 2, 3 and 4 correspond to proteins pulled down. αA-crystallin interacts with PAR-2-GST (lane 2 in a) and not with GFP (lane 4 in a). αB-crystallin interacts with PAR-2-GFP (lane 2 in b) and not with GST (lane 4 in b). All the experiments were repeated three times with comparable results.

3.3.2 Identification of the interaction of PAR-2 with α-crystallin by co-immunoprecipitation

To further confirm that the interaction of the full length PAR-2 with α-crystallin occurs in live cells, we performed co-immunoprecipitation experiments. We generated HEK293 cell lines stably co-expressing PAR-2-GFP/α-crystallin-myc-his or PAR-2-GFP/α-crystallin-HA. The whole cell lysates were immunoprecipitated by anti-GFP antibody, and the interaction of PAR-2-GFP with α-crystallin was examined by western blot analysis using the anti-myc or anti-

HA antibody. As shown in Fig. 3.4 (a) and (b), α-crystallin was specifically co-immunoprecipitated by PAR-2-GFP in the HEK293-PAR-2-GFP + αA-crystallin-myc-his (CRYAA-MH, see Fig. 3.4 a, lane 2) or αB-crystallin-HA (CRYAB-HA, see Fig. 3.4 b, lane 2) cells, but not in the negative control HEK293-GFP + αA-crystallin-myc-his (see Fig. 3.4 a, lane 4) or αB-crystallin-HA (CRYAB-HA, Fig. 3.4 b, lane 4).

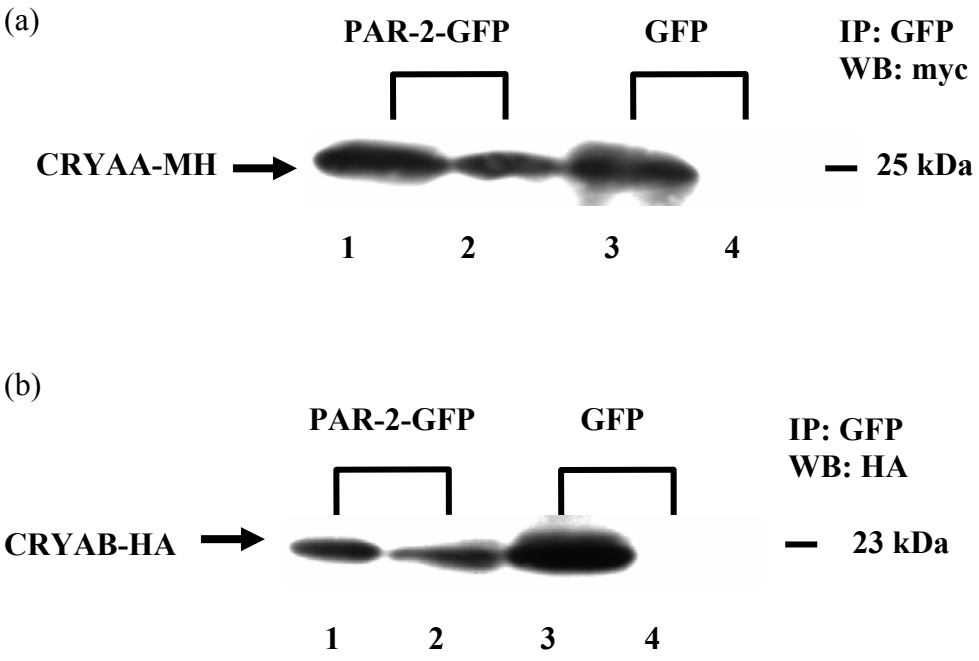

Figure 3.4 Identification of the interaction of PAR-2 with α-crystallin by co-immunoprecipitation

(a). αA-crystallin interacts with PAR-2. (b). αB-crystallin interacts with PAR-2. HEK293 cells were stably co-transfected with PAR-2-GFP/CRYAA-MH or PAR-2-GFP/αB-crystallin-HA (CRYAB-HA) or with GFP/CRYAA-MH or GFP/CRYAB-HA, respectively. The whole cell lysates were immunoprecipitated by anti-GFP antibody in the presence of protein A Sepharose beads and the immunocomplex was determined by western blot using the anti-myc (1:5000, Invitrogen) or anti-HA antibody (1:10000, Sigma). Lanes 1 and 3 correspond to the lysates from HEK293 co-transfected with PAR-2-GFP and CRYAA-MH (a) or PAR-2-GFP and CRYAB-HA (b) or with GFP and CRYAA-MH (a) or GFP and CRYAB-HA (b), respectively. Lanes 2 and 4 correspond to immunoprecipitated proteins. αA-crystallin interacts with PAR-2-GFP (a, lane 2) and not with GFP (a, lane 4). αB-crystallin interacts with PAR-2-GFP (b, lane 2) and not with GFP (b, lane 4). The experiments were repeated three times with comparable results.

3.3.3 Identification of the interaction of PAR-2 with α-crystallin by immunostaining

To further demonstrate the interaction of PAR-2 with α-crystallin, we studied the co-localization of PAR-2 with α-crystallin in HEK293 cells co-expressing PAR-2-GFP + α-

crystallin-myc-his using immunofluorescence staining. PAR-2-GFP and α-crystallin-myc-his were shown to be similarly distributed and mostly co-localized at the plasma membrane in transfected HEK293 cells (Fig. 3.5).

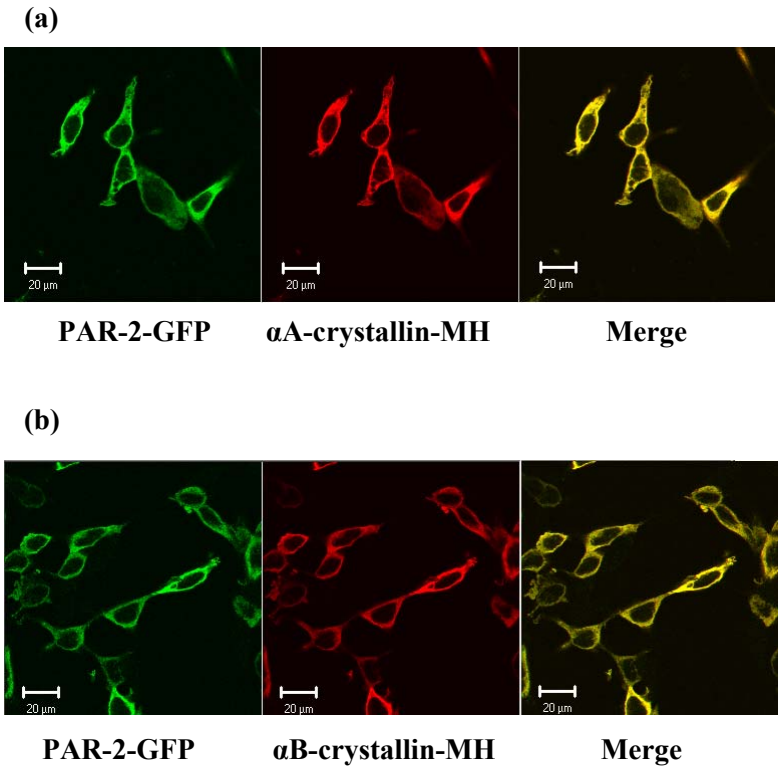

Figure 3.5 Colocalisation of PAR-2 and α-crystallin in transfected HEK293 cells. HEK293 cells were stably co-transfected with PAR-2-GFP and α-crystallin-MH. Cells were fixed, permeabilized, stained, and observed by a confocal microscope. PAR-2 (green) was visualized directly and α-crystallin (red) were visualized by monoclonal anti-myc primary antibody and Alexa^{TM}555 goat anti-mouse IgG as secondary antiboy. The overlay image (Merge) revealed in yellow the colocalisation of PAR-2 and α-crystallin. Scale bar, 20 μm. The experiments were repeated three times with comparable results.

3.3.4 Only PAR-2 interacts with α-crystallin in the PARs family

As we know, there are four members in the PAR family (PAR-1, PAR-2, PAR-3 and PAR-4). Whether α-crystallin is a specific partner of PAR-2 is not clear. We next investigated whether the other PARs (PAR-1, PAR-3 and PAR-4) could also interact with α-crystallin by carrying out co-immunoprecipitation assays. As confirmed in Fig. 3.6, PAR-2-GFP interacts with αA-crystallin and αB-crystallin (Fig. 3.6 a, lane 4 and b, lane 4). However, PAR-1-GFP (Fig. 3.6 a, lane 2 and 3.6 b, lane 2), PAR-3-GFP (Fig. 3.6 a, lane 6 and 3.6 b, lane 6) and PAR-4-GFP (Fig. 3.6 a, lane 8 and 3.6 b, lane 8) do not interact with α-crystallin under the same conditions. As an additional negative control, we showed that GFP proteins do not interact with α-crystallin (Fig. 3.6 a, lane 10 and 3.6 b, lane 10). These findings imply that PAR-2 specifically interacts with α-crystallin.

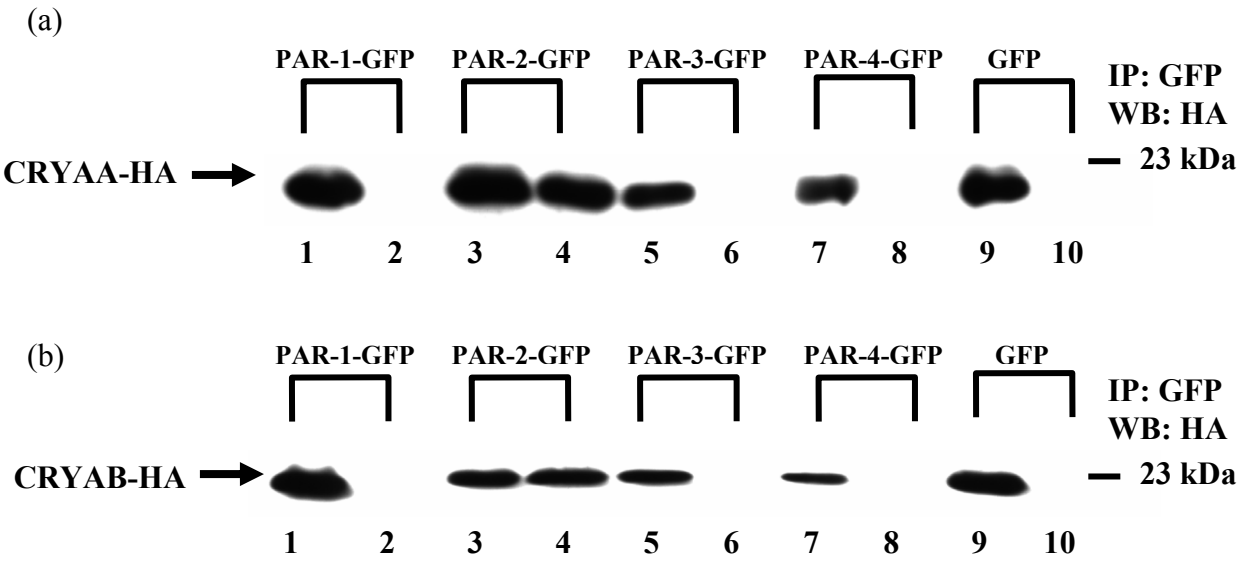

Figure 3.6 Lack of interaction of α-crystallin with PAR-1, PAR-3 and PAR-4.

(a). αA-crystallin interacts with PAR-2-GFP (lane 4), but does not interact with PAR-1-GFP (lane 2), PAR-3-GFP (lane 6) and PAR-4-GFP (lane 8). (b). αB-crystallin interacts with PAR-2-GFP (lane 4), but does not interact with PAR-1-GFP (lane 2), PAR-3-GFP (lane 6) and PAR-4-GFP (lane 8). HEK293 cells were stably co-transfected with PAR-X-GFP (X: 1, 2, 3, 4) and α-crystallin-HA, respectively. The whole cell lysates were immunoprecipitated by anti-GFP antibody in the presence of protein A Sepharose beads and the immunocomplex was determined by western blot using the anti-HA antibody (1:10000, Sigma). Lanes 1, 3, 5, 7 and 9 correspond to the lysates from HEK293 co-transfected with PAR-2-GFP and CRYAA-HA (a) or PAR-2-GFP and CRYAB-HA (b) or with GFP and CRYAA-HA (a) or GFP and CRYAB-HA (b), respectively. Lanes 2, 4, 6, 8 and 10 correspond to immunoprecipitated proteins. αA-crystallin interacts with PAR-2 (a, lane 4) and not with PAR-1 (a, lane 2), PAR-3 (a, lane 6) and PAR-4 (a, lane 8). In parallel, αB-crystallin only interacts with PAR-2-GFP (b, lane 4). As a negative control, α-crystallin does not interact with GFP (lanes 10 in a and b). The experiments were repeated three times with comparable results.

3.3.5 Identification of the interaction of C-tail of PAR-2 with α-crystallin

We also wanted to confirm the interaction between αA-crystallin and the C-tail of PAR-2 which was suggested from our previous yeast-two-hybrid protein interaction studies (Rohatgi, 2003). Therefore, protein pull-down assay was performed. The C-tail of PAR-2-GST (C-tail-PAR-2-GST) fusion protein expressed in sf.9 cells was purified by glutathione-sepharose beads. These beads with immobilized C-tail of PAR-2-GST fusion proteins were incubated overnight with the lysate from HEK293-α-crystallin-myc-his cells to examine the interaction of the C-tail of PAR-2-GST with α-crystallin-MH. The interaction was determined by western blot analysis using anti-myc antibody. As shown in Fig. 3.7, αA-crystallin specifically interacted with the C-

tail of PAR-2-GST fusion protein (lane 2). To exclude the possible interaction of αA-crystallin with the GST tag protein, we incubated GST protein with the crude HEK293-α-crystallin-myc-his cell lysate. The western blot analysis showed that αA-crystallin did not interact with GST protein alone (lane 3). Similarly, no signal was detectable when the C-tail of PAR-2-GST protein was incubated with wild-type lysate of HEK293 cells (lane 4). This served as a negative control.

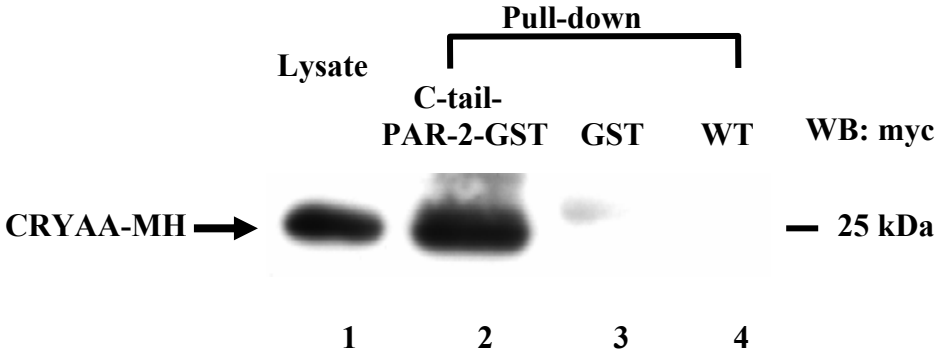

Figure 3.7 Interaction of αA-crystallin with C-tail of PAR-2 *in vitro.*

For the pull-down experiments, the whole cell lysates from HEK293 cells or HEK293-αA-crystallin-MH (CRYAA-MH) cells were incubated overnight with glutathione S-transferase (GST) protein alone or C-tail of PAR-2-GST (C-tail-PAR-2-GST) fusion proteins immobilized on glutathione beads followed by western blot analysis with the anti-myc antibody. Lysate from HEK293-CRYAA-MH cells (lane 1) shows 2% of lysate used for the pull-down experiments. Lanes 2, 3 and 4 correspond to proteins pulled down. The experiments were repeated three times with comparable results.

To unequivocally confirm the interaction between αA-crystallin and the C-tail of PAR-2 in live cells, co-immunoprecipitation assay was performed. HEK293 cells transiently co-expressing C-tail of PAR-2-GFP (C-tail-PAR-2-GFP) and αA-crystallin-HA (CRYAA-HA) were used. The whole cell lysates were immunoprecipitated by anti-GFP antibody, and the interaction of C-tail of PAR-2-GFP with αA-crystallin was examined by western blot analysis using anti-HA antibody. As shown in Fig. 3.8 (a), αA-crystallin was specifically co-immunoprecipitated by C-tail of PAR-2-GFP in the HEK293-C-tail-PAR-2-GFP + αA-crystallin-HA (lane 2), but not in the negative control HEK293-GFP + αA-crystallin-HA (lane 4). In parallel, the interaction of αB-crystallin with the C-tail of PAR-2 was identified (see Fig. 3.8 b). These results indicated that C-tail of PAR-2 is involved in the interaction with αA-crystallin and αB-crystallin.

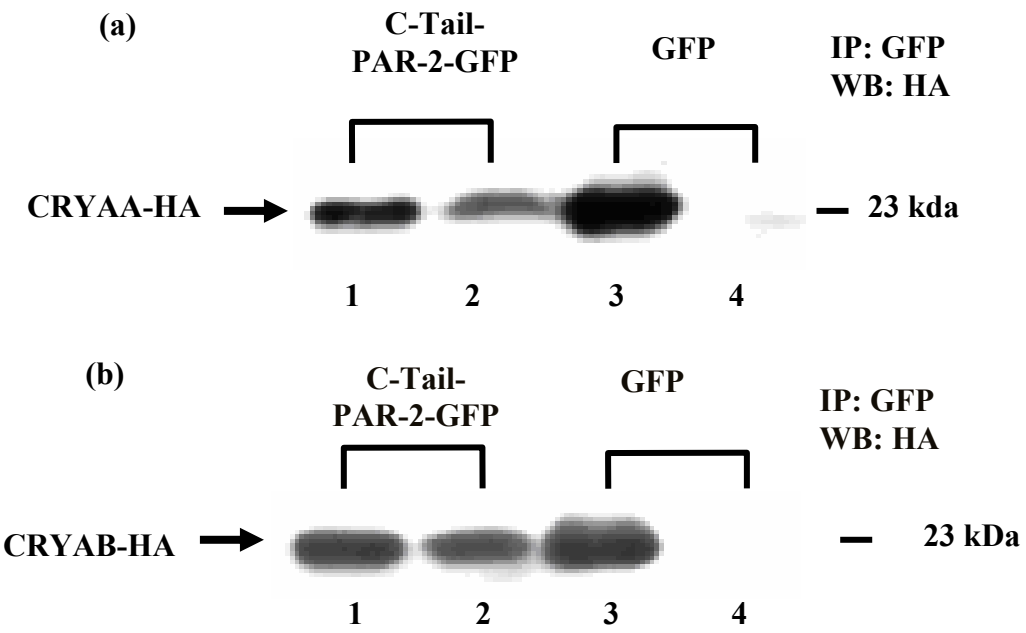

Figure 3.8 Interaction of α-crystallin with C-tail of PAR-2 in live cells.

(a). Interaction of αA-crystallin with C-tail of PAR-2 *in vivo*. (b). Interaction of αB-crystallin with C-tail of PAR-2 *in vivo*. HEK293 cells were transiently co-transfected with C-tail of PAR-2-GFP (C-tail-PAR-2-GFP) and αA-crystallin-HA (CRYAA-HA) or C-tail of PAR-2-GFP (C-tail-PAR-2-GFP) and αB-crystallin-HA (CRYAB-HA) or with GFP and αA-crystallin-HA, or with GFP and αB-crystallin-HA, respectively. The whole cell lysates from HEK293-C-tail-PAR-2-GFP + α-crystallin-HA cells, as well as HEK293-GFP + α-crystallin-HA cells (negative control) were immunoprecipitated (IP) by anti-GFP antibody in the presence of protein A Sepharose beads and the immunocomplex was determined by western blot using the anti-HA antibody. Lanes 1 and 3 correspond to the lysates from HEK293 co-transfected with C-tail of PAR-2-GFP and α-crystallin-HA or with GFP and α-crystallin-HA, respectively. Lanes 2 and 4 correspond to immunoprecipitated proteins. The experiments were repeated three times with comparable results.

3.3.6 Interaction domains of αA-crystallin with PAR-2

The small heat shock proteins, αA-crystallin and αB-crystallin share high similarity in their secondary structure. α-Crystallin is predominantly a β-sheet protein with less α-helical structure (Fig. 1.3). The N-terminal domain of α-crystallin contains three α-helices (numbered α1 to α3). The 'α-crystallin domain' consists of eight β-sheets (designated β2 to β9). The C-terminal extension includes another β-sheet (designated β10).

Sequence analysis using software antheprot (http://antheprot-pbil.ibcp.fr) of the αA-crystallin interaction suggests that four regions of αA-crystallin might be important for the interaction of PAR-2 with αA-crystallin. To map the regions of αA-crystallin responsible for

interaction with PAR-2, we generated a series of deleted αA-crystallin-myc-his fusion proteins, which are explained schematically in Figure 3.9 (a). CRYAA-MH corresponds to the full-length αA-crystallin with the myc-his tag (denoted as MH) at the C-terminus. Del 49-MH (parts of α3 and β2 are deleted), Del 95-MH (parts of β5 and β6 are deleted), Del 120-MH (parts of β7 and β8 are deleted, including the phosphorylation site Ser122) and Del 136-MH (part of β9 is deleted, including the phosphorylation site Ser148) are the αA-crystallin mutants tested with indicated internal deletion and a myc-his tag at the C-terminus, respectively.

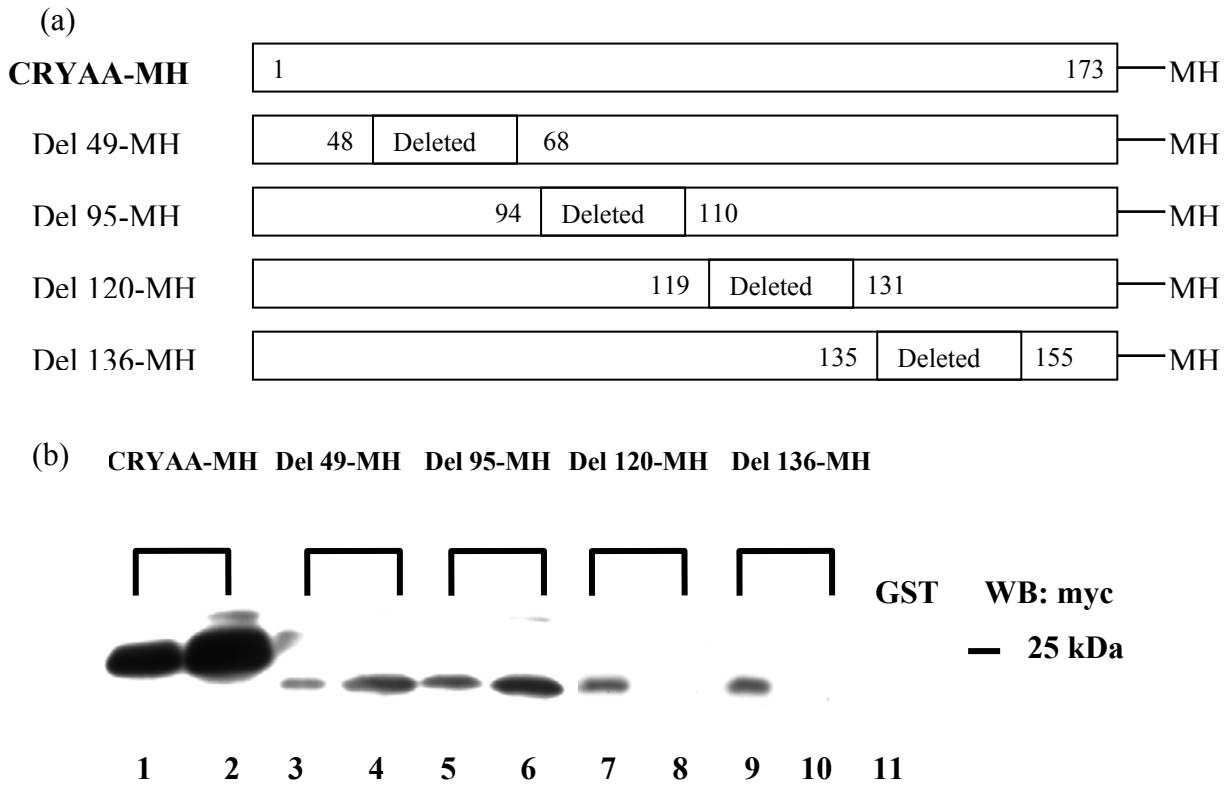

Figure 3.9 Regions of αA-crystallin involved in the interaction with full length PAR-2 *in vitro*.
(a). Schematic representation of CRYAA-deletion MH constructs. The respective deleted part of αA-crystallin is shown by the gray bar. The numbers in the bars represent amino acid residues of αA-crystallin. (b). Identification of interacting regions of αA-crystallin with PAR-2 by pull-down assays. The whole cell lysates from HEK293-CRYAA-MH or HEK293-CRYAA-Deletion-MH cells were incubated overnight with GST protein alone or full length PAR-2-GST fusion proteins immobilized on glutathione beads followed by western blot analysis with the anti-myc antibody. Lanes 1, 3, 5, 7 and 9 correspond to lysates from HEK293 cells transfected with indicated MH constructs. Lanes 2, 4, 6, 8, 10, and 11 correspond to proteins pulled down in the assay. Full length CRYAA-MH, Del 49-MH and Del 95-MH proteins interact with PAR-2-GST proteins (Lanes 2, 4 and 6). Del 120-MH and Del 136-MH proteins do not interact with PAR-2-GST (lanes 8 and 10). As a control, full length CRYAA-MH does not interact with GST protein (lane 11). The experiments were repeated four times with comparable results.

As shown in Fig. 3.9 (b), the deleted fusion proteins were expressed in HEK293 cells transfected with the respective constructs. These deleted fusion proteins were tested for their capacities to bind to the PAR-2-GST protein. Fig. 3.9 (a), lanes show lysates of HEK293 cells transfected with the indicated constructs, and lanes give pull-down of respective proteins. As demonstrated in the pull-down results, CRYAA-MH (Fig. 3.9 b, lane 2), Del 49-MH (Fig. 3.9 b, lane 4), and Del 95-MH (Fig. 3.9 b, lane 6) can interact with PAR-2-GST. However, Del 120-MH (deleted aa 120-130 of αA-crystallin) and Del 136-MH (deleted aa 136-154 of αA-crystallin) fusion proteins do not interact with PAR-2 (Fig. 3.9 b, lane 8 and lane 10). These results suggest that the regions of the amino acids 120-130 and amino acids 136-154 of αA-crystallin are required for the interaction with PAR-2.

3.4 The role of PAR-2 in astrocytes

Activation of PAR-2 may be beneficial or toxic to brain according to the physiological or pathophysiological situation (Fiorucci et al., 2001; Jin et al., 2005; Steinhoff et al., 2005).

To explore the role of PAR-2 in astrocytes, we treated astrocytes with C2-ceramide or staurosporine to induce astrocyte cell death. C2-ceramide or staurosporine are useful reagents for inducing apoptosis of cells in different research. Astrocytes underwent cell death in response to C2-ceramide or staurosporine in a time-dependent manner (up to 48 h, data not shown). In our further experiments, astrocytes were treated with these toxic agents for 18 hours. Activation of PAR-2 by activating peptide significantly decreased C2-ceramide or staurosporine-induced cell death in astrocytes (Fig. 3.10). Thus, PAR-2 activation inhibited C2-ceramide and staurosporine-induced cell death in our experimental conditions. In the current research, we observed protective role of PAR-2 in astrocytes treated with ceramide and staurosporine. This is a novel evidence to show PAR-2 is protective in astrocytes during stress.

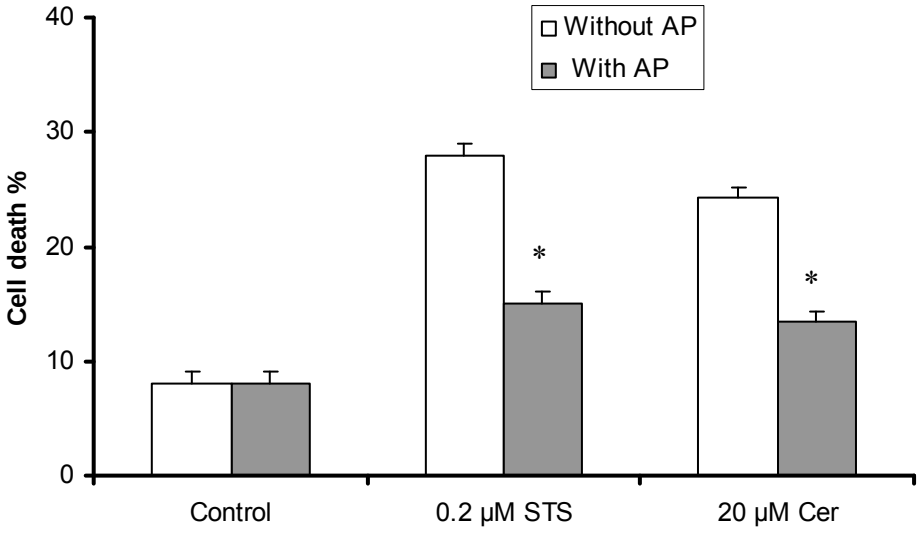

Figure 3.10 Cytoprotection of astrocytes by PAR-2 activation.

Astrocytes were treated with 20 μM of C2-ceramide (Cer) alone or with 20 μM of C2-ceramide + 500 μM of PAR-2 activating peptide (AP, SLIGRL) or with 0.2 μM of staurosporine (STS) alone or with 0.2 μM of staurosporine + 500 μM of PAR-2-activating peptide for 18 h, respectively. Cell death was measured by LDH activity assay. The cell death data were obtained for each sample and the results were averaged. The values of astrocytes death under the treatment with staurosporine or C2-ceramide in the absence or presence of PAR-2-activating peptide were compared. The statistical significance level for difference in cell death between PAR-2 AP treatment and without PAR-2 AP treatment is given as * $p<0.05$. The experiments were repeated six times with comparable results. As indicated, C2-ceramide- and staurosporine-induced cell death in astrocytes was significantly inhibited by activation of PAR-2.

3.5 The role of α-crystallin in astrocytes

3.5.1 Overexpression of α-crystallin rescues astrocytes from death induced by C2-ceramide and staurosporine

To obtain a first clue about the functional role of α-crystallin in astrocytes, we studied astrocytes over-expressing the αA-crystallin and αB-crystallin after transfection of αA-crystallin-MH and αB-crystallin-MH into these cells.

As shown in Fig. 3.11, after transfection, expression of αA-crystallin and αB-crystallin was increased (compare lanes 1 and 2 in Fig. 3.11 a and b). Only native α-crystallin is expressed in astrocytes with transfection of empty vector (lanes 1, native α-crystallin about 20 kDa). However, highly expressed α-crystallin (lanes 2, including native α-crystallin of 20 kDa and fusion protein of α-crystallin of 25 kDa) was detectable.

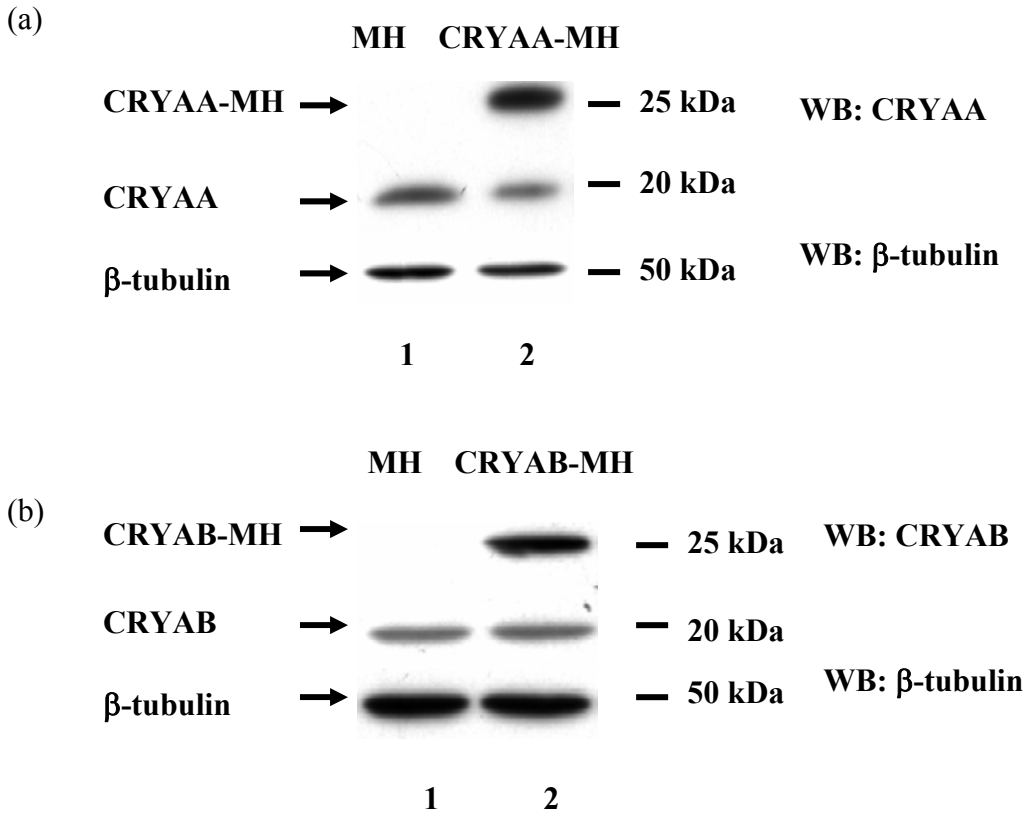

Figure 3.11 Overexpression of α-crystallin.

(a). Overexpression of αA-crystallin in astrocytes. (b). Overexpression of αB-crystallin in astrocytes. Astrocytes were transfected with empty vector (MH), αA-crystallin-MH (CRYAA-MH) or αB-crystallin-MH (CRYAB-MH), respectively. Overexpression of αA-crystallin or αB-crystallin in astrocytes was determined by western blot with anti-αA-crystallin antibody (a) or anti-αB-crystallin antibody (b). Native αA-crystallin (CRYAA) or αB-crystallin (CRYAB) was visible at 20 kDa. Overexpression of fusion proteins αA-crystallin-MH (CRYAA-MH) or αB-crystallin-MH (CRYAB-MH) was detectable at 25 kDa. Expression of internal β-tubulin was measured as a control for normalization of expression of α-crystallin. The experiments were repeated six times with comparable results.

Interestingly, overexpression of α-crystallin significantly inhibited the C2-ceramide- and staurosporine-induced cell death in astrocytes (Fig. 3.12 a). PAR-2-activating peptide can specifically activate PAR-2 in astrocytes (Wang et al., 2007b). In addition, activation of PAR-2 by the activating peptide significantly decreased C2-ceramide- or staurosporine-induced cell death in astrocytes (Fig. 3.10). Our data also show that activation of PAR-2 increases the protective effect in astrocytes over-expressing αA-crystallin, and but does not affect the protective effect in astrocytes over-expressing αB-crystallin (Fig. 3.12).

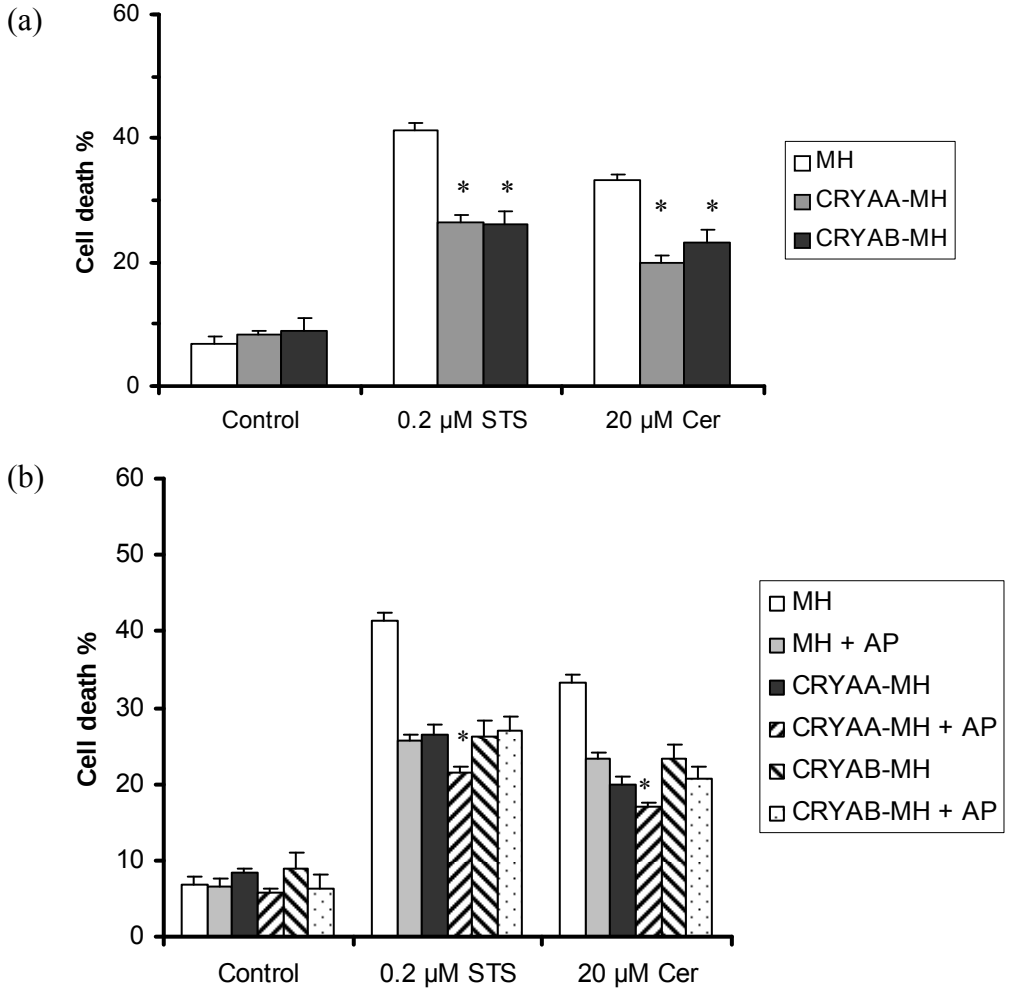

Figure 3.12 Cytoprotection of astrocytes by overexpression of α-crystallin (a) and the role of PAR-2 activation in cytoprotection by α-crystallin (b). Astrocytes were transfected like described previously (see Fig. 3.11). After 48 h, cultures with transfection were treated with 20 µM of C2-ceramide or with 0.2 µM of staurosporine for 18 h in the absence (a) or presence (b) of 500 µM of PAR-2 activating peptide for 18 h, respectively. Cell death was measured by LDH activity assay. The cell death data were obtained for each sample and the results were averaged. The values of cell death in astrocytes transfected with empty vector (MH), αA-crystallin (CRYAA-MH) or αB-crystallin (CRYAB-MH) under the treatment with staurosporine or C2-ceramide were compared in (a). The statistical significance level for difference in astrocytes death caused by C2-ceramide or staurosporine between empty vector (MH) transfection and αA-crystallin (CRYAA-MH) or αB-crystallin (CRYAB-MH) transfection is given as * $p<0.05$ in (a). In (b), the values of cell death in astrocytes overexpressing αA-crystallin (CRYAA-MH) or αB-crystallin (CRYAB-MH) under the treatment with staurosporine or C2-ceramide in the absence or presence of PAR-2-activating peptide (AP) were compared. The statistical significance level for difference in astrocytes death caused by C2-ceramide or staurosporine between PAR-2 AP treatment and without PAR-2 AP treatment is given as * $p<0.05$ in (b). As shown in (a), overexpression of α-crystallin significantly reduced C2-ceramide- and staurosporine-induced cell death in astrocytes. Interestingly, activation of PAR-2 has higher protective effect than in astrocytes overexpressing αA-crystallin, and has similar protective effect like in astrocytes overexpressing αB-crystallin (b). The experiments were repeated six times with comparable results.

3.5.2 Downregulation of α-crystallin increases astrocytes death induced by C2-ceramide and staurosporine

To confirm the protective effect of α-crystallin in astrocytes, we applied siRNA of αA-crystallin and αB-crystallin to knockdown expression of α-crystallin. Two siRNAs targeting different regions of each α-crystallin were applied for the experiments. After transfection with siRNA, expression of αA-crystallin and αB-crystallin was measured by real-time PCR and western blot. mRNA level of αA-crystallin (Fig. 3.13 a, CRYAA-1 and CRYAA-2) and αB-crystallin (Fig. 3.13 c, CRYAB-2 and CRYAB-3) was significantly decreased. Obviously, siRNA CRYAA-1 of αA-crystallin has more efficiency than siRNA CRYAA-2 of αA-crystallin. Similarily, siRNA CRYAB-3 of αB-crystallin has more efficiency than siRNA CRYAB-2 of αB-crystallin. Therefore, we used siRNA CRYAA-1 of αA-crystallin and siRNA CRYAB-3 of αB-crystallin in the following experiments. We next studied the effect of siRNA on downregulation of α-crystallin at protein level (Fig. 3.13 b and d). Transfection of siRNA of αA-crystallin (CRYAA-1) or αB-crystallin (CRYAB-3), protein level of αA-crystallin (Fig. 3.13 b) and αB-crystallin (Fig. 3.13 d) was apparently reduced. Furthermore, we observed the influence of downregulation by sRNA of αA-crystallin and αB-crystallin on astrocytes death caused by staurosporine and C2-ceramide. As shown in Fig. 3.14, staurosporine and C2-ceramide treatment significantly caused astrocytes death. Compared with control cells (primary culture), transfection with scrambled RNA has no effect on astrocytes death. However, when we knocked down α-crystallin by siRNA, decreased α-crystallin results in about 5% of increase in astrocytes death caused by C2-ceramide and staurosporine. It means that decreased expression of α-crystallin reduced the ability of astrocytes to resist against staurosporine and C2-ceramide. These results suggest that α-crystallin plays a protective role in astrocytes.

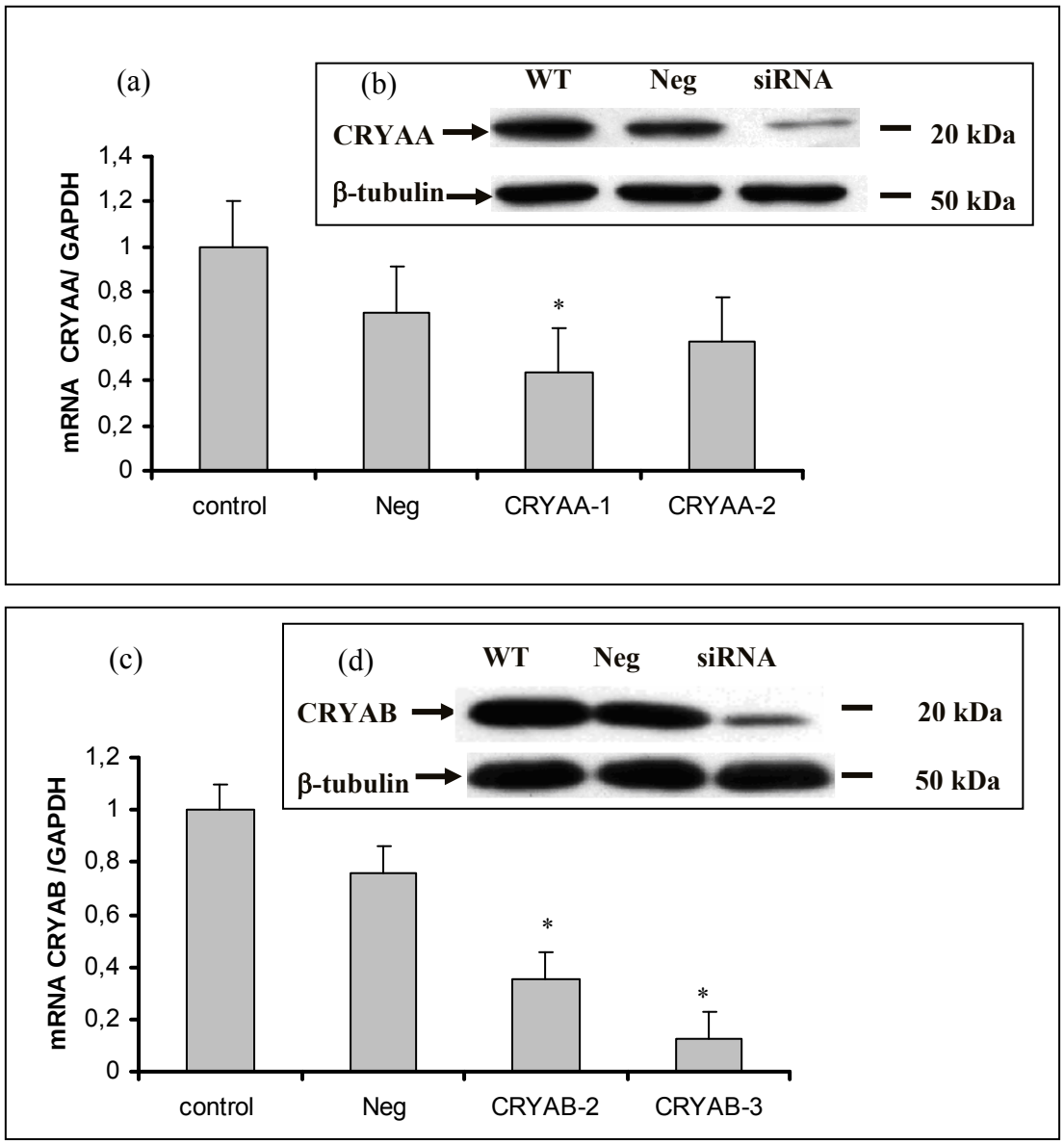

Figure 3.13 Downregulation of α-crystallin in astrocytes by siRNA of α-crystallin.

(a). Comparison of effect of different siRNA of αA-crystallin in astrocytes by real-time PCR. (b). Detection of effect of siRNA of αA-crystallin in astrocytes by western blot. (c) Comparison of effect of different siRNA of αB-crystallin in astrocytes by real-time PCR. (d). Detection of effect of siRNA of αB-crystallin in astrocytes by western blot. Astrocytes were transfected with scrambled RNA (Neg), siRNA of αA-crystallin or αB-crystallin, respectively. Efficiency of downregulation of either αA-crystallin (a) or αB-crystallin (c) by siRNAs in astrocytes was determined by real-time PCR. The mRNA signal for αA-crystallin and αB-crystallin was normalized to the GAPDH signal. The expression of the control (untreated) was set as 1. The PCR data were obtained for each sample and the results were averaged. The cumulative normalized data were presented as value ± SEM ($n \geq 3$). The statistical significance level for difference from control value is given as * $p<0.05$. The siRNAs of CRYAA-1 (for αA-crystallin) and (CRYAB-3 for αB-crystallin) showed good effect on knockdown of αA-crystallin or αB-crystallin. The effect of siRNAs of CRYAA-1 (for αA-crystallin) or CRYAB-3 (for αB-crystallin) on downregulation of αA-crystallin or αB-crystallin by αA-crystallin antibody (c) or anti-αB-crystallin antibody (d). The experiments were repeated six times with comparable results.

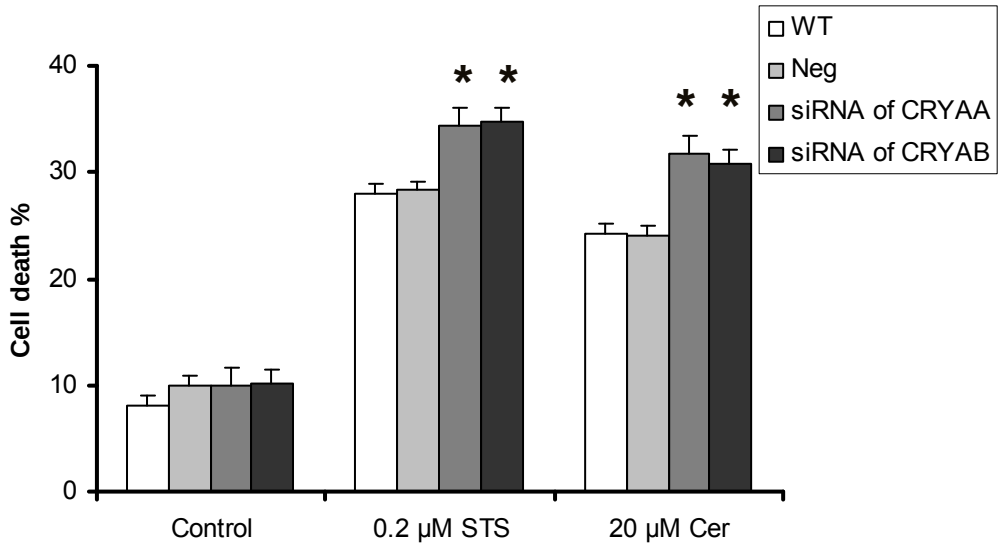

Figure 3.14 Increased astrocytes death by decreased expression of α-crystallin.

Astrocytes were transfected with scrambled RNA (Neg), siRNA of αA-crystallin (CRYAA-1) or αB-crystallin (CRYAB-3), respectively. After 48 h, cultures with transfection were treated with 20 μM of C2-ceramide or with 0.2 μM of staurosporine for 18 h, respectively. Cell death was measured by LDH activity assay. The cell death data were obtained for each sample and the results were averaged. The values of cell death caused by C2-ceramide or staurosporine in primary astrocytes (WT) and astrocytes transfected with siRNA of αA-crystallin or αB-crystallin were compared. The statistical significance level for difference in cell death caused by C2-ceramide or staurosporine between primary astrocytes (WT) and astrocytes transfected with siRNA of αA-crystallin or with siRNA of αB-crystallin is given as * $p<0.05$. Downregulation of α-crystallin significantly increased C2-ceramide- and staurosporine-induced cell death in astrocytes. The experiments were repeated five times with comparable results.

We also tried to knock down the expression of both αA-crystallin and αB-crystallin with siRNAs. As shown in Fig. 3.15 (a) and (b), with different combinations of siRNAs of αA-crystallin and αB-crystallin, expression of αA-crystallin and αB-crystallin are significantly deceased at the same time in astrocytes. We applied the combination of siRNA of αA-crystallin (CRYAA-1) and αB-crystallin (CRYAB-3) for cell death experiments. Increase of cell death was observed in astrocytes downregulating both αA-crystallin and αB-crystallin (Fig. 3.15 c) under C2-ceramide and staurosporine treatment. These results confirm the protective role of α-crystallin in astrocytes.

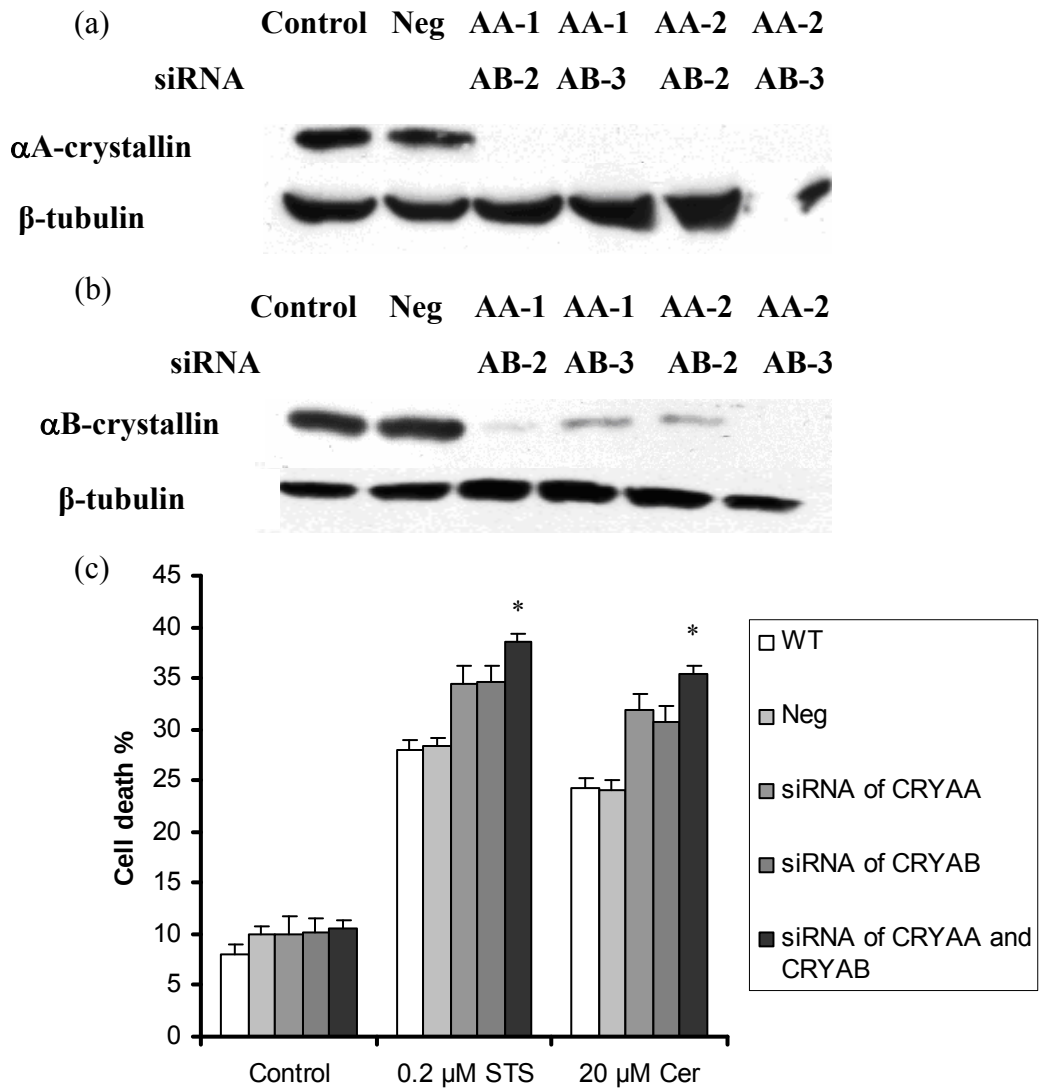

Figure 3.15 Astrocytes death under the downregulation of both αA-crystallin and αB-crystallin. (a). Detection of downregulation of αA-crystallin in astrocytes by different combinations of siRNAs of αA-crystallin and αB-crystallin using western blot. (b). Detection of downregulation of αB-crystallin in astrocytes by different combinations of siRNAs of αA-crystallin and αB-crystallin using western blot. (c). Increased astrocytes death by decreased expression of α-crystallin. siRNAs for both αA-crystallin (CRYAA-1) and αB-crystallin (CRYAB-3) were used for knockdown of expression of α-crystallin in (c). Astrocytes were transfected with scrambled RNA (Neg), siRNAs of αA-crystallin and αB-crystallin, respectively. Efficiency of downregulation of either αA-crystallin (a) or αB-crystallin (b) by siRNAs in astrocytes was determined using western blot. After 48 h, astrocytes with transfection were treated with 20 μM of C2-ceramide or with 0.2 μM of staurosporine for 18 h, respectively. Cell death was measured by LDH activity assay. The cell death data were obtained for each sample and the results were averaged. The values of cell death in astrocytes transfected with siRNA of αA-crystallin or αB-crystallin and with siRNAs of both αA-crystallin and αB-crystallin under the treatment with staurosporine or C2-ceramide were compared. The statistical significance level for difference in cell death caused by C2-ceramide or staurosprine between astrocytes transfected with siRNA of αA-crystallin or αB-crystallin and with siRNAs of both αA-crystallin and αB-crystallin is given as * $p<0.05$. Downregulation of both αA-crystallin and αB-crystallin significantly increased C2-ceramide- and staurosporine-induced cell death in astrocytes. The experiments were repeated six times with comparable results.

3.6 The mechanism of cytoprotection by PAR-2 and α-crystallin

3.6.1 PAR-2 activation activates p38, ERK and JNK MAP kinases

PAR-2 has dual role in different situations either protective or toxic (Coelho et al., 2003; Steinhoff et al., 2005; Wang and Reiser, 2003b). Our current data demonstrated that PAR-2 activation rescued cells from C2-ceramide- and staurosporine-induced cell death in astrocytes (see Fig. 3.10). These evidences suggest that PAR-2 activation might protect cells from damage in brain. PAR-2 mediates activation of mitogen-activated protein kinase family, like extracellular signal regulated kinase, c-Jun N-terminal kinase and p38 MAPK and nuclear factor kappa B in a cell-type specific manner. Evidence suggests that MAP kinases play a key role in PAR-2-mediated cellular responses. We speculate that MAP kinases might be involved in protective processes in astrocytes.

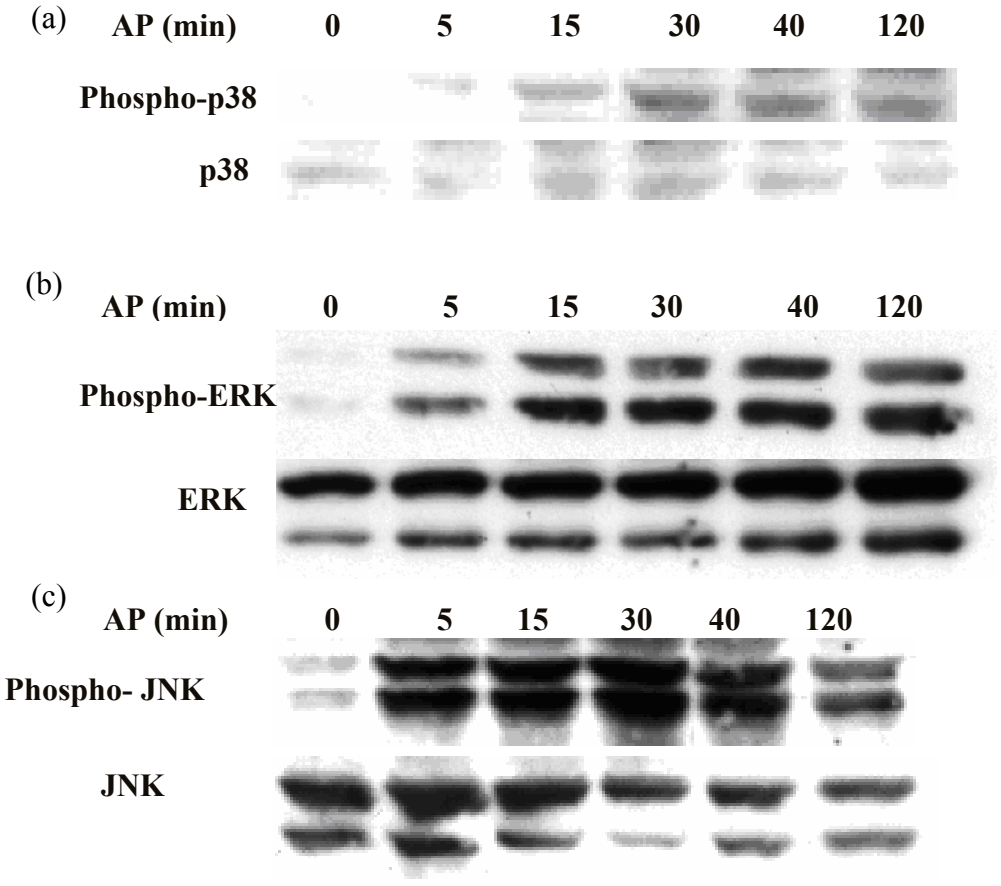

Figure 3.16 Activation of p38, ERK and JNK by PAR-2 activating peptide in astrocytes.

Astrocytes were treated with PAR-2-activating peptide (AP, 500 μM) for 5 min, 15 min, 30 min, 40 min and 120 min. Activation of p38, ERK and JNK by PAR-2 activating peptide in astrocytes was determined by western blot with anti-phospho-p38 antibody, anti-phospho-ERK andtibody and anti-phospho-JNK antibody. Obviously, all the MAP kinases of p38, ERK and JNK were activated by PAR-2 activation. The experiments were repeated three times with comparable results.

To know whether all MAP kinases (p38, ERK and JNK) are activated in astrocytes, we measured activated states of p38, ERK and JNK by western blot. We clearly found the activation of p38 (Fig. 3.16 a), ERK (Fig. 3.16 b) and JNK (Fig. 3.16 c).

3.6.2 Application of inhibitors of p38, ERK and JNK reduces cytoprotection by PAR-2 activation in astrocytes

To explore the mechanism of activation of PAR-2 and α-crystallin in astrocytes, we applied specific inhibitors of MAP kinases to see whether and which MAP kinases mediate the protection in astrocytes. As shown in Fig. 3.17, specific inhibitors of p38 (SB203580), ERK (PD98059) and JNK (SP600125) block the protection of astrocytes by PAR-2 activation. Theses results sugguest that p38, ERK and JNK modulate the protection of astrocytes by PAR-2. Previous data in our lab indicated that PAR-2 rescued astrocytes from C2-ceramide-induced death in short term (6 h) by JNK-mediated chemokine secretion. These evidences indicate that all MAP kinases (p38, ERK and JNK) participate in the protective process by PAR-2 in astrocytes.

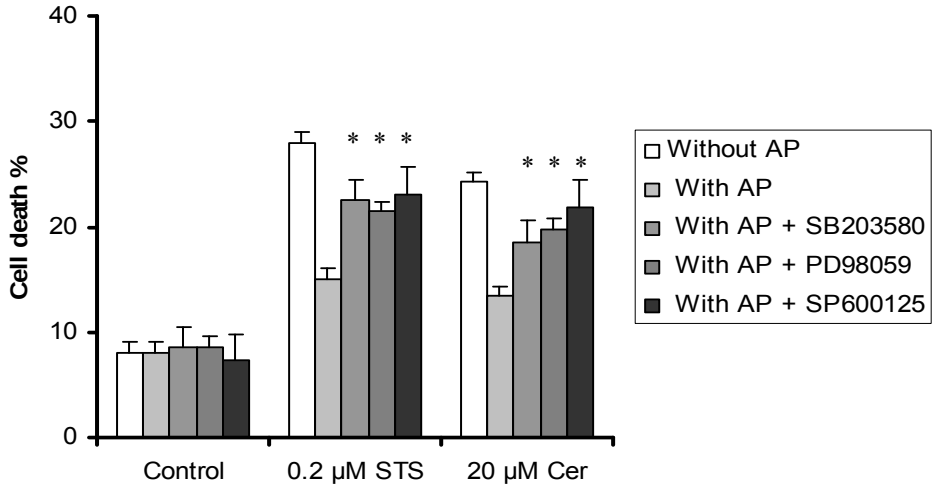

Figure 3.17 Inhibitors of p38, ERK and JNK block the protection of astrocytes by PAR-2 activation. Astrocytes were treated with C2-ceramide or staurosporine in the absence or presence of PAR-2-activating peptide (AP, 500 μM) or 10 μM of inhibitor of p38 (SB203580) and 100 μM of inhibitor of ERK (PD98059) or 20 μM of inhibitor of JNK (SP600125) for 18 h (additions were indicated in the figure). Cell death was measured by LDH assay. The cell death data were obtained for each sample and the results were averaged. The values of cell death caused by C2-ceramide or staurosporine in astrocytes under the treatment with PAR-2-activating peptide in the absence or presence of inhibitors of p38, ERK and JNK were compared. The statistical significance level for difference in astrocytes death caused by C2-ceramide or staurosporine in the presence of PAR-2-activating peptide between application and no application of inhibitors of p38, ERK and JNK is given as * $p<0.05$. Protection of astrocytes by PAR-2 activation was significantly reduced by addition of inhibitors of p38, ERK and JNK. The experiments were repeated six times with comparable results.

3.6.3 Application of inhibitors of p38 and ERK reduces cytoprotection caused by overexpression of α-crystallin

αA-crystallin and αB-crystallin are chaperones, which prevent the precipitation of denatured proteins to increase cellular tolerance to stress. Studies indicate that α-crystallin especially αB-crystallin are protective in lens and heart. Evidences reveal that αB-crystallin plays an important role in neurodegenerative diseases, such as Alzheimer, Parkinson and amyotrophic lateral sclerosis. For example, αB-crystallin is upregulated in Alzheimer's brains and interacts with amyloid-β, thereby affecting amyloid production in brain. Our results showed that αA-crystallin and αB-crystallin are protective in astrocytes (see Fig. 3.12, Fig. 3.14 and Fig. 3.15).

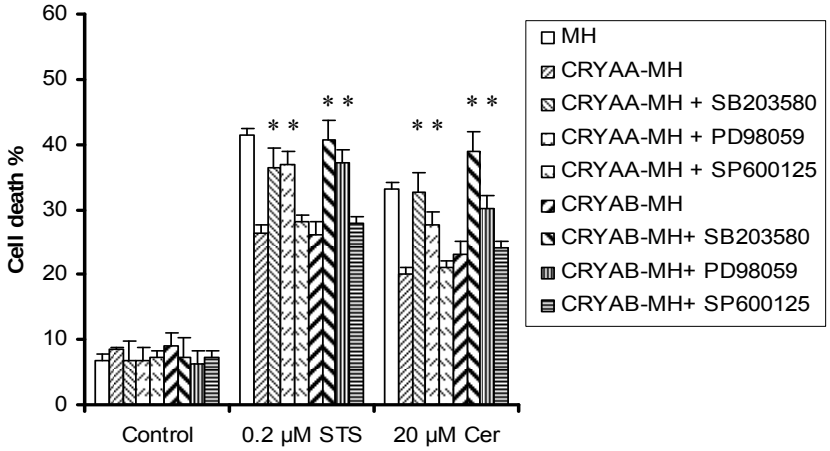

Figure 3.18 Inhibitors of p38 and ERK block the protection of astrocytes by overexpression of α-crystallin. Astrocytes were transfected with either pcDNA3.1 (MH) or CRYAA-MH. After 48 h, astrocytes with transfection were treated with C2-ceramide or staurosporine in the absence or presence of inhibitors of p38 (SB203580, 10 μM) or ERK (PD98059, 100 μM) or JNK (SP600125, 20 μM) for 18 h. Cell death was measured by LDH activity assay. The cell death data were obtained for each sample and the results were averaged. The values of cell death caused by C2-ceramide or staurosporine in astrocytes overexpressing αA-crystallin or αB-crystallin in the absence or presence of inhibitors of p38, ERK and JNK were compared. The statistical significance level for difference in cell death caused by C2-ceramide or staurosporine in astrocytes overexpressing αA-crystallin or αB-crystallin between application and no application of inhibitors of p38, ERK and JNK is given as * $p<0.05$. Protection of astrocytes by overexpression of α-crystallin was significantly reduced by addition of inhibitors of both p38 and ERK. The experiments were repeated six times with comparable results.

Further experiments with inhibitors of MAP kinases proved that inhibition of p38 and ERK significantly reduced the protection by αA-crystallin and αB-crystallin (Fig. 3.18). However, specific inhibitor of JNK (SP600125) does not have any effect on protection by αA-crystallin and αB-crystallin. These results suggest that p38 and ERK regulate the protective processes by αA-crystallin and αB-crystallin. As mediators, p38 and ERK modulate the

protective process by both PAR-2 and α-crystallin. It seems that PAR-2 and α-crystallin are functionally connected via p38 and ERK.

3.7 The functional connection of PAR-2 with α-crystallin

As indicated above, PAR-2 and α-crystallin play a protective role in astrocytes. MAP kinases are involved in protection by PAR-2 and α-crystallin. PAR-2 activation can evoke all MAP kinases. Highly expressed α-crystallin protects astrocytes. Accumulating evidences also suggest that phosphorylation of αB-crystallin is mediated by p38 and ERK (Hoover et al., 2000; Webster, 2003). Phoshphorylation state of α-crystallin contributes to the protective activity of α-crystallin (Ito et al., 2001; Morrison et al., 2003). It seems that PAR-2 and α-crystallin are functionally connected in cytoprotection in astrocytes. We proposed that PAR-2 activation could regulate expression of α-crystallin or phosphorylation states of α-crystallin to protect astrocytes.

3.7.1 PAR-2 activation regulates expression of α-crystallin

Firstly, we determined the mRNA level of α-crystallin under the PAR-2 activation by real-time PCR. Increased mRNA level of αA-crystallin was observed after short-term (1 h) and long-term stimulation (18 h, Fig. 3.19 a). Interestingly, mRNA level of αB-crystallin was significantly decreased (from 1 h to 18 h, Fig. 3.19 b). αA-crystallin and αB-crystallin behave differently. The mechanism is unknown.

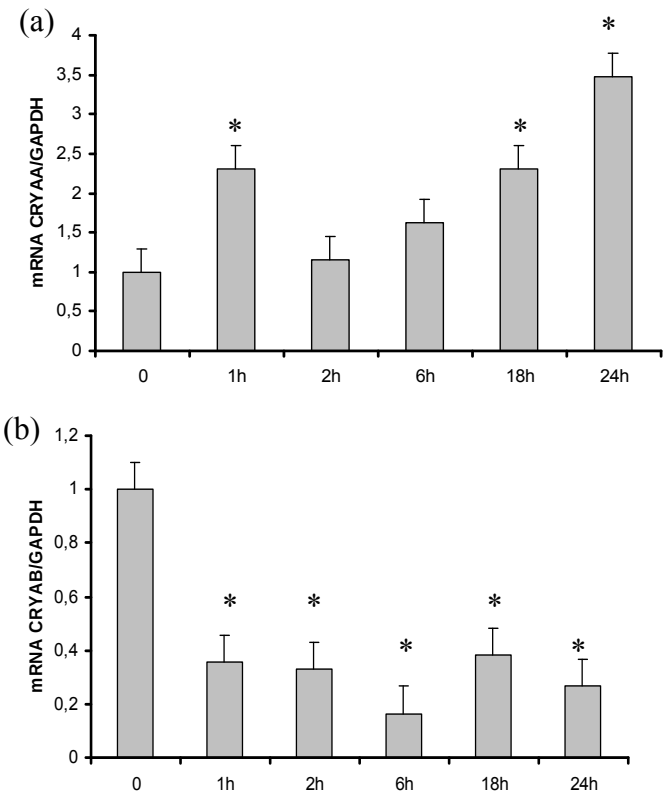

Figure 3.19 PAR-2 activation modulates expression of αA-crystallin (a) and αB-crystallin (b) at mRNA level. Astrocytes were treated with PAR-2-activating peptide (500 μM) for 1 h, 2 h, 6 h, 18 h and 24 h. mRNA level of α-crystallin was measured by real-time PCR. The mRNA signal for α-crystallin was normalized to the GAPDH signal. The expression of the control (untreated) was set as 1. The PCR data were obtained for each sample and the results were averaged. The cumulative normalized data are presented as value ± SEM ($n \geq 3$). The statistical significance level for difference from control value (time 0) is given as * $p<0.05$. As shown in (a), mRNA level of αA-crystallin is increased at time point 1 h, 18 h and 24 h. In (b), mRNA level of αB-crystallin is decreased from time point 1 h to 24 h. The experiments were repeated six times with comparable results.

To see whether the protein level of α-crystallin is changed by PAR-2 activation, western blot was performed. As shown in Fig. 20 (a) and (b), expression of αA-crystallin was increased from 2 h by PAR-2 activation. Regarding the results of mRNA in Fig. 3.19 and protein profile in Fig. 3.20, it seems that there is a mechanism of rapidly regulating the expression of αA-crystallin in response to stimulation in astrocytes. Moreover, αA-crystallin can be accumulated in astrocytes. However, there is no change of αB-crystallin under PAR-2 activation at protein level (Fig. 20 c and d).

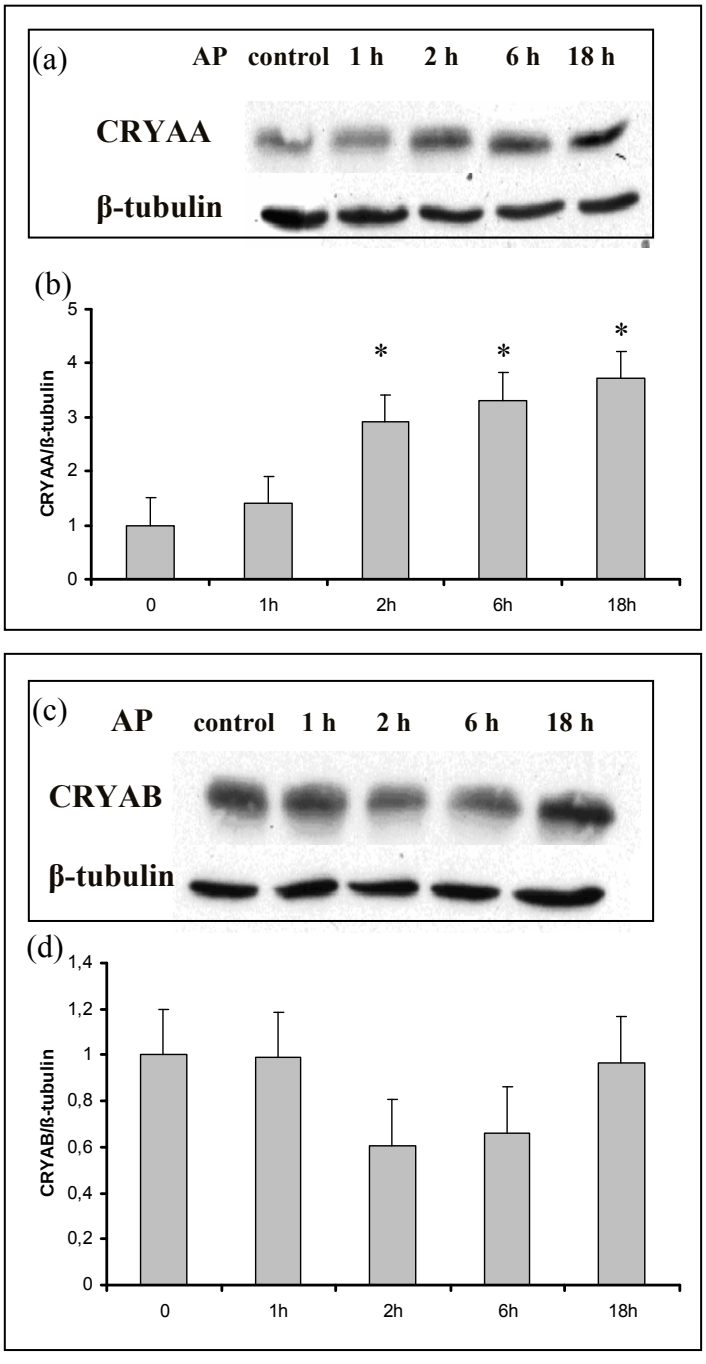

Figure 3.20 PAR-2 activation modulates expression of αA-crystallin (a) and (b), and do not affect expression of αB-crystallin (c) and (d) at protein level. Astrocytes were treated with PAR-2-activating peptide (AP, 500 μM) for 1h, 2h, 6 h and 18 h. Protein level of α-crystallin at different time point was measured by western blot in (a) and (c). Quantification of protein level was shown in (b) for αA-crystallin and (d) for αB-crystallin. The protein level for αA-crystallin and αB-crystallin was normalized to the β-tubulin level. The expression of the control (untreated) was set as 1. The quantification data were obtained for each sample and the results were averaged. The cumulative normalized data were presented as value ± SEM ($n \geq 3$). The statistical significance level for difference from control value (time 0) is given as * $p<0.05$. As shown in (b), protein level of αA-crystallin increased from time point 2 h to 18 h. However, the protein level of αB-crystallin was not changed by PAR-2 activation. The experiments were repeated four times with comparable results.

3.7.2 PAR-2 activation increases phosphorylated Ser59-αB-crystallin level

As mentioned above, we also proposed that PAR-2 activation modulates phosphorylation of α-crystallin. We measured the phosphorylated Ser59-αB-crystallin level under PAR-2 activation by western blot. As indicated in Fig. 3.21, phosphorylated Ser59-αB-crystallin level is increased up to 2.3 fold under the PAR-2 activation by AP. These experiments demonstrated that phosphorylated Ser59-αB-crystallin is modulated by PAR-2 activation. Treatment with C2-ceramide and staurosporine does not induce increase in phosphorylated Ser59-αB-crystallin. Whether PAR-2 activation also modulates phosphorylation of αA-crystallin is not clear. There is no available antibody of phosphorylated αA-crystallin.

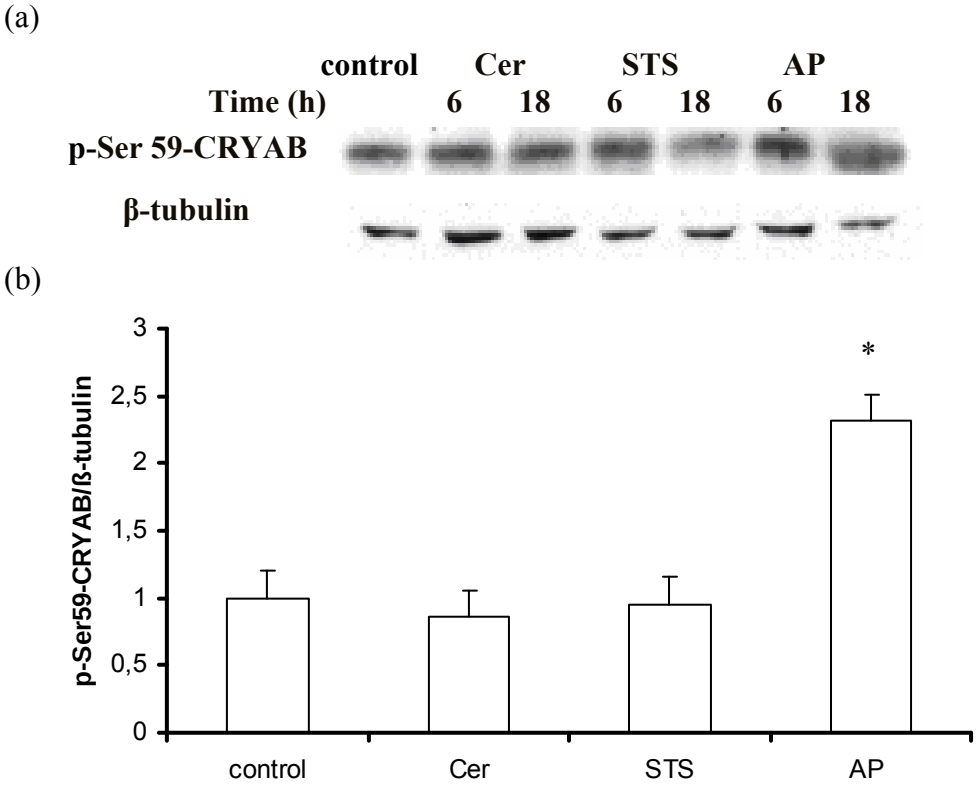

Figure 3.21 PAR-2 activation increases phosphorylated Ser59-αB-crystallin level.

Astrocytes were treated with C2-ceramide, staurosporine or PAR-2-activating peptide (AP, 500 μM) for 6 h and 18 h. Protein level of phosphorylated Ser59-αB-crystallin was measured by western blot with anti-phospho-Ser59-αB-crystallin antibody in (a). Quantification of protein level of αB-crystallin was analyzed in (b). The protein level for phosphorylated αB-crystallin at Ser 59 was normalized to the β-tubulin level. The expression of the control cells (untreated) was set as 1. The quantification data were obtained for each sample and the results were averaged. The cumulative normalized data are presented as value ± SEM ($n \geq 3$). The statistical significance level for difference from control value is given as * $p<0.05$. At time point 18h, expression of phosphorylated Ser59-αB-crystallin level significantly increased up to about 2.3 fold. The experiments were repeated three times with comparable results.

3.7.3 Phosphorylation of α-crystallin contributes to protective activity in astrocytes

3.7.3.1 Generation of α-crystallin mutants

Phosphorylation of α-crystallin is an important issue for understanding the role of α-crystallin. Multiple stimuli induce phosphorylation of α-crystallin. The change of phosphorylation state of α-crystallin results in the translocation, decreased or increased chaperone activity and cytoprotection. Up to now, several phosphorylation sites of αA-crystallin and αB-crystallin have been identified. αA-crystallin can be phosphorylated at two sites, Ser122 and Ser148. αB-crystallin can be phosphorylated at three different sites, Ser19, Ser45 and Ser59. Our data shown above indicate that PAR-2 activation is protective in astrocytes. p38 and ERK MAP kinases are activated and increasingly phosphorylated Ser59-αB-crystallin occurs during protection by PAR-2 activation. Previous studies from other groups suggest that phosphorylation of Ser59-αB-crystallin is mediated by p38 MAP kinase. This suggests that phosphorylation of α-crystallin could be required in the protective process by PAR-2. However, it is unknown which sites are involved in cytoprotection. We constructed mutants of α-crystallin to mimic lack of phosphorylation (Ser is mutated to Ala) or pseudophosphorylation (Ser is mutated to Glu) for figuring out which sites are essential for protection (see table 3.1). All the mutants were cloned into pcDNA 3.1 with myc-his tag.

Table 3.1 mutants of α-crystallin (S: Ser, A: Ala, E: Glu)

	Unphosphorylation	**Pseudophosphorylation**
αA-crystallin	**S122A, S148A, S122A/S148A**	**S122E, S148E, S122E/S148E**
αB-crystallin	**S19A, S45A, S59A** **S19A/S45A, S19A/S59A, S45A/S59A** **S19A/S45A/S59A**	**S19E, S45E, S59E** **S19E/S45E, S19E/S59E,** **S45ES/59E, S19E/S45E/S59E**

3.7.3.2 Mimicking of phosphorylation/unphosphorylation of α-crystallin

To look for the important phosphorylation sites of α-crystallin for protection, mutants of α-crystallin were transfected into astrocytes. Cell death caused by C2-ceramide and staurosporine in astrocytes with transfection was measured.

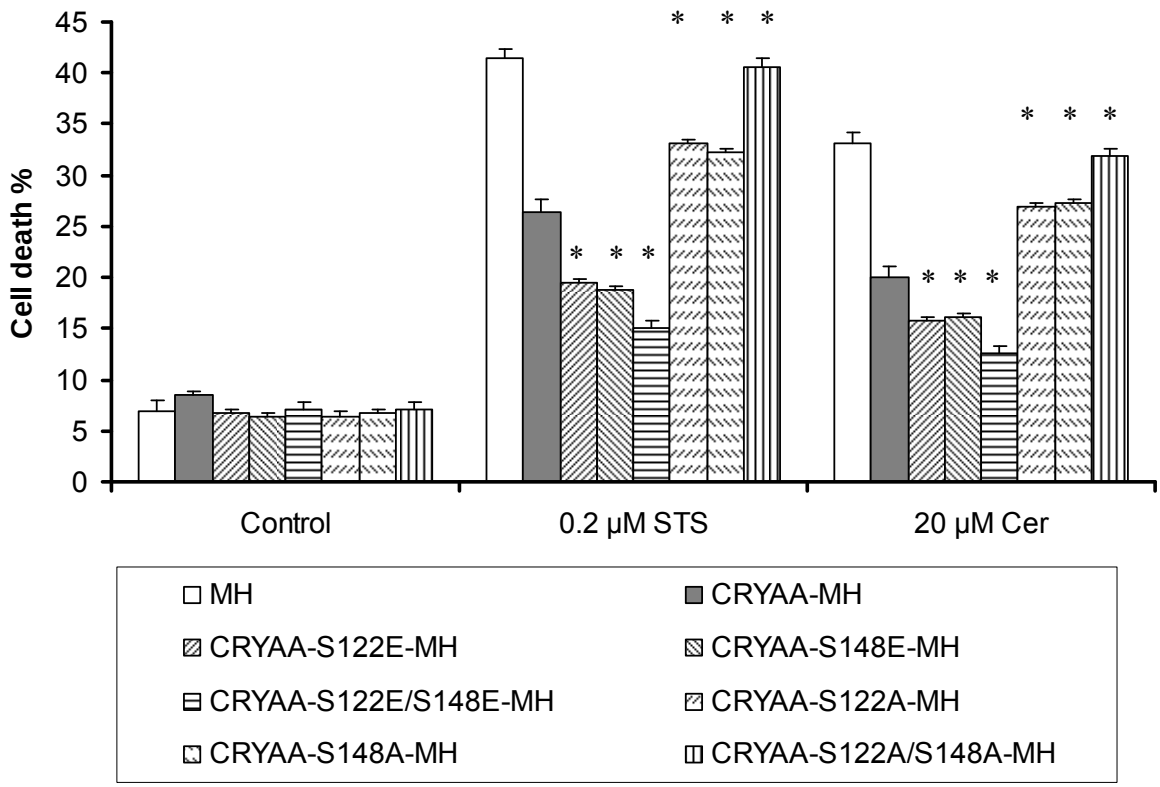

Figure 3.22 Ser122 and Ser148 of αA-crystallin are required for protection.

Astrocytes were transfected with empty vector (MH), αA-crystallin-MH (CRYAA-MH) or mutants of αA-crystallin-MH (as indicated in the figure), respectively. After 48 h, cultures with transfection were treated with 20 μM of C2-ceramide or with 0.2 μM of staurosporine for 18 h, respectively. Cell death was measured by LDH activity assay. The cell death data were obtained for each sample and the results were averaged. The values of cell death in astrocytes transfected with full-length of αA-crystallin were compared with that in astrocytes transfected with mutants of αA-crystallin under staurosporine or C2-ceramide treatment. The statistical significance level for difference in cell death caused by C2-ceramide or staurosporine in astrocytes between full-length of αA-crystallin transfection and mutants of αA-crystallin transfection is given as * $p<0.05$. As shown in figure, overexpression of mutants CRYAA-S122E/S148E, CRYAA-S122E and CRYAA-S148E rescues more astrocytes than CRYAA-MH. However, overexpression of mutants CRYAA-S122A and CRYAA-S148A has lower protective activity than CRYAA-MH. With overexpression of mutants CRYAA-S122A/S148A cytoprotection is completely lost. This suggests that phosphorylation of αA-crystallin at Ser122 and Ser148 is required for cytoprotection. The experiments were repeated six times with comparable results.

As shown in Fig. 3.22, overexpression of mutants CRYAA-S122E/S148E, CRYAA-S122E and CRYAA-S148E rescues more astrocytes than CRYAA-MH. However, overexpression of mutants CRYAA-S122A and CRYAA-S148A has low protective activity than CRYAA-MH. Overexpression of mutants CRYAA-S122A/S148A completely loses cytoprotection. These data suggest that the phosphorylation of Ser122 and Ser148 is required for cytoprotection. The analysis of data was shown in table 4.1.

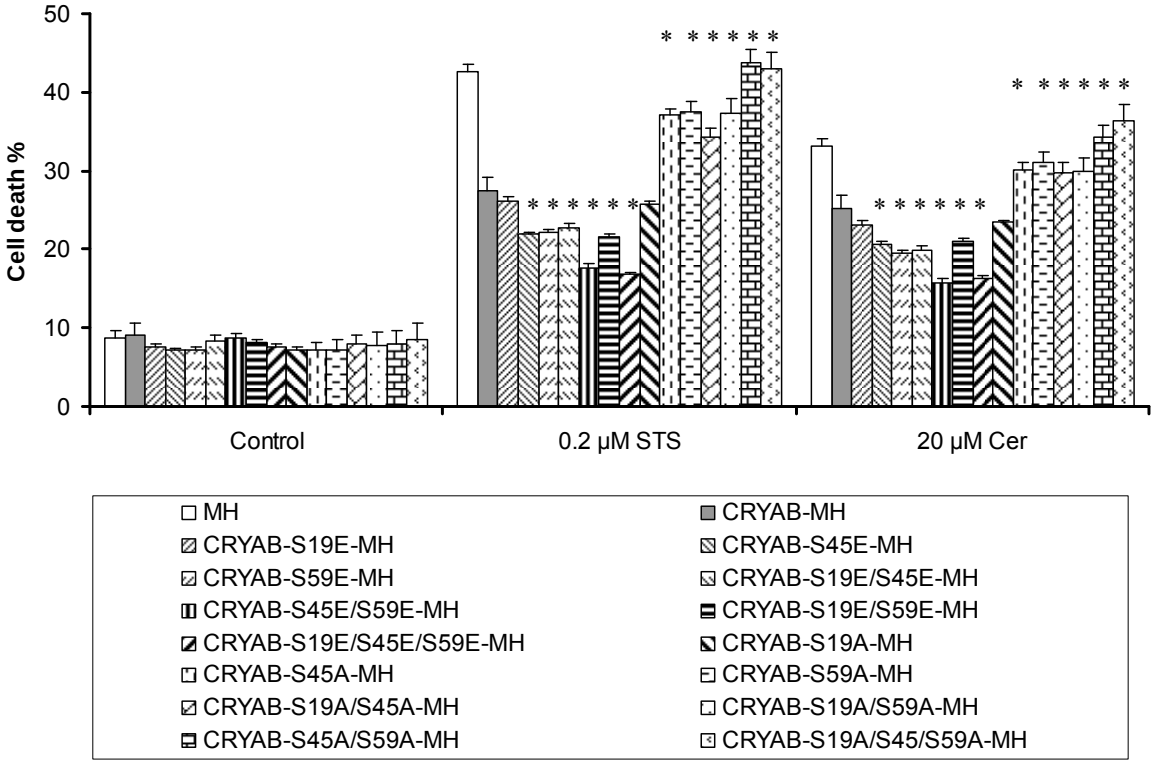

Figure 3.23 Ser45 and Ser59 of αB-crystallin are required for protection.
Astrocytes were transfected with empty vector (MH), αB-crystallin-MH (CRYAB-MH) or mutants of αB-crystallin-MH (as indicated in the figure), respectively. After 48 h, cultures with transfection were treated with 20 μM of C2-ceramide or with 0.2 μM of staurosporine for 18 h, respectively. Cell death was measured by LDH activity assay. The cell death data were obtained for each sample and the results were averaged. The values of cell death in astrocytes transfected with full-length of αB-crystallin were compared with that in astrocytes transfected with mutants of αA-crystallin under staurosporine or C2-ceramide treatment. The statistical significance level for difference in cell death caused by C2-ceramide or staurosporine in astrocytes between full-length of αB-crystallin transfection and mutants of αB-crystallin transfection is given as * $p<0.05$. As shown in figure, overexpression of mutants CRYAB-S19E/S45E/59E, CRYAB-S19E/S45E, CRYAB-S45E/S59E, CRYAB-S19E/S59E, CRYAB-S45E and CRYAB-S59E rescues more astrocytes than CRYAB-MH. Overexpression of mutants CRYAB-S45A, CRYAB-S59A, CRYAB-S19A/S45A and CRYAB-S19A/S59A has lower protective activity than CRYAB-MH. Overexpression of mutants CRYAB-S45A/S59A and CRYAB-S19A/S45A/S59A completely loses cytoprotection. Interestingly, Overexpression of mutants CRYAB-S19E or CRYAB-S19A has similar protective activity as CRYAB-MH. These results suggest that Ser19 of αB-crystallin does not contribute to cytoprotection. Phosphorylation sites of αB-crystallin at Ser45 and Ser59 are involved in protection. The experiments were repeated six times with comparable results.

For αB-crystallin, as shown in Fig. 3.23, overexpression of mutants CRYAB-S45E, CRYAB-S59E, CRYAB-S19E/S45E, CRYAB-S45E/S59E, CRYAB-S19E/S59E and CRYAB-S19E/S45E/S59E rescues significantly more astrocytes than CRYAB-MH. Overexpression of mutants CRYAB-S45A, CRYAB-S59A, CRYAB-S19A/S45A and CRYAB-S19A/S59A has low protective activity than CRYAB-MH. Overexpression of mutants CRYAB-S45A/S59A and CRYAB-S19A/S45A/S59A completely loses cytoprotection. Importantly, overexpression of mutants CRYAB-S19E or CRYAB-S19A has similar protective activity as CRYAB-MH. These results indicate that Ser19 of αB-crystallin does not contribute to cytoprotection. Ser45 and Ser59 of αB-crystallin are required for protection. The analysis of data was shown in table 4.2.

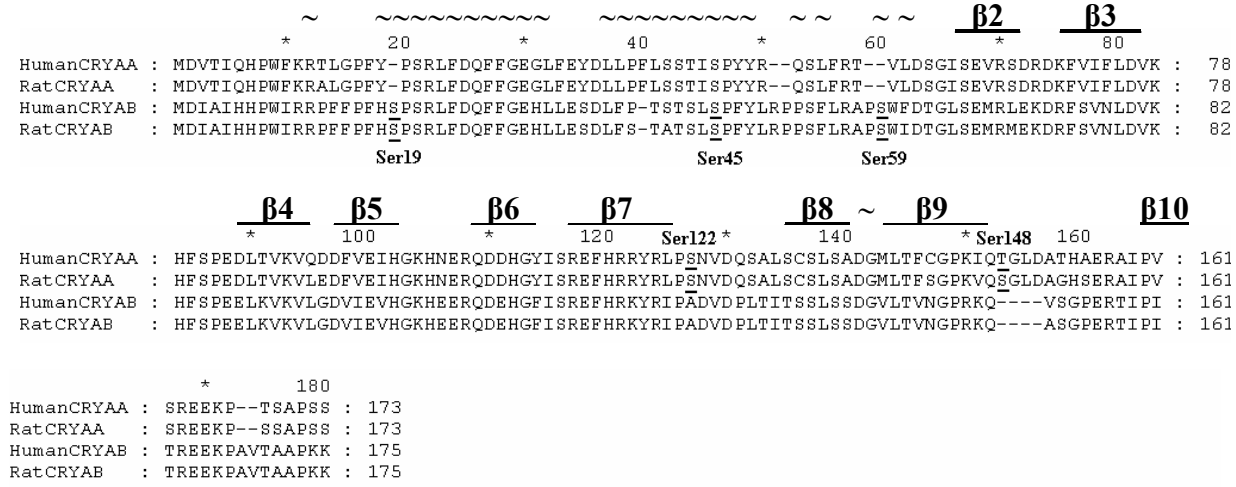

Figure 3.24 The important phosphorylation sites of α-crystallin for protection.

The phosphorylation sites of αA-crystallin at Ser122 and Ser148 and αB-crystallin at Ser45 and Ser59 are required for protection in astrocytes. Ser19 of αB-crystallin does not contribute to protective activity. ~ represents helix and — represents β strand.

3.8. Extracellular expression of α-crystallin and its function

3.8.1 Expression of α-crystallin in bacteria and purification

Previous research indicated that α-crystallin is accumulated in the brain in neurodegenerative diseases. α-crystallin may participate in the formation of plaques in Alzheimer's disease. Phosphorylated αB-crystallin at Ser59 is found at high levels in the brain of patients with Alexander's disease. These findings suggest that α-crystallin functions also in the extracellular environments. To explore the role α-crystallin in the extracellular medium, we cloned α-crystallin into intein vectors PTXB1 and PTYB11.

The fusion protein α-crystallin-intein was transformed and expressed in E.coli ER2566 induced by IPTG. As indicated in Fig. 3.25 (a) and (b), α-crystallin with PTXB1 vector was well expressed in E.coli ER2566 (Fig. 3.25 lanes 3 in a and b). With the pTXB1, recombinant α-crystallin-intein protein possesses a chitin binding domain and a reactive C-terminal thioester. The chitin binding domain can be used for the affinity purification of the fusion protein on a chitin resin. Using thiol reagents such as dithiothreitol (DTT), the target protein is released from the intein tag. Therefore, the purification of α-crystallin can be performed without the use of proteases to remove the affinity tag. To isolate α-crystallin, α-crystallin-intein ER2566 cells were disrupted by sonication. The crude cell extract was centrifuged and the clarified supernatant was loaded on the chitin column. After washing with 20 bed volumes of the column buffer, cleavage buffer containing 50 mM DTT was applied to release the target protein. Following on-column cleavage, the target protein was eluted from the column using different buffers in the absence or presence of urea (Fig. 3.26 a and b). α-Crystallin remaining on the beads or in the elution fractions was measured by coomassie stain. Unfortunately, pure α-crystallin can not be eluted from chitin beads under the undenatured conditions (Fig. 3.26 a, lane 2). Therefore, we applied urea (Fig. 3.26 a, lanes 4 and 6), ethanol (Fig. 3.26 a, lane 8) and isoproponal (Fig. 3.26 a, lane 10) to elute pure α-crystallin. As shown in Fig. 3.26 (a), pure α-crystallin can't be eluted using buffer containing 2 M of urea (Fig. 3.26 a, lane 7). To get more pure α-crystallin, we tried different elution times and concentrations of urea. As shown in Fig. 3.26 (b), purified α-crystallin was obtained with washing buffer containing 4 M or 6 M of urea with less recombinant protein α-crystallin-intein. Non-detergent sulfobetaines (NDSB) are useful chemicals in purifying proteins under the undenatured conditions. To purify pure α-crystallin, undenaturing detergent NDSB 256 was applied in the experiments. Pure α-crystallin was eluted with buffer containing 0.5 M-1 M of NDSB 256 (Fig. 3.27).

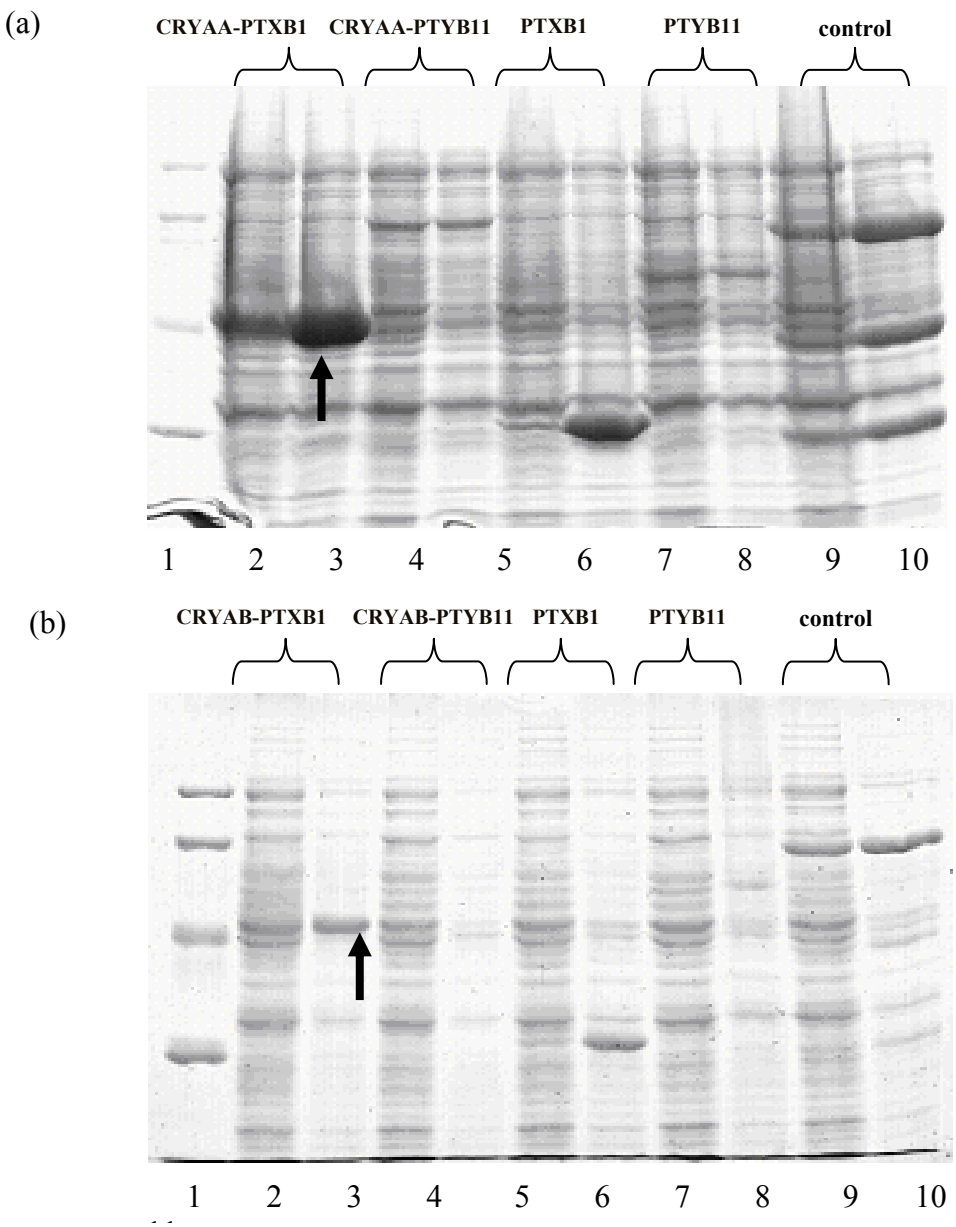

Figure 3.25 Expression of α-crystallin in E. coli ER2566.

αA-crystallin and αB-crystallin genes were cloned into PTXB1 and PTYB11 vectors. E. coli ER2566 was transformed with empty vectors of PTXB1 or PTYB11 or with recombinant plasmids of CRYAA-PTXB1, CRYAA-PTYB11, CRYAB-PTXB1 or CRYAB-PTYB11 as described in method 2.2.4. Incubated the cultures in the shaker at 37°C until the OD_{600} reached 0.5. Then, IPTG was added to a final concentration of 0.4 mM for induction of protein expression. After 2 hours' incubation, we took 40 µl of cultures and determined the proteins with 12.5 % SDS-PAGE gel and coomassie stain. The culture of ER2566 without transformation was used as control. Lanes 1 show the protein mass marker LWM. Lanes 2, 4, 6, 8 and 10 correspond to proteins in different cultures (as indicated in the figure) without IPTG induction. Lanes 3, 5, 7, 9 and 11 correspond to proteins in different cultures (as indicated in the figure) with IPTG induction. As shown in the figure, αA-crystallin (as pointed out with arrow in a, lane 3) and αB-crystallin (as pointed out with arrow in b, lane 3) can be strongly expressed in ER2566 with vector PTXB1. The experiments were repeated five times with comparable results.

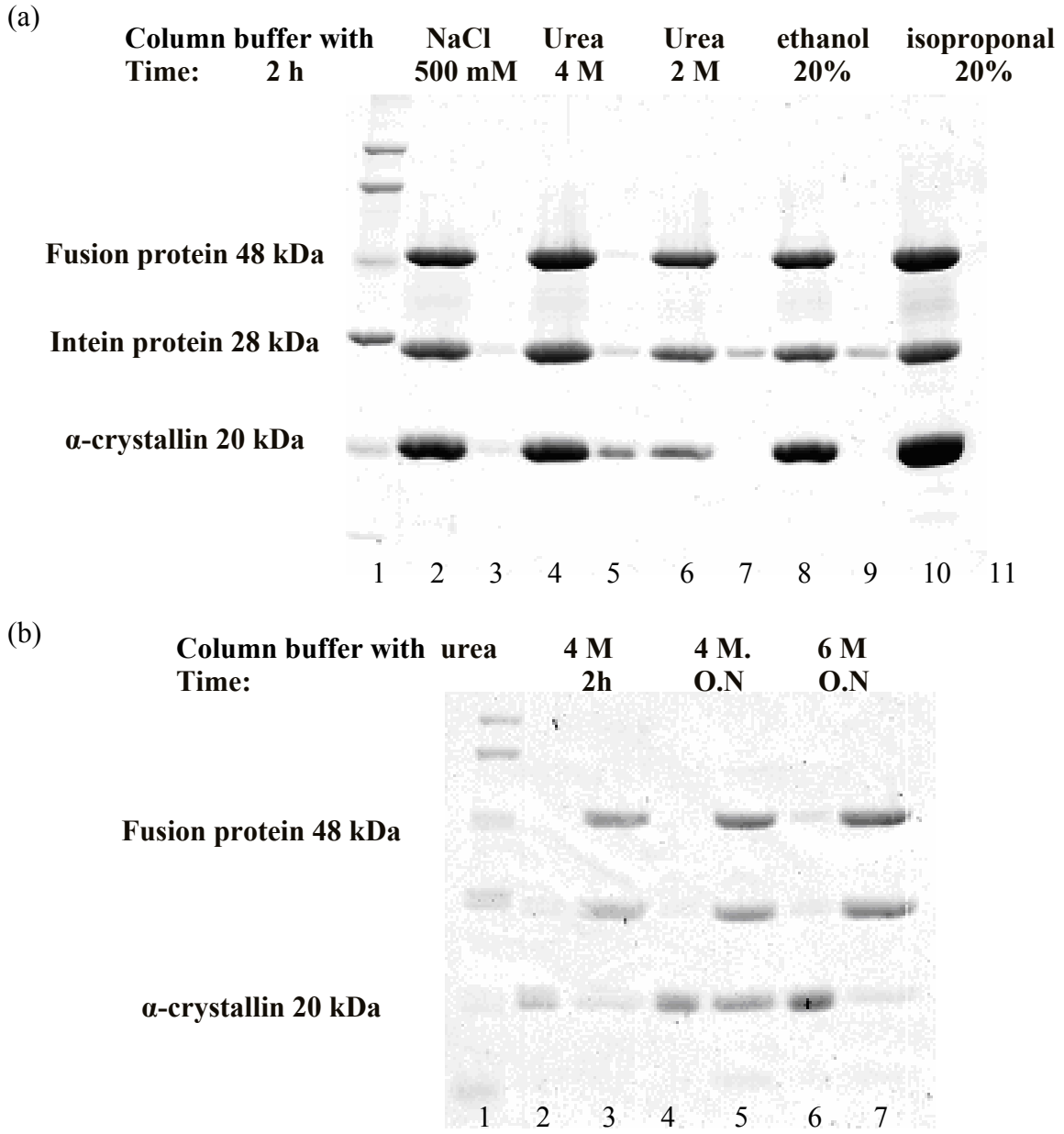

Figure 3.26 Purification of α-crystallin with different elution buffers.

CRYAA-PTXB1 and CRYAB-PTXB1 were expressed in ER2566 and purified with chitin beads according to the protocol described in method 2.2.4 and 2.2.11. Different elution buffers (as indicated in the figure) were used to elute pure αA-crystallin and αB-crystallin from chitin beads. Elution time was also changed to optimize the purification conditions. The protein level in the elution fractions and chitin beads was analyzed by coomassie stain. Lanes 1 show the protein mass marker LWM. Lanes 2, 4, 6, 8 and 10 in (a) and Lanes 3, 5 and 7 in (b) correspond to proteins remaining on the chitin beads. Lanes 3, 5, 7, 9 and 11 in (a) and Lanes 2, 4 and 6 in (b) correspond to proteins in the elution fractions. Obviously, high concentration of urea (more than 4 M, lanes 4 and 6 in b) was helpful to get pure α-crystallin under denaturing conditions. The experiments were repeated five times with comparable results. O.N represents overnight.

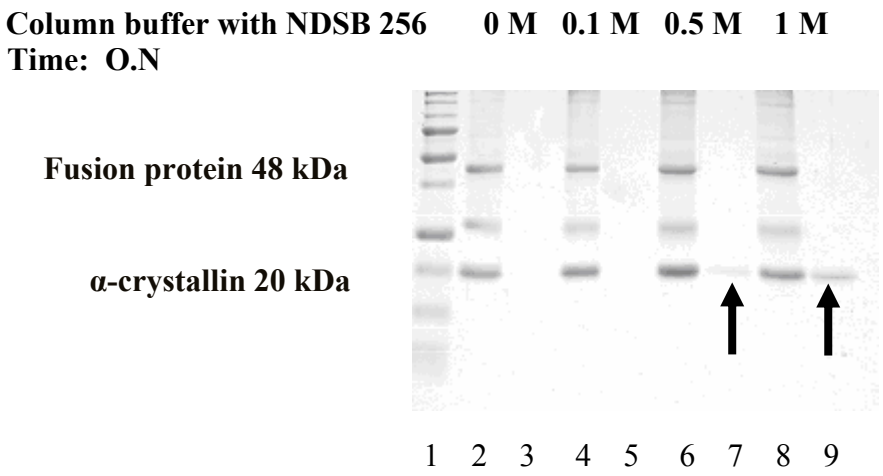

Figure 3.27 Purification of α-crystallin with elution buffer containing NDSB 256.

CRYAA-PTXB1 and CRYAB-PTXB1 were expressed in ER2566 and purified with chitin beads according to the protocol described in method 2.2.4 and 2.2.11. Elution buffer containing different concentrations of NDSB 256 (as indicated in the figure) was used to elute pure α-crystallin from chitin beads. The protein level in the elution fractions and chitin beads was analyzed by coomassie stain. Lane 1 shows the protein mass marker LWM. Lanes 2, 4, 6 and 8 correspond to proteins remaining on the chitin beads. Lanes 3, 5, 7 and 9 correspond to proteins in the elution fractions. With buffer with 0.5 M-1 M (as indicated with arrow) of NDSB 256, we are able to get pure α-crystallin under non-denaturing conditions. The experiments were repeated ten times with comparable results. O.N represents overnight.

3.8.2 Extracellular application of α-crystallin protects astrocytes

To understand the function of α-crystallin in the extracellular environment, purified α-crystallin at different concentrations was added into culture medium. Astrocytes death was induced by 20 μM of C2-ceramide, 0.2 μM of staurosporine or 25 nM of typsin. αA-crystallin and αB-crystallin significantly rescued astrocytes from death caused by C2-ceramide and staurosporine (Fig. 3.28 a) and trypsin (Fig. 3.28 b). Compared with maximal value of induced cell death, astrocytes death was reduced by 1 μg/ml of αA-crystallin under C2-ceramide (about 47%), staurosporine (about 41%) and trypsin (about 62%) treatment. Similarly, 1 μg/ml of αB-crystallin reduced astrocytes death induced by C2-ceramide (about 66%) and staurosporine (about 31%) and trypsin (about 62%). These results demonstrate that α-crystallin plays a protective role in the extracellular medium. Interestingly, at low concentrations (100 ng/ml), αA-crystallin had higher protective effect for astrocytes than αB-crystallin in the case of C2-ceramide and staurosporine treatment. This suggests that αA-crystallin has higher protective activity than αB-crystallin in the extracellular medium under C2-ceramide and staurosporine treatment. Further analysis of data is shown in table 4.3 and table 4.4.

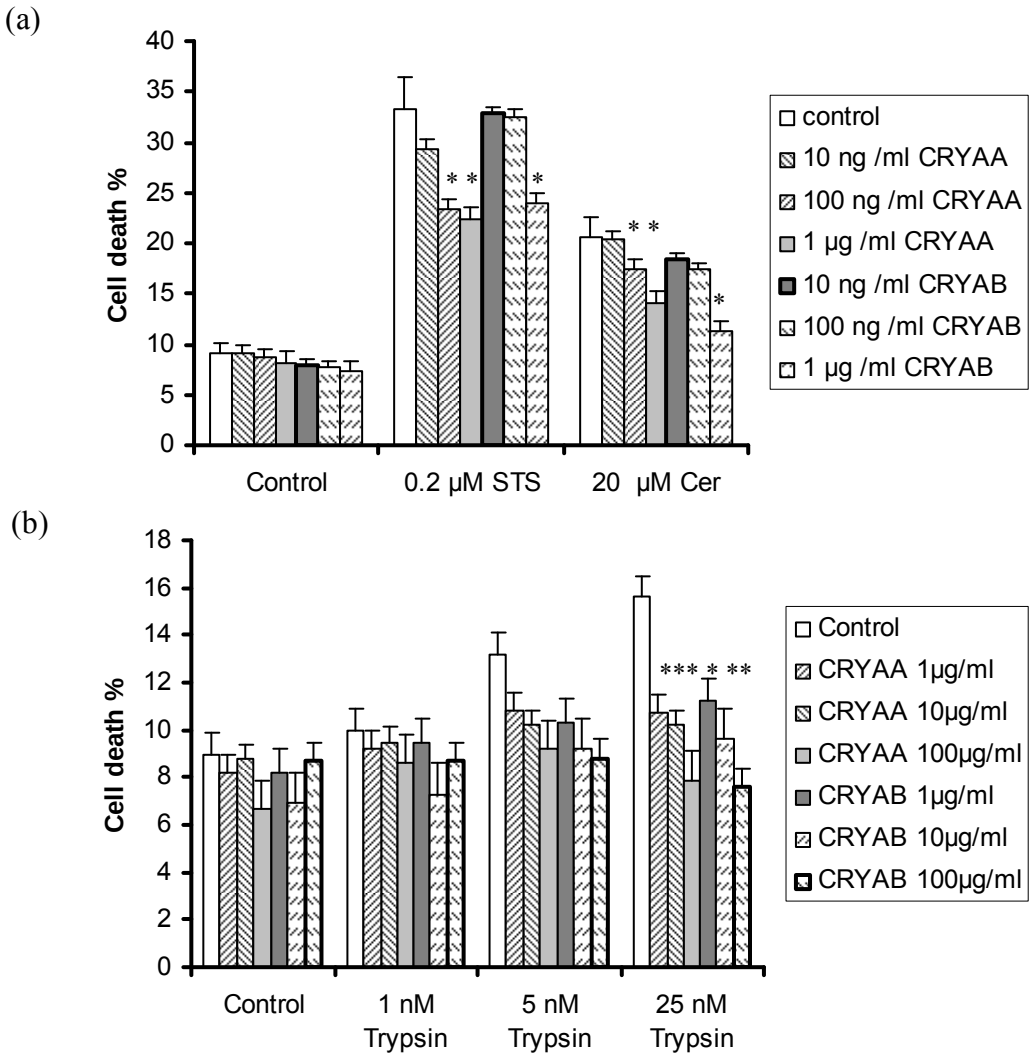

Figure 3.28 Extracellular application of α-crystallin rescued astrocytes from C2-ceramide, staurosporine and trypsin induced death. (a). Extracellular α-crystallin protects astrocytes against C2-ceramide and staurosporine treatment. (b). Extracellular α-crystallin protects astrocytes against high concentration of trypsin treatment. αA-crystallin and αB-crystallin were expressed in ER2566 and purified with chitin beads. Astrocytes were treated with 20 µM of C2-ceramide or with 0.2 µM of staurosporine or with 1 nM, 5 nM or 25 nM trypsin in the absence or presence of αA-crystallin and αB-crystallin in the culture medium for 18 h. Cell death was measured by LDH activity assay. The cell death data were obtained for each sample and the results were averaged. The values of cell death in astrocytes under staurosporine, C2-ceramide or trypsin treatment in the absence or presence of α-crystallin in the extracellular medium were compared. The statistical significance level for difference in astrocytes death caused by C2-ceramide, staurosporine or trypsin between addition and no addition of α-crystallin in the extracellular medium is given as * $p<0.05$. Compared with maximal value of induced cell death, addition of αA-crystallin in the culture medium significantly reduced astrocytes death caused by C2-ceramide (up to 47%), staurosporine (up to 41%) and trypsin (up to 82%). Similarly, addition of αB-crystallin in the culture medium significantly reduced astrocytes death caused by C2-ceramide (up to 66%), staurosporine (up to 31%) and trypsin (up to 100%). Further analysis of data was shown in table 4.3 and table 4.4. The experiments were repeated three times with comparable results.

4. Discussion

4.1 Interaction of α-crystallin with PAR-2

4.1.1 Interaction domains of α-crystallin with PAR-2

In the present study, we for the first time report that the α-crystallins, that is αA-crystallin and αB-crystallin, are two novel PAR-2 interacting proteins. We demonstrated the *in vitro* and *in vivo* interaction of PAR-2 with αA-crystallin and αB-crystallin by different assays. PAR-2 is a G protein-coupled receptor with seven transmembrane domains. Previous studies with yeast-two-hybrid assays suggested the C-terminus of PAR-2 interacts with αA-crystallin and cytoplasmic loop-2 and cytoplasmic loop-3 of rat PAR-2 are not involved in the interaction with αA-crystallin (Rohatgi, 2003). To confirm the results from yeast two-hybrid assays, protein pull-down assay was performed. Our results demonstrated that αA-crystallin specifically interacted with the C-tail of PAR-2-GST fusion protein (Fig. 3.7). To identify the interaction between α-crystallin and the C-tail of PAR-2 in live cells, co-immunoprecipitation assay was performed. Our results demonstrate that the C-terminus of PAR-2 interacts with αA-crystallin and αB-crystallin (Fig. 3.8).

As indicated in Fig. 1.3, the secondary structure of α-crystallin comprises an ordered N-terminus, a conserved domain 'α-crystallin domain', and a C-terminal extension. Sequence analysis with software suggests that four regions of αA-crystallin might be important for the interaction of PAR-2 with αA-crystallin. Therefore, we generated mutants of αA-crystallin with internal deletions (Fig. 3.9 a). These mutants were applied to explore the possible interaction regions of αA-crystallin with PAR-2. Two mutants of αA-crystallin did not interact with PAR-2 (Fig. 3.9 b). This indicates that the regions of amino acids 120-130 and amino acids 136-154 of αA-crystallin are required for the interaction with PAR-2. This interpretation has to be taken with some caution, because internal deletions of αA-crystallin might result in improper folding, resulting in a loss of the interaction with PAR-2. Interestingly, the phosphorylation sites of αA-crystallin at Ser122 and Ser148 are included in these interaction domains. Perhaps, phosphorylation of αA-crystallin could contribute to the regulation of the interaction of αA-crystallin with PAR-2.

4.1.2 Specificity of the interaction of α-crystallin with PAR-2

PARs are members of the superfamily of seven-transmembrane domain, G protein-coupled receptors. PARs are activated by proteolytic cleavage by serine proteases. Four PAR

subtypes are known, PAR-1, PAR-2, PAR-3 and PAR-4 (Wang and Reiser, 2003b; Wang et al., 2002). PAR-1, PAR-3 and PAR-4 are receptors for thrombin, whereas PAR-1, PAR-2 and PAR-4 are receptors for trypsin. To investigate whether αA-crystallin and αB-crystallin are specific interacting partners of PAR-2 in the PAR family, co-immunoprecipitation experiments were carried out to determine the possible *in vivo* cellular interaction of PAR-1, PAR-3 and PAR-4 with α-crystallin. Our results demonstrate that within the PAR family, only PAR-2 interacts with the α-crystallin (see Fig. 3.6). These results suggest that α-crystallin might be involved in uniquely PAR-2-mediated events.

4.2 PAR-2 activation and change in expression of α-crystallin

PAR-2 is diversely expressed in many tissues. Up to now, PAR-2 was found in airway, gastrointestinal tract, liver, vasculature, heart, skin, kidney, immune cells, brain and peripheral nervous system. PAR-2 can be activated by serine proteases, like trypsin, tryptase and coagulation factors VIIa and Xa. Of course, synthetic peptides, so called PAR-2-activating peptides can mimic the tethered ligand of PAR-2 in activation of PAR-2. Normally, short peptides SLIGKV for human and SLIGRL for rat are applied for PAR-2 activation in the research of PAR-2. These peptides activate PAR-2 at concentration in the micromolar range compared with nanomolar potencies of proteases. Unfortunately, antagonists of PAR-2 are not yet available. Interestingly, PARs are activated by a unique mechanism. Proteases cleave the N-terminus of the receptor to expose a tethered ligand which interacts with the extracellular loop, and results in activation. Unlike 'typical' receptors, the specific receptor-activating ligand is part of the receptor. The proteolytic activation of PAR-2 is irreversible. Desensitization of activated PAR-2 occurs by rapid phosphorylation and arrestin binding, which promotes uncoupling of the receptor from G protein signalling within seconds. PAR-2 internalizes within minutes and removes activated receptor from G-proteins and signalling effectors at the plasma membrane. This is an ERK-dependent process. PAR-2 activation evokes G protein-coupled signalling events.

Recent findings point to an important role for PAR-2 in regulating the expression of proteins under physiological and pathophysiological conditions in many tissues. For example, tryptase upregulates IL-1β, IL-6 and IL-8 secretion, cell adhesion molecules (ICAM-1), and selectins (Eselectin) in endothelial cells, CD11b/CD18 in neutrophils, and the release of chemokine GRO/CINC-1 from rat astrocytes (Steinhoff et al. 2005; Wang et al. 2007). Previous studies also suggested that PAR-2-mediated regulation of proteins is modulated by MAP kinases and NFκB. In the present research, we found that PAR-2 activation upregulates the expression of

αA-crystallin (Fig. 3.20 a and b). Interestingly, PAR-2 activation does not significantly influence the expression of αB-crystallin (Fig. 3.20 c and d).

4.3 Mechanism of cytoprotection by PAR-2 and α-crystallin in astrocytes

PAR-2 is widely expressed in the brain and upregulated during neurodegeneration. Numerous evidences demonstrate that low concentrations of PAR-2 agonists will protect the brain. However, high concentration of PAR-2 agonists is toxic to neural cells. The mechanism of cytoprotection of PAR-2 activation is still uncertain. Previous studies suggest that PAR-2 activation will evoke JNK MAP kinase to release chemokine to protect astrocytes (Wang et al., 2007a, b).

In the current research, we report a novel way for PAR-2 to provide cytoprotection in astrocytes. Our data indicate that PAR-2 activation modulates either expression or phosphorylation of α-crystallin to protect astrocytes. α-Crystallin is a chaperone with protective activity. Highly expressed α-crystallin protects cells against stress in lens (Mao et al., 2004). We could show for the first time that increased α-crystallin level is protective for astrocytes. The results from real-time PCR and western blot reveal that PAR-2 activation upregulates αA-crystallin expression. mRNA level of αA-crystallin under PAR-2 activation is about 1.3-fold increase at 18 hours and 2.5-fold increase at 24 hours above control. The protein level of αA-crystallin at 18 hours of stimulation with PAR-2 activating peptide is about 3.7-fold of the control levels. Interestingly, PAR-2 activation results in a rapid increase in mRNA level of αA-crystallin in the early stage (1 h) and a continuously high level of mRNA of αA-crystallin in the late stage (after 18 h). However, the expression pattern of αB-crystallin under PAR-2 activation is quite different. mRNA level of αB-crystallin is downregulated quickly after PAR-2 activation. The protein level of αB-crystallin is not changed by PAR-2 activation. The mechanism how PAR-2 activation regulates expression of αA-crystallin and αB-crystallin is unknown.

We also studied the influence of downregulation of αA-crystallin and αB-crystallin on astrocytes death caused by C2-ceramide and staurosporine. Our data demonstrate that low expression level of αA-crystallin and αB-crystallin results in high percentage of astrocytes death. These data suggest that the amount of αA-crystallin and αB-crystallin in astrocytes is also important for the protective activity of α-crystallin. Upregulation of expression of αA-crystallin by PAR-2 activation could protect astrocytes. Moreover, we measured the phosphorylation level of αB-crystallin at Ser59 site by western blot. We found that at least part of αB-crystallin is phosphorylated at Ser59 site in primary astrocytes. Phosphorylation level of αB-crystallin at

Ser59 site is increased by PAR-2 activation (about 2.3-fold of the control levels), which could contribute to the protective activity of αB-crystallin. Some experiments already showed that αB-crystallin is a stress-related protein in lens cells. Phosphorylation of αB-crystallin is also associated with the formation of oligomers of αB-crystallin, which influences the chaperone activity *in vitro*. Therefore, PAR-2 activation will protect astrocytes by modulating the phosphorylation of αB-crystallin.

To understand the role of phosphorylation of α-crystallin in protection of astrocytes, we generated mutations in α-crystallin for mimicking phosphorylation or unphosphorylation of α-crystallin. Up to now, phosphorylation sites of αA-crystallin at Ser122 and Ser148 and αB-crystallin at Ser19, Ser45 and Ser59 are identified. As shown in table 3.1, we made different mutants of αA-crystallin and αB-crystallin at different sites. Our results in Fig. 3.22 show that pseudophosphorylation of αA-crystallin at Ser122 and Ser 148 provides powerful protection to astrocytes against C2-ceramide and staurosporine. However, unphosphorylation of αA-crystallin at Ser122 and Ser 148 results in the loss of protection for astrocytes.

Table 4.1 Cytoprotection of astrocytes by mutants of αA-crystallin (S: Ser, A: Ala, E: Glu, STS: staurosporine, Cer: C2-ceramide). Data analysis of results as shown in Fig. 3.22 (see for details).

Astrocytes; transfected plasmids	STS treatment		Cer treatment	
	Cell death (values Fig. 3.22)	Cytoprotection (%)	Cell death (values Fig. 3.22)	Cytoprotection (%)
Control (empty vector, MH)	34	—	26	—
CRYAA-MH	18	48	12	56
S122E-MH	13	63	9	66
S148E-MH	12	64	10	63
S122E/S148E-MH	8	77	5	79
S122A-MH	27	23	20	22
S148A-MH	26	26	20	22
S122A/S148A-MH	34	0	25	0

Compared with maximal value of induced cell death in astrocytes caused by C2-ceramide and staurosporine, as indicated in table 4.1, overexpression of full-length αA-crystallin rescued 48% of astrocytes from death caused by staurosporine and 56% of astrocytes from death induced by C2-ceramide. Phosphorylation of αA-crystallin at both Ser122 and Ser148 increased up to 77% (under staurosporine treatment) or 79% (under C2-ceramide treatment) of protection

compared with full-length αA-crystallin. However, unphosphorylation of αA-crystallin at both Ser122 and Ser148 resulted in almost complete loss of protection. These data suggest that the phosphorylation of αA-crystallin at Ser122 and Ser148 is required for cytoprotection of astrocytes.

Table 4.2 Cytoprotection of astrocytes by mutants of αB-crystallin (S: Ser, A: Ala, E: Glu, STS: staurosporine, Cer: C2-ceramide). Data analysis of results as shown in Fig. 3.23 (see for details).

Astrocytes; transfected plasmids	STS treatment		Cer treatment	
	Cell death (values Fig. 3.23)	Cytoprotection (%)	Cell death (values Fig. 3.23)	Cytoprotection (%)
Control (empty vector, MH)	34	—	26	—
CRYAB-MH	18	47	16	38
CRYAB-S19E-MH	19	46	16	40
CRYAB-S45E-MH	15	57	14	48
CRYAB-S59E-MH	15	57	12	53
CRYAB-S19E/S45E-MH	14	59	12	56
CRYAB-S45E/S59E-MH	9	74	7	74
CRYAB-S19E/S59E-MH	13	61	13	51
CRYAB-S19E/S45E/S59E-MH	9	73	9	67
CRYAB-S19A-MH	19	46	16	38
CRYAB-S45A-MH	30	14	23	13
CRYAB-S59A-MH	30	12	24	9
CRYAB-S19A/S45A-MH	26	24	22	17
CRYAB-S19A/S59A-MH	30	14	22	17
CRYAB-S45A/S59A-MH	36	0	26	0
CRYAB-S19A/S45/S59A-MH	34	0	28	0

Regarding the phosphorylation of αB-crystallin at Ser19, Ser45 and Ser59, we found that phosphorylation site Ser19 of αB-crystallin has no correlation to cytoprotection and phosphorylation of αB-crystallin at Ser45 and Ser59 is necessary for cytoprotection (see Fig. 3.23). As shown in table 4.2, overexpression of full-length αB-crystallin rescued 47% of astrocytes from death caused by staurosporine and 38% of astrocytes from death induced by C2-ceramide. Phosphorylation of αB-crystallin at both Ser45 and Ser59 increased up to 74% (under staurosporine treatment) or 74% (under C2-ceramide treatment) of protection compared with full-length αB-crystallin. However, unphosphorylation of αB-crystallin at both Ser45 and Ser59 resulted in complete loss of protection. Interestingly, overexpression of pseudophosphorylated mutant of αB-crystallin at Ser19 generated similar protection as full-length αB-crystallin. These data suggest that the phosphorylation of αB-crystallin at Ser45 and Ser59 is required for cytoprotection of astrocytes. Phosphorylation site of αB-crystallin at Ser19 had no effect on protection of astrocytes.

Accumulating evidences suggest that MAP kinases are involved in PAR-2-mediated processes, like release of proteins. We proposed that MAP kinases could modulate cytoprotection by PAR-2. As indicated in Fig. 3.16, we determined that PAR-2 activation activates all MAP kinases, including p38, ERK and JNK. To know which of the MAP kinases are involved in protective process by PAR-2 and α-crystallin, we applied specific inhibitors of p38, ERK and JNK to block each pathway. We found that the inhibitors of p38, ERK and JNK blocked protection by PAR-2 activation in astrocytes (Fig. 3.17). Interestingly, cytoprotection by overexpression of α-crystallin is inhibited by application of inhibitors of p38 and ERK, but not by application of inhibitor of JNK (Fig. 3.18). This means that p38 and ERK regulate the PAR-2-α-crystallin mediated cytoprotection. Finally, we can get the following conclusion: PAR-2 and α-crystallin are involved in cytoprotection. Two possible pathways underlying the protective mechanisms could be: 1) PAR-2 activation increases the expression of α-crystallin. 2) PAR-2 activation activates p38 and ERK to phosphorylate α-crystallin (See Fig. 4.1).

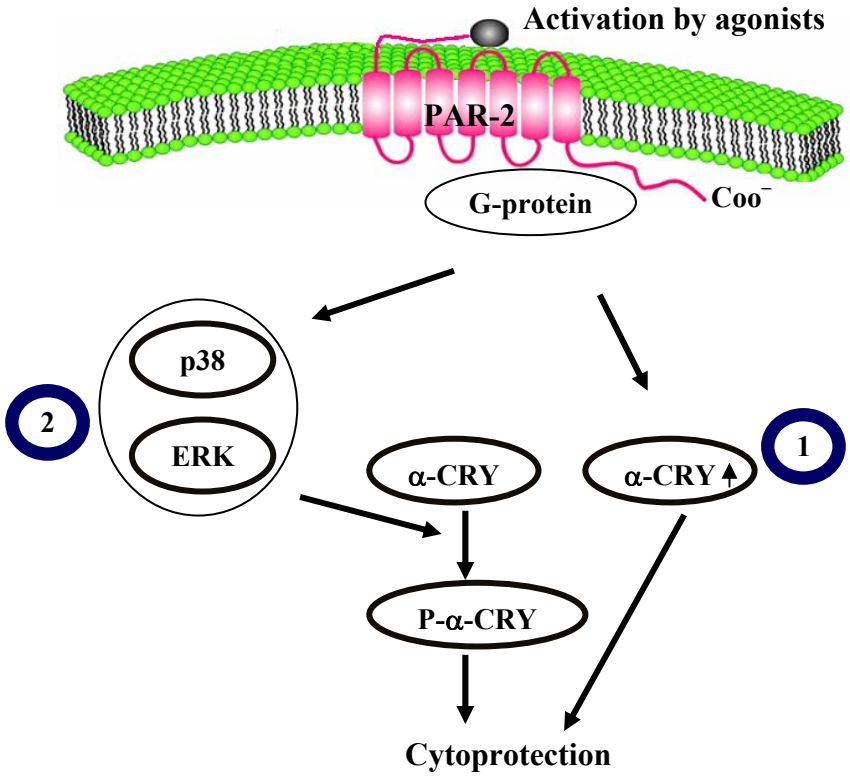

α-CRY: α-crystallin; P- α-CRY: phosphorylated α-crystallin

Figure 4.1 Mechanism of cytoprotection by PAR-2 and α-crystallin in astrocytes.

α-Crystallin and PAR-2 activation protect astrocytes via two pathways in astrocytes:
① PAR-2 activation upregulates the expression of α-crystallin.
② PAR-2 activation activates p38 and ERK which could mediate phosphorylation of α-crystallin.

4.4 Potential functions of α-crystallin in the extracellular medium

α-Crystallin plays a protective role inside cells. α-Crystallin also exists in the extracellular medium. For example, αB-crystallin was found in the plaques in Alzheimer's disease. α-Crystallin is a cytosolic protein and highly expressed in damaged tissue. We propose that α-crystallin comes out from broken cells and functions in the extracellular medium. To generate large amounts of α-crystallin, we optimized the IMPACT (Intein Mediated Purification with an Affinity Chitin-binding Tag) system. The inducible self-cleavage activity of protein splicing elements (termed intein) is applied to separate the target protein from the affinity tag without the use of protease in this protein purification system. Each intein tag contains a chitin binding domain for affinity purification of the fusion protein on a chitin resin. The target protein can be released from the intein tag using thiol reagents like dithiothreitol. In the current research, we used PTXB1 and PTYB11 vectors for expression in the E. coli strain ER2566. As indicated in Fig. 3.25 (a) and (b), PTYB11 does not work well. The fusion protein α-crystallin-intein with PTXB1 was strongly expressed in ER2566 by induction of IPTG. After purification by chitin beads, the fusion protein α-crystallin-intein was treated with DTT buffer to release α-crystallin. Unfortunately, α-crystallin strongly attaches to the chitin resin. To separate α-crystallin from chitin resin, we tried different buffers in the absence or presence of urea. We found that buffer with high concentration of urea (more than 4 M) can elute α-crystallin from chitin resin. However, α-crystallin should be renatured after purification with urea buffer. This is difficult to detect. To get pure renatured α-crystallin, we optimized the purification conditions by using non-detergent sulfobetaines (NDSB). Non-detergent sulfobetaines are a family of solubilizing and stabilizing agents for proteins. We applied NDSB 201 and NDSB 256 for purification of α-crystallin. We found that NDSB 201 is not helpful for purification of α-crystallin (data not shown). Pure α-crystallin can be eluted with buffer with NDSB 256 (Fig. 3.27).

As mentioned above, highly expressed α-crystallin protects astrocytes against staurosporine and C2-ceramide. In the current experiments, we also treated astrocytes with staurosporine and C2-ceramide in the presence of purified α-crystallin in the culture medium. Interestingly, application of α-crystallin rescued astrocytes from death caused by staurosporine and C2-ceramide at low concentration of α-crystallin (100 ng/ml) (see table 4.3).

Table 4.3 Cytoprotection of astrocytes by α-crystallin in the extracellular medium under staurosporine or C2-ceramide treatment (STS: staurosporine, Cer: C2-ceramide, CRYAA: αA-crystallin, CRYAB: αB-crystallin). Data analysis of results as shown in Fig. 3.28 a (see for details).

Cell treatment	STS treatment		Cer treatment	
	Cell death (values Fig. 3.28 a)	Cytoprotection (%)	Cell death (values Fig. 3.28 a)	Cytoprotection (%)
Control	24	—	11	—
100 ng /ml of CRYAA	15	39	9	23
1 µg/ml of CRYAA	14	41	6	47
100 ng /ml of CRYAB	25	0	10	15 (#)
1 µg/ml of CRYAB	17	31	4	66

#, not significant

As indicated in table 4.3, 100 ng/ml of αA-crystallin in the extracellular medium rescued 39% of astrocytes from death caused by staurosporine and 23% of astrocytes from death induced by C2-ceramide. The increase in concentration of αA-crystallin in the medium did not provide further protection under staurosporine treatment. It is interesting that 1 µg/ml of αA-crystallin in the medium resulted in up to 47% of protection of astrocytes under C2-ceramide treatment. However, addition of low concentrations (100 ng/ml) of αB-crystallin in the medium did not protect astrocytes against staurosporine and C2-ceramide. High concentrations (1 µg/ml) of αB-crystallin rescued astrocytes from both staurosporine and C2-ceramide treatment.

Table 4.4 Cytoprotection of astrocytes by α-crystallin in the extracellular medium under trypsin treatment (STS: staurosporine, Cer: C2-ceramide, CRYAA: αA-crystallin, CRYAB: αB-crystallin). Data analysis of results as shown in Fig. 3.28 b (see for details).

Cell treatment	Trypsin treatment	
	Cell death (values Fig. 3.28 b)	Cytoprotection (%)
Control	7	—
1 µg/ml of CRYAA	3	62
10 µg/ml of CRYAA	1	79
100 µg/ml of CRYAA	1	82
1 µg/ml of CRYAB	3	62
10 µg/ml of CRYAB	3	62
100 µg/ml of CRYAB	0	100

We also studied whether astrocytes were protected by application of α-crystallin in the extracellular medium under trypsin treatment. We found that low concentrations (10 ng/ml and 100 ng/ml) of α-crystallin in the extracellular medium did not protect astrocytes (data not shown). As indicated in table 4.4, when we increased the concentration of α-crystallin, astrocytes were significantly protected by addition of α-crystallin in the extracellular medium. Regarding trypsin-induced astrocytes death, high percentage of astrocytes was protected by addition of 1 μg/ml (62% by αA-crystallin and 62% by αB-crystallin), 10 μg/ml of α-crystallin (79% by αA-crystallin and 62% by αB-crystallin) and 100 μg/ml of α-crystallin (82% by αA-crystallin and 100% by αB-crystallin) in the extracellular medium under trypsin treatment.

Mechanism for protection of α-crystallin given as extracellular agent is unkown. One explanation could be that α-crystallin could stabilize the plasma membrane and proteins on the plasma membrane. Whether α-crystallin can also enter cells is not clear. A low concentration of trypsin is protective under physiological conditions in the brain (Wang and Reiser, 2003a). High concentrations of trypsin are toxic to neural cells, which could be dependent on protease activity of trypsin. Treatment with high concentration of trypsin induced astrocytes death (Fig. 3.28 b). When we added different concentrations of α-crystallin into the medium, we found that high concentration (more than 1 μg /ml) of α-crystallin was protective to astrocytes (Fig. 3.28 b). The mechanism is still unclear. One hypothesis is that α-crystallin directly interacts with trypsin to block the protease activity of trypsin, except for stabilization of plasma components. All these evidences suggest that α-crystallin could be protective for cells in the extracellular medium.

4.5 The role of PAR-2 and α-crystallin in the nervous system

4.5.1 Widespread expression and multiple roles of PAR-2

Identification of the family of PARs demonstrates that systemic serine proteases play a role also as activators of G protein-coupled receptor. These proteases transmit extracellular stimuli into intracellular signalling events (Asokananthan et al., 2002; Berger et al., 2001; Cottrell et al., 2003). The second member of this family of receptors is PAR-2, which was originally identified as a receptor activated by trypsin. PAR-2 has attracted great attention by its prospective functions, which are distinct from the functions of the other PARs activated by thrombin (Steinhoff et al., 2005). Widespread expressed PAR-2 was already identified in many tissues and cells, like brain, kidney, heart, pancreas, airway, eye, gastrointestinal tract, lia, liver, prostate, ovary, testes, skin, immune cells, such as T cell, eosinophils, neutrophils, and mast cells. Activation of PAR-2 elicits diverse cellular responses, including cell proliferation, differentiation,

and production and release of proteins such as, interleukin-5, cytokines, chemokines and neurotransmitters (Cocks et al., 1999; Darmoul et al., 2004; Hirota et al., 2005; Kanke et al., 2005). PAR-2 has many effects that are inflammatory. In the vasculature, agonists of PAR-2 increase IL-6 production. In the skin, PAR-2 activation induces inflammatory changes and contributes to the pathophysiology of atopic dermatitis and psoriasis. In the immune system, PAR-2 activating peptides cause the increase of leukocyte migration. In human respiratory epithelial cells, PAR-2 stimulates IL-6, IL-8, and PGE_2 release. In the gastrointestinal tract, PAR-2 modulates Ca^{2+}, Cl^- and K^- channels. In the nervous system, PAR-2 is involved in neurogenic inflammation and pain. PAR-2 also regulates shape changes of astrocytes.

In the nervous system, PAR-2 has been localized in various compartments, such as brain, spinal cord, and peripheral nerves, with different receptor densities found during stages of development (Bushell et al., 2006; Wang and Reiser, 2003a; Wang and Reiser, 2003b). In the brain, PAR-2 is widely expressed on hippocampal, cortical, thalamic, hypothalamic, and striatal neurons, astrocytes, oligodendrocytes and even in microvascular endothelium (Smith-Swintosky et al., 1997). The extrapancreatic trypsin and trypsin-like serine proteases have been detected in the brain. They are involved in neural development, plasticity, neurodegeneration and neuroregeneration (Wang et al., 2008). Brain-expressed trypsinogen IV and mast cell-derived tryptase are considered to be potential PAR-2-activating proteases. Other trypsin-like serine proteases like neurosin, neuropsin and neurotrypsin are also PAR-2 agonists found in the brain (Wang et al., 2008). Several studies have demonstrated important roles for PAR-2 in neurodegenerative/inflammatory disorders in the brain. However, the function of PAR-2 in the nervous system is still largely unclear.

4.5.2 The role of PAR-2 in cell death

Previous work in our laboratory revealed that PAR-2 activation protects astrocytes from C2-ceramide treatment (Wang et al., 2007b). In the present study, C2-ceramide and staurosporine were applied to induce cell death. Numerous studies have described intracellular ceramide accumulation upon triggering of apoptotic cell death signals. Short chain analogs of ceramide, in particular C2-ceramide, are interesting tools to study apoptosis of cells, since C2-ceramide efficiently triggers apoptosis in almost any cell (Wang et al., 2007a). Staurosporine inhibits protein kinase C and is a potent apoptosis inducer, as demonstrated in a broad spectrum of cells. Staurosporine causes apoptosis through the mitochondrial death pathway (Mao et al., 2004). In the present case, we explored the role of PAR-2 activation in astrocytes. PAR-2 activation has a significant cytoprotection against C2-ceramide and staurosporine treatment in

astrocytes. This result is consistent with our previous report showing that PAR-2 activation led to the release of the chemokine GRO/CINC-1 to rescue astrocytes from C2-ceramide treatment (Wang et al., 2007b). The release of GRO/CINC-1 from astrocytes can consequently protect neurons from apoptosis by inhibition of C2-ceramide-induced cytochrome c release from mitochondria (Wang et al., 2007a). Moreover, we could show earlier that PAR-2 activation also rescued astrocytes from staurosporine treatment, even though the mechanism of protection is still unclear.

4.5.3 The role of α-crystallin in cell death

Except for the different expression patterns of αA-crystallin and αB-crystallin, also their difference in the amino acid sequence indicates different properties and functions for them. αB-crystallin, but not αA-crystallin is heat-inducible. αA-crystallin has higher protective activity than αB-crystallin against staurosporine or UVA-induced apoptosis in mouse lens epithelial cells (Andley et al., 2000). αA-crystallin can activate the protein kinase B pathway to induce cell survival. αB-crystallin can inhibit cell apoptosis by blocking Ras activation. In knockout mice, deletion of αB-crystallin has little effect on lens morphology; however, removal of the αA-crystallin gene causes early onset of cataract (Van Rijk and Bloemendal, 2000; Xi et al., 2006). These observations suggest that αA-crystallin and αB-crystallin are functionally not equivalent.

In the heart and lens epithelial cells, evidence was obtained indicating that α-crystallin provides protection against ischemia and stress, like UVA-irradiation and exposure to staurosporine. The possible mechanism implies that α-crystallin acts on apoptotic regulators, such as Bax and caspases to consequently block mitochondrial apoptotic processes and cause cell survival (Li et al., 2005; Liu et al., 2004; Mao et al., 2004). It is unclear whether α-crystallin has similar effects in the nervous system.

4.5.4 The role of PAR-2 and α-crystallin in neurodegenerative diseases

PAR-2 may play an important regulatory role in the central and peripheral nervous system in normal and disease states. PAR-2 is abundantly expressed in various subareas of the brain and regulates neurologic pro- and anti-inflammatory reactions. Normally, PAR-2 is upregulated during brain injury, like oxygen and glucose deprivation (Striggow et al., 2001). Of course, cytokines such as TNF-α and IL-1α also induce upregulation of PAR-2. PAR-2 activation has different effects on neurons and astrocytes. The PAR-2 agonist is toxic for neurons

(Smith-Swintosky et al., 1997). However, PAR-2 activation is protective for astrocytes (Li et al., 2009). Therefore, the role of PAR-2 in brain injury depends on cell types and experimental conditions.

An important finding obtained in the α-crystallin research of the past decade has been the association of increased levels of αB-crystallin with various neurological diseases, such as Alexander's disease, Creutzfeldt-Jacob disease, and Alzheimer's disease (Van Rijk and Bloemendal, 2000; Xi et al., 2006). For example, the Rosenthal fibers, which are typical of Alexander's disease are composed of glial fibrillary acidic protein, αB-crystallin and heat shock protein 27. It is assumed that the formation of Rosenthal fibers is due to chronic stress by yet unknown stimuli which evoke the elevated expression of αB-crystallin and heat shock protein 27. Recent studies have shown that αB-crystallin participates in neuroinflammation (Masilamoni et al., 2006). αB-crystallin level is elevated in oligodendrocytes and astrocytes in areas of active demyelination in multiple sclerosis, in reactive astrocytes and microglia in or near the senile plaques, and the neurofibrillary tangles of Alzheimer's disease (Bajramovic et al., 1997; Renkawek et al., 1994). αB-crystallin is also observed after kainic acid-induced seizure in astrocytes in the CA3 region of the hippocampus (Xi et al., 2006). Furthermore, accumulating evidence indicates the association of αB-crystallin with tau inclusions, which are generated in various neuropathological conditions (Dabir et al., 2004). Recent studies indicate that Ser59 is the major phosphorylation site of αB-crystallin accumulated in the brain of patients with Alexander's disease (Kato et al., 2001). This suggests that there is some relationship between phosphorylation of αB-crystallin and the neurodegenerative disease states.

The data from our research and from other groups suggest that PAR-2 and α-crystallin could be involved in brain injury and neurodegenerative diseases which will be an issue for future investigations. In the current studies, we provide evidence for cytoprotection by α-crystallin and PAR-2 in astrocytes. Astrocytes underwent cell death in response to C2-ceramide and staurosporine in time-dependent and concentration-dependent manner. Our results indicate that PAR-2 activation rescues astrocytes from both C2-ceramide- and staurosporine-induced cell death (Fig. 3.10). Overexpression of αA-crystallin and αB-crystallin significantly inhibits cell death in astrocytes (see Fig. 3.12). We speculate that α-crystallin protects also astrocytes in pathological conditions, because it has been shown that increased expression of α-crystallin is induced in stress situations. We tried to explore how cytoprotection in astrocytes derived from PAR-2 activation and from α-crystallin expression are related. Previous studies suggest that phosphorylation of α-crystallin is required for the protective activity (Ito et al., 1997; Morrison

et al., 2003; Wang and Spector, 1996), and the phosphorylation process of α-crystallin is mediated by the MAPK pathway (Hoover et al., 2000). One possible way might be that PAR-2 activation activates the MAPK pathway to regulate α-crystallin activity by altering phosphorylation of α-crystallin. Indeed, our data demonstrate that PAR-2 activation increases the phosphorylation level of αB-crystallin at Ser59 (Fig. 3.21). The phosphorylation of α-crystallin is required for protection (Fig. 3.22 and 3. 23). Moreover, PAR-2 activation also results in the increased expression of αA-crystallin (Fig. 3.20). In addition, we also found that some concentration of α-crystallin in the extracellular medium is protective for astrocytes (Fig. 3. 28). These data suggest that PAR-2 and α-crystallin could be protective inside and outside astrocytes during brain injury.

4.6 Further possible functional connections of PAR-2 and α-crystallin

Another possible consequence of the interaction of PAR-2 with α-crystallin is that α-crystallin might be involved in the endocytosis of PAR-2, which is a critical process for recruitment of PAR-2. On the one hand, the binding of α-crystallin might stabilize the PAR-2 structure and affect its conformational change. On the other hand, the phosphorylation site of the C-terminus of PAR-2 is required for the interaction of β-arrestin, which mediates PAR-2 endocytosis (Stalheim et al., 2005). The interaction of α-crystallin with PAR-2 might interfere with the C-terminal phosphorylation of PAR-2 to regulate PAR-2 internalization. Previous studies indicate that α-crystallin directly interacts with plasma membrane complexes and cytoskeleton components to stabilize the plasma membrane (Cobb and Petrash, 2000; Djabali et al., 1997; Nicholl and Quinlan, 1994). These findings suggest that α-crystallin might modulate the internalization of PAR-2. Moreover, the dissociation of G-proteins is important for PAR-2-mediated signalling. The binding of α-crystallin might interfere with conformational changes of G proteins in PAR-2 activation to subsequently influence downstream signals, like Ca^{2+} influx.

Astrocytes play a crucial role in maintaining normal brain physiology during development and in adulthood. In addition to their physiological functions, astrocytes have an important role in responding to injury and disease. There is an increasing body of data implicating astrocyte apoptosis in brain injury. Thus, the regulation of astrocyte apoptosis is essential in physiological and pathological processes in the central nervous system. The current findings provide a new possible way to regulate astrocyte apoptosis. Our data suggest that the occurrence of PAR-2 activation and increased expression of α-crystallin during injury will attenuate the damage of the brain.

5. Zusammenfassung

Der Protease-aktivierte Rezeptor 2 (PAR2) ist ein G Protein-gekoppelter Rezeptor, der durch Trypsin und trypsinähnliche Serinproteasen aktiviert wird. Der in vielen Geweben exprimierte PAR-2 ist an Entzündungsprozessen beteiligt, jedoch ist seine physiologische /pathologische Rolle im Nervensystem unklar. In der vorliegenden Arbeit konnten wir αA-Crystallin und αB-Crystallin als neue Interaktionspartner für PAR-2 aufzeigen. Für diese 20 kDa Proteine wurde berichtet, dass sie bei neurodegenerativen Krankheiten, wie Alexanders-Krankheit, Creutzfeld-Jakob, Alzheimer und Parkinson beteiligt sind. Vorarbeiten aus einem Hefe-2-Hybrid Assay, bei denen der cytosolisch lokalisierte C-Terminus von PAR-2 als Köder verwendet wurde, gaben einen Hinweis darauf, dass αA-Crystallin mit PAR-2 interagiert. Wir konnten in dieser Studie zeigen, dass sowohl *in vitro*, wie auch in vivo, der C-terminale Teil von PAR-2, wie auch der vollständige PAR-2 in der Lage sind, mit αA(αB)-Crystallinen zu interagieren. Für diesen Nachweis benutzten wir Pull-Down, Co-Immunpräzipitation und Kolokalisationsexperimente. Die Analyse der Interaktion mit Hilfe von Deletionsmutanten von α-Crystallin zeigte, dass die Aminosäurereste 120-130 und 136-154 für die Interaktion mit PAR-2 notwendig sind. Die Interaktion von αA(αB)-Crystallin mit anderen PARs (PAR-1, PAR-3, PAR-4) konnte ausgeschlossen werden. Dies beweist, dass αA(αB)-Crystallin spezifisch mit PAR-2 interagiert.

Weiterhin untersuchten wir in Astrozyten die funktionelle Rolle von PAR-2 und α-Crystallin. Wir konnten beweisen, dass die Aktivierung von PAR-2 und eine erhöhte Expression von α-Crystallin, den Zelltod in Astrozyten reduzieren. Zelltod wurde durch C2-Ceramid und Staurosporin induziert. Wir untersuchten weiterhin den Mechanismus, durch den PAR-2 und α-Crystallin die Astrozyten schützen können. Das Expressionsniveau von αA(αB)-Crystallin bei Aktivierung von PAR-2 wurde mit Hilfe von Real-Time-PCR und Western Blot untersucht. Unsere Daten zeigen, dass die Aktivierung von PAR-2 die Expression von αA-Crystallin nach 18 –stündiger Stimulation erhöht.

Wir konnten auch durch Western Blot nachweisen, dass die Aktivierung von PAR-2 eine Phosphorylierung des Ser59 von αB-Crystallin induziert. Um die Rolle der Phosphorylierung des αA(αB)-Crystallins auf den Schutz der Zellen zu untersuchen, stellten wir Mutanten her, die eine Phosphorylierung oder eine Nicht-phosphorylierung des Crystallins nachahmen können, indem wir das entsprechende Serin zu Glutamat bzw. Alanin mutierten. Ergebnisse, die durch die Expression von pseudo-phosphoryliertem αA-Crystallin (Ser122 und 148) erhalten wurden, zeigten eine starke Protektion der Astrozyten bei Behandlung mit

Staurosporin und C2-Ceramid. Hoch exprimiertes nicht-phosphoryliertes αA-Crystallin (an Ser122 und 148) verursachte einen Verlust dieser protektiven Eigenschaft. Parallel dazu zeigt hoch exprimiertes phosphoryliertes αB-Crystallin (Ser45 und Ser59) eine protektive Wirkung auf Astrozyten. Expression von nicht-phosphoryliertem αB-Crystallin (Ser122 und Ser148) zeigt jedoch keine schützende Funktion in Astrozyten. Interessanterweise zeigt nicht-phosphoryliertes αB-Crystallin (Ser19) eine ähnliche protektive Wirkung wie normales αB-Crystallin. Diese Daten lassen vermuten, dass die Phosphorylierung von Ser122 und Ser148 bei αA-Crystallin und Ser45 und Ser59 bei αB-Crystallin für den Schutz der Astrozyten notwendig sind. Somit weisen unsere Ergebnisse darauf hin, dass PAR-2 und α-Crystallin durch die Regulation der Expression und des Phosphorylierungsstatus von α-Crystallin bei Kontrolle des Überlebens der Astrozyten beteiligt sind.

Um herauszufinden, ob MAP-Kinasen bei diesem Protektionsvorgang beteiligt sind, wurden spezifische Inhibitoren von p38, ERK und JNK angewendet. Die Aktivierung von p38 und JNK wurde bei PAR-2 Aktivierung mittels Western Blot bestimmt. Die PAR-2 Aktivierung löst die Aktivierung von p38, ERK und JNK in Astrozyten aus. Die Anwendung spezifischer Inhibitoren von p38 (SB203580), ERK (PD98059) und JNK (SP600125), reduzierte den Schutz durch PAR-2. Dies deutet darauf hin, dass alle MAP-Kinasen den Schutz durch PAR-2 vermitteln. Inhibitoren von p38 und ERK blockieren den Schutz durch α-Crystallin. Der Inhibitor von JNK hatte keinen Einfluß auf die protektive Wirkung von α-Crystallin.

Diese Ergebnisse weisen auf einen funktionellen Zusammenhang zwischen PAR-2 und α-Crystallin mit den MAP-Kinasen p38 und ERK hin. Die dabei möglichen 3 Signal- und Aktivierungswege, die bei der protektiven Wirkung von PAR-2 und α-Crystallin beteiligt sind, sind 1) PAR-2 Aktivierung erhöht die Expression von αA-Crystallin, 2) PAR-2 Aktivierung moduliert die Phosphorylierung von α-Crystallin über die Aktivierung von p38 und ERK; 3) PAR-2 Aktivierung ruft die Freisetzung von Chemokinen über JNK hervor. Letzteres wurde in früheren Arbeiten gezeigt.

Zusätzlich untersuchten wir auch die Rolle von α-Crystallin in der extrazellulären Matrix. α-Crystallin wurde in Bakterien exprimiert und aufgereinigt. Wir optimierten die Bedingungen für die Aufreinigung, um reines αA(αB)-Crystallin herzustellen. Zugabe dieser aufgereinigten α-Crystalline zum extrazellulären Medium rettete Astrozyten von Staurosporin- und C2-Ceramid und Trypsin-induziertem Zelltod. Dies weist darauf hin, dass auch extrazelluläres α-Crystallin bei neurodegenerativen Erkrankungen eine protektive Rolle haben kann.

6. Abstract

Protease activated receptor 2 (PAR-2) belongs to the family of G protein-coupled receptors and is activated by trypsin and tryptase after brain insults. PAR-2 has been implicated in multiple biological functions, such as inflammation, apoptosis, modulation in morphology, proliferation, mitogenesis and immunomodulation. In the current research, we could show earlier that α-crystallin (comprising αA-crystallin and αB-crystallin), a small heat shock protein functioning as structural protein and chaperone, specifically interacts with the PAR-2 protein. Our data indicate that in the PAR family, only PAR-2 interacts with α-crystallin. To understand the interaction of PAR-2 with α-crystallin in detail, mutants of PAR-2 and α-crystallin are used in the experiments. Results from immunoprecipitation and GST pull-down experiments demonstrate that the C-tail of PAR-2 is involved in the interaction with α-crystallin. Specific regions of αA-crystallin (amino acids 120-130 and 136-154) are required for the interaction with PAR-2.

Moreover, we investigated the functional role of PAR-2 and α-crystallin in astrocytes. Evidence is presented to show that PAR-2 activation and increased the expression of α-crystallin reduced C2-ceramide- and staurosporine-induced cell death in astrocytes. Thus, both PAR-2 and α-crystallin are involved in cytoprotection in astrocytes. We further investigate the mechanism of protection by PAR-2 and α-crystallin in astrocytes. PAR-2 activation increases expression of αA-crystallin and induces phosphorylation of Ser59 of αB-crystallin. The experiments by mimicking of phosphorylation or unphosphorylation of α-crystallin show that phosphorylation of αA-crystallin at Ser122 and Ser148 and αB-crystallin at Ser45 and Ser59 is required for protection. Ser19 of αB-crystallin has no connection with protection. PAR-2 activation activates p38, ERK and JNK in astrocytes. Application of inhibitors of p38 and ERK reduces the protection by PAR-2 and α-crystallin. Inhibitor of JNK blocks the protection by PAR-2 and does not have any effect on protection by α-crystallin. These findings suggest that PAR-2 and α-crystallin are involved in astrocytes survival by regulating the expression and the phosphorylation status of α-crystallin.

In addition, we explored the role of α-crystallin in extracellular matrix. α-Crystallin was expressed in bacteria and purified using chitin resin. Addition of α-crystallin into the extracellular medium rescues astrocytes from staurosporine, C2-ceramide and trypsin treatment. This hints that α-crystallin could be protective in the extracellular medium in neurodegenerative disease conditions.

7. References

Al-Ani B, Saifeddine M, Kawabata A, Renaux B, Mokashi S, Hollenberg MD (1999) Proteinase-activated receptor 2 (PAR(2)): development of a ligand-binding assay correlating with activation of PAR(2) by PAR(1)- and PAR(2)-derived peptide ligands. J Pharmacol Exp Ther 290:753-760.

Andley UP, Song Z, Wawrousek EF, Bassnett S (1998) The molecular chaperone alphaA-crystallin enhances lens epithelial cell growth and resistance to UVA stress. J Biol Chem 273:31252-31261.

Andley UP, Song Z, Wawrousek EF, Fleming TP, Bassnett S (2000) Differential protective activity of alpha A- and alphaB-crystallin in lens epithelial cells. J Biol Chem 275:36823-36831.

Asokananthan N, Graham PT, Fink J, Knight DA, Bakker AJ, McWilliam AS, Thompson PJ, Stewart GA (2002) Activation of protease-activated receptor (PAR)-1, PAR-2, and PAR-4 stimulates IL-6, IL-8, and prostaglandin E2 release from human respiratory epithelial cells. J Immunol 168:3577-3585.

Augusteyn RC (2004) alpha-crystallin: a review of its structure and function. Clin Exp Optom 87:356-366.

Bajramovic JJ, Lassmann H, van Noort JM (1997) Expression of alphaB-crystallin in glia cells during lesional development in multiple sclerosis. J Neuroimmunol 78:143-151.

Benarroch EE (2005) Neuron-astrocyte interactions: partnership for normal function and disease in the central nervous system. Mayo Clin Proc 80:1326-1338.

Berger P, Perng DW, Thabrew H, Compton SJ, Cairns JA, McEuen AR, Marthan R, Tunon De Lara JM, Walls AF (2001) Tryptase and agonists of PAR-2 induce the proliferation of human airway smooth muscle cells. J Appl Physiol 91:1372-1379.

Buddenkotte J, Stroh C, Engels IH, Moormann C, Shpacovitch VM, Seeliger S, Vergnolle N, Vestweber D, Luger TA, Schulze-Osthoff K, Steinhoff M (2005) Agonists of proteinase-activated receptor-2 stimulate upregulation of intercellular cell adhesion molecule-1 in primary human keratinocytes via activation of NF-kappa B. J Invest Dermatol 124:38-45.

Bushell TJ, Plevin R, Cobb S, Irving AJ (2006) Characterization of proteinase-activated receptor 2 signalling and expression in rat hippocampal neurons and astrocytes. Neuropharmacology 50:714-725.

Chiesa R, Spector A (1989) The dephosphorylation of lens alpha-crystallin A chain. Biochem Biophys Res Commun 162:1494-1501.

Cobb BA, Petrash JM (2000) Characterization of alpha-crystallin-plasma membrane binding. J Biol Chem 275:6664-6672.

Cocks TM, Fong B, Chow JM, Anderson GP, Frauman AG, Goldie RG, Henry PJ, Carr MJ, Hamilton JR, Moffatt JD (1999) A protective role for protease-activated receptors in the airways. Nature 398:156-160.

Coelho AM, Ossovskaya V, Bunnett NW (2003) Proteinase-activated receptor-2: physiological and pathophysiological roles. Curr Med Chem Cardiovasc Hematol Agents 1:61-72.

Cottrell GS, Amadesi S, Schmidlin F, Bunnett N (2003) Protease-activated receptor 2: activation, signalling and function. Biochem Soc Trans 31:1191-1197.

Coughlin SR (1999) How the protease thrombin talks to cells. Proc Natl Acad Sci U S A 96:11023-11027.

Coughlin SR (2000) Thrombin signalling and protease-activated receptors. Nature 407:258-264.

D'Andrea MR, Derian CK, Leturcq D, Baker SM, Brunmark A, Ling P, Darrow AL, Santulli RJ, Brass LF, Andrade-Gordon P (1998) Characterization of protease-activated receptor-2 immunoreactivity in normal human tissues. J Histochem Cytochem 46:157-164.

Dabir DV, Trojanowski JQ, Richter-Landsberg C, Lee VM, Forman MS (2004) Expression of the small heat-shock protein alphaB-crystallin in tauopathies with glial pathology. Am J Pathol 164:155-166.

Darmoul D, Gratio V, Devaud H, Laburthe M (2004) Protease-activated receptor 2 in colon cancer: trypsin-induced MAPK phosphorylation and cell proliferation are mediated by epidermal growth factor receptor transactivation. J Biol Chem 279:20927-20934.

den Engelsman J, Gerrits D, de Jong WW, Robbins J, Kato K, Boelens WC (2005) Nuclear import of {alpha}B-crystallin is phosphorylation-dependent and hampered by hyperphosphorylation of the myopathy-related mutant R120G. J Biol Chem 280:37139-37148.

den Engelsman J, Bennink EJ, Doerwald L, Onnekink C, Wunderink L, Andley UP, Kato K, de Jong WW, Boelens WC (2004) Mimicking phosphorylation of the small heat-shock protein alphaB-crystallin recruits the F-box protein FBX4 to nuclear SC35 speckles. Eur J Biochem 271:4195-4203.

Dery O, Corvera CU, Steinhoff M, Bunnett NW (1998) Proteinase-activated receptors: novel mechanisms of signaling by serine proteases. Am J Physiol 274:C1429-1452.

Djabali K, de Nechaud B, Landon F, Portier MM (1997) AlphaB-crystallin interacts with intermediate filaments in response to stress. J Cell Sci 110 (Pt 21):2759-2769.

Eaton P, Fuller W, Bell JR, Shattock MJ (2001) AlphaB crystallin translocation and phosphorylation: signal transduction pathways and preconditioning in the isolated rat heart. J Mol Cell Cardiol 33:1659-1671.

Fan L, Yotov WV, Zhu T, Esmailzadeh L, Joyal JS, Sennlaub F, Heveker N, Chemtob S, Rivard GE (2005) Tissue factor enhances protease-activated receptor-2-mediated factor VIIa cell proliferative properties. J Thromb Haemost 3:1056-1063.

Fiorucci S, Mencarelli A, Palazzetti B, Distrutti E, Vergnolle N, Hollenberg MD, Wallace JL, Morelli A, Cirino G (2001) Proteinase-activated receptor 2 is an anti-inflammatory signal for colonic lamina propria lymphocytes in a mouse model of colitis. Proc Natl Acad Sci U S A 98:13936-13941.

Golenhofen N, Ness W, Koob R, Htun P, Schaper W, Drenckhahn D (1998) Ischemia-induced phosphorylation and translocation of stress protein alpha B-crystallin to Z lines of myocardium. Am J Physiol 274:H1457-1464.

Hirade K, Kozawa O, Tanabe K, Niwa M, Matsuno H, Oiso Y, Akamatsu S, Ito H, Kato K, Katagiri Y, Uematsu T (2002) Thrombin stimulates dissociation and induction of HSP27 via p38 MAPK in vascular smooth muscle cells. Am J Physiol Heart Circ Physiol 283:H941-948.

Hirota Y, Osuga Y, Hirata T, Harada M, Morimoto C, Yoshino O, Koga K, Yano T, Tsutsumi O, Taketani Y (2005) Activation of protease-activated receptor 2 stimulates proliferation and interleukin (IL)-6 and IL-8 secretion of endometriotic stromal cells. Hum Reprod 20:3547-3553.

Hoover HE, Thuerauf DJ, Martindale JJ, Glembotski CC (2000) alpha B-crystallin gene induction and phosphorylation by MKK6-activated p38. A potential role for alpha B-crystallin as a target of the p38 branch of the cardiac stress response. J Biol Chem 275:23825-23833.

Horwitz J (1992) Alpha-crystallin can function as a molecular chaperone. Proc Natl Acad Sci U S A 89:10449-10453.

Ito H, Okamoto K, Nakayama H, Isobe T, Kato K (1997) Phosphorylation of alphaB-crystallin in response to various types of stress. J Biol Chem 272:29934-29941.

Ito H, Kamei K, Iwamoto I, Inaguma Y, Nohara D, Kato K (2001) Phosphorylation-induced change of the oligomerization state of alpha B-crystallin. J Biol Chem 276:5346-5352.

Iwaki T, Kume-Iwaki A, Goldman JE (1990) Cellular distribution of alpha B-crystallin in non-lenticular tissues. J Histochem Cytochem 38:31-39.

Jin G, Hayashi T, Kawagoe J, Takizawa T, Nagata T, Nagano I, Syoji M, Abe K (2005) Deficiency of PAR-2 gene increases acute focal ischemic brain injury. J Cereb Blood Flow Metab 25:302-313.

Kamradt MC, Chen F, Cryns VL (2001) The small heat shock protein alpha B-crystallin negatively regulates cytochrome c- and caspase-8-dependent activation of caspase-3 by inhibiting its autoproteolytic maturation. J Biol Chem 276:16059-16063.

Kamradt MC, Chen F, Sam S, Cryns VL (2002) The small heat shock protein alpha B-crystallin negatively regulates apoptosis during myogenic differentiation by inhibiting caspase-3 activation. J Biol Chem 277:38731-38736.

Kanke T, Takizawa T, Kabeya M, Kawabata A (2005) Physiology and pathophysiology of proteinase-activated receptors (PARs): PAR-2 as a potential therapeutic target. J Pharmacol Sci 97:38-42.

Kanke T, Macfarlane SR, Seatter MJ, Davenport E, Paul A, McKenzie RC, Plevin R (2001) Proteinase-activated receptor-2-mediated activation of stress-activated protein kinases and inhibitory kappa B kinases in NCTC 2544 keratinocytes. J Biol Chem 276:31657-31666.

Kato K, Ito H, Kamei K, Inaguma Y, Iwamoto I, Saga S (1998) Phosphorylation of alphaB-crystallin in mitotic cells and identification of enzymatic activities responsible for phosphorylation. J Biol Chem 273:28346-28354.

Kato K, Inaguma Y, Ito H, Iida K, Iwamoto I, Kamei K, Ochi N, Ohta H, Kishikawa M (2001) Ser-59 is the major phosphorylation site in alphaB-crystallin accumulated in the brains of patients with Alexander's disease. J Neurochem 76:730-736.

Kozawa O, Matsuno H, Niwa M, Hatakeyama D, Kato K, Uematsu T (2001) AlphaB-crystallin, a low-molecular-weight heat shock protein, acts as a regulator of platelet function. Cell Stress Chaperones 6:21-28.

Li DW, Liu JP, Mao YW, Xiang H, Wang J, Ma WY, Dong Z, Pike HM, Brown RE, Reed JC (2005) Calcium-activated RAF/MEK/ERK signaling pathway mediates p53-dependent apoptosis and is abrogated by alpha B-crystallin through inhibition of RAS activation. Mol Biol Cell 16:4437-4453.

Li R, Rohatgi T, Hanck T, Reiser G (2009) Alpha A-crystallin and alpha B-crystallin, newly identified interaction proteins of protease-activated receptor-2, rescue astrocytes from C2-ceramide- and staurosporine-induced cell death. J Neurochem 110:1433-1444.

Liu JP, Schlosser R, Ma WY, Dong Z, Feng H, Liu L, Huang XQ, Liu Y, Li DW (2004) Human alphaA- and alphaB-crystallins prevent UVA-induced apoptosis through regulation of PKCalpha, RAF/MEK/ERK and AKT signaling pathways. Exp Eye Res 79:393-403.

Lozada A, Maegele M, Stark H, Neugebauer EM, Panula P (2005) Traumatic brain injury results in mast cell increase and changes in regulation of central histamine receptors. Neuropathol Appl Neurobiol 31:150-162.

Macfarlane SR, Sloss CM, Cameron P, Kanke T, McKenzie RC, Plevin R (2005) The role of intracellular Ca2+ in the regulation of proteinase-activated receptor-2 mediated nuclear factor kappa B signalling in keratinocytes. Br J Pharmacol 145:535-544.

Maddala R, Rao VP (2005) alpha-Crystallin localizes to the leading edges of migrating lens epithelial cells. Exp Cell Res 306:203-215.

Mao YW, Liu JP, Xiang H, Li DW (2004) Human alphaA- and alphaB-crystallins bind to Bax and Bcl-X(S) to sequester their translocation during staurosporine-induced apoptosis. Cell Death Differ 11:512-526.

Masilamoni JG, Jesudason EP, Baben B, Jebaraj CE, Dhandayuthapani S, Jayakumar R (2006) Molecular chaperone alpha-crystallin prevents detrimental effects of neuroinflammation. Biochim Biophys Acta 1762:284-293.

Morozov V, Wawrousek EF (2006) Caspase-dependent secondary lens fiber cell disintegration in alphaA-/alphaB-crystallin double-knockout mice. Development 133:813-821.

Morrison LE, Hoover HE, Thuerauf DJ, Glembotski CC (2003) Mimicking phosphorylation of alphaB-crystallin on serine-59 is necessary and sufficient to provide maximal protection of cardiac myocytes from apoptosis. Circ Res 92:203-211.

Napoli C, Cicala C, Wallace JL, de Nigris F, Santagada V, Caliendo G, Franconi F, Ignarro LJ, Cirino G (2000) Protease-activated receptor-2 modulates myocardial ischemia-reperfusion injury in the rat heart. Proc Natl Acad Sci U S A 97:3678-3683.

Nicholl ID, Quinlan RA (1994) Chaperone activity of alpha-crystallins modulates intermediate filament assembly. Embo J 13:945-953.

Noorbakhsh F, Vergnolle N, McArthur JC, Silva C, Vodjgani M, Andrade-Gordon P, Hollenberg MD, Power C (2005) Proteinase-activated receptor-2 induction by neuroinflammation prevents neuronal death during HIV infection. J Immunol 174:7320-7329.

Ossovskaya VS, Bunnett NW (2004) Protease-activated receptors: contribution to physiology and disease. Physiol Rev 84:579-621.

Ousman SS, Tomooka BH, van Noort JM, Wawrousek EF, O'Connor KC, Hafler DA, Sobel RA, Robinson WH, Steinman L (2007) Protective and therapeutic role for alphaB-crystallin in autoimmune demyelination. Nature 448:474-479.

Pai KS, Mahajan VB, Lau A, Cunningham DD (2001) Thrombin receptor signaling to cytoskeleton requires Hsp90. J Biol Chem 276:32642-32647.

Park GH, Ryu JR, Shin CY, Choi MS, Han BH, Kim WK, Kim HC, Ko KH (2006) Evidence that protease-activated receptor-2 mediates trypsin-induced reversal of stellation in cultured rat astrocytes. Neurosci Res 54:15-23.

Piao CS, Kim SW, Kim JB, Lee JK (2005) Co-induction of alphaB-crystallin and MAPKAPK-2 in astrocytes in the penumbra after transient focal cerebral ischemia. Exp Brain Res 163:421-429.

Renkawek K, Voorter CE, Bosman GJ, van Workum FP, de Jong WW (1994) Expression of alpha B-crystallin in Alzheimer's disease. Acta Neuropathol 87:155-160.

Rohatgi T (2003) Effect of CNS injury on expression of protease-activated receptors (PARs) in brain and identification of a putative PAR-2-interacting protein in retina. PhD thesis submitted, Faculty of Natural Sciences, Otto-von-Guericke University Magdeburg.

Rohatgi T, Sedehizade F, Reymann KG, Reiser G (2004) Protease-activated receptors in neuronal development, neurodegeneration, and neuroprotection: thrombin as signaling molecule in the brain. Neuroscientist 10:501-512.

Sharma A, Tao X, Gopal A, Ligon B, Andrade-Gordon P, Steer ML, Perides G (2005) Protection against acute pancreatitis by activation of protease-activated receptor-2. Am J Physiol Gastrointest Liver Physiol 288:G388-395.

Sharma KK, Olesen PR, Ortwerth BJ (1987) The binding and inhibition of trypsin by alpha-crystallin. Biochim Biophys Acta 915:284-291.

Smith-Swintosky VL, Cheo-Isaacs CT, D'Andrea MR, Santulli RJ, Darrow AL, Andrade-Gordon P (1997) Protease-activated receptor-2 (PAR-2) is present in the rat hippocampus and is associated with neurodegeneration. J Neurochem 69:1890-1896.

Sokolova E, Reiser G (2007) A novel therapeutic target in various lung diseases: airway proteases and protease-activated receptors. Pharmacol Ther 115:70-83.

Srinivasan AN, Nagineni CN, Bhat SP (1992) alpha A-crystallin is expressed in non-ocular tissues. J Biol Chem 267:23337-23341.

Stalheim L, Ding Y, Gullapalli A, Paing MM, Wolfe BL, Morris DR, Trejo J (2005) Multiple independent functions of arrestins in the regulation of protease-activated receptor-2 signaling and trafficking. Mol Pharmacol 67:78-87.

Steinhoff M, Buddenkotte J, Shpacovitch V, Rattenholl A, Moormann C, Vergnolle N, Luger TA, Hollenberg MD (2005) Proteinase-activated receptors: transducers of proteinase-mediated signaling in inflammation and immune response. Endocr Rev 26:1-43.

Steinhoff M, Vergnolle N, Young SH, Tognetto M, Amadesi S, Ennes HS, Trevisani M, Hollenberg MD, Wallace JL, Caughey GH, Mitchell SE, Williams LM, Geppetti P, Mayer EA, Bunnett NW (2000) Agonists of proteinase-activated receptor 2 induce inflammation by a neurogenic mechanism. Nat Med 6:151-158.

Striggow F, Riek-Burchardt M, Kiesel A, Schmidt W, Henrich-Noack P, Breder J, Krug M, Reymann KG, Reiser G (2001) Four different types of protease-activated receptors are widely expressed in the brain and are up-regulated in hippocampus by severe ischemia. Eur J Neurosci 14:595-608.

Sun Y, MacRae TH (2005) The small heat shock proteins and their role in human disease. Febs J 272:2613-2627.

Temkin V, Kantor B, Weg V, Hartman ML, Levi-Schaffer F (2002) Tryptase activates the mitogen-activated protein kinase/activator protein-1 pathway in human peripheral blood eosinophils, causing cytokine production and release. J Immunol 169:2662-2669.

Tseng WC, Lu KS, Lee WC, Chien CL (2006) Redistribution of GFAP and alphaB-crystallin after thermal stress in C6 glioma cell line. J Biomed Sci 13:681-694.

Van Rijk AF, Bloemendal H (2000) Alpha-B-crystallin in neuropathology. Ophthalmologica 214:7-12.

Wang H, Reiser G (2003a) Thrombin signaling in the brain: the role of protease-activated receptors. Biol Chem 384:193-202.

Wang H, Reiser G (2003b) Signal transduction by serine proteases in astrocytes: Regulation of proliferation, morphological changes and survival via protease-activated receptors. Drug Dev Res 60:43-50.

Wang H, Ubl JJ, Reiser G (2002) Four subtypes of protease-activated receptors, co-expressed in rat astrocytes, evoke different physiological signaling. Glia 37:53-63.

Wang K, Spector A (1996) alpha-crystallin stabilizes actin filaments and prevents cytochalasin-induced depolymerization in a phosphorylation-dependent manner. Eur J Biochem 242:56-66.

Wang Y, Luo W, Reiser G (2007a) Activation of protease-activated receptors in astrocytes evokes a novel neuroprotective pathway through release of chemokines of the growth-regulated oncogene/cytokine-induced neutrophil chemoattractant family. Eur J Neurosci 26:3159-3168.

Wang Y, Luo W, Reiser G (2007b) Proteinase-activated receptor-1 and -2 induce the release of chemokine GRO/CINC-1 from rat astrocytes via differential activation of JNK isoforms, evoking multiple protective pathways in brain. Biochem J 401:65-78.

Wang Y, Luo W, Reiser G (2008) Trypsin and trypsin-like proteases in the brain: proteolysis and cellular functions. Cell Mol Life Sci 65:237-252.

Webster KA (2003) Serine phosphorylation and suppression of apoptosis by the small heat shock protein alphaB-crystallin. Circ Res 92:130-132.

Xi JH, Bai F, McGaha R, Andley UP (2006) Alpha-crystallin expression affects microtubule assembly and prevents their aggregation. Faseb J 20:846-857.

Yan SJ, Blomme EA (2003) In situ zymography: a molecular pathology technique to localize endogenous protease activity in tissue sections. Vet Pathol 40:227-236.

8. Abbreviations

AP	Activating peptide
bp	Base pair
α-CRY	α-crystallin
cDNA	Complementary deoxyribonucleic acid
Cer	C2-ceramide
CNS	Central nervous system
CAPS	3-(Cyclohexylamino)-1-propansulfonic acid
CRYAA	αA-crystallin
CRYAB	αB-crystallin
DAG	Diacylglycerol
DMEM	Dulbecco's Modified Eagle's Medium
DNA	Deoxyribonucleic acid
dNTP	Deoxyribonucleoside triphosphate
DEPC	Diethyl pyrocarbonate
DMSO	Dimethyl sulfoxide
DTT	Dithiothreitol
ERK	Extracellular signal regulated kinase
FCS	Fetal calf serum
FTP	FCS-Triton-X100-PBS
GFAP	Glial fibrillary acidic protein
GAPDH	Glyceraldehyde phosphate dehydrogenase
GFP	Green fluorescent protein
GPCR	G-protein coupled receptor
GRO/CINC-1	Growth related oncogene/Cytokine-induced neutrophil chemoattractant-1
GST	Glutathione S-transferase
HA	Hemagglutinin
HBSS	Hank's balanced salt solution
HEK	Human embryonic kidney
H_2O_2	Hydrogen peroxide
IKK	I kappa B kinase
IL	Interleukine
IMPACT	Intein Mediated Purification with an Affinity Chitin-binding Tag
IP	Immunoprecipitation

IP3	Inositol 1,4,5-trisphosphate
IPTG	Isopropyl β-D-1-thiogalactopyranoside
JNK	c-jun related kinase
Kana	Kanamycin
KCM	KCl- $CaCl_2$- $MgCl_2$
LB	Luria bertini
LDH	Lactate dehydrogenase
MAPK	Mitogen-activated protein kinase
MH	Myc-his
MOPS	N-Morpholino-3-propansulphonic acid
mRNA	Messenger ribonucleic acid
NDSB	Non-detergent sulfobetaines
NFκB	Nuclear factor kappa B
OD	Optical density
p38 MAP	p38 mitogen activated protein
PARs	Protease-activated receptors
PBS	Phosphate buffered saline
PCR	Polymerase Chain Reaction
PAR-2	Protease-activated receptor-2
PFA	Paraformaldehyde
PKC	Protein kinase C
PLC	Phospholipase C
PVDF	Polyvinyliden difluoride
Real-Time-PCR	Real-Time-Polymerase Chain Reaction
RT	Reverse Transcription
SDS-PAGE	Sodium dodecyl sulphate-polyacrylamide gel electrophoresis
sf.9	*Spodoptera frugiperda*
TCM	Tris/HCl-$CaCl_2$- $MgCl_2$
Tm	Melting temperature
TRag	Thrombin receptor agonist
TBE	Tris-boric acid-EDTA
TE	Tris-EDTA
UV	Ultraviolet
WB	Western blot

9. Publication during Ph. D studies

Li R, Rohatgi T, Hanck T, Reiser G. αA-crystallin and αB-crystallin, newly identified interaction proteins of protease-activated receptor-2, rescue astrocytes from C2-ceramide- and staurosporine-induced cell death. J Neurochem. 2009 Sep; 110 (5):1433-44.

Poster Presentations

Li R., Hanck T. and Reiser G. (2008) Astrocytes are protected from cell death by α-crystallins (αA and αB) and protease-activated receptor-2. ELSO 2008 Conference in Nice.

Li R., Hanck T. and Reiser G. (2009) Protease-activated receptor-2 and its interaction partner alpha-crystallin play a protective role in astrocytes. ESN 2009 Conference in Leipzig.

Curriculum Vitae

Name: Rongyu Li

Birthday: Jun 24, 1973

Place of birth: Liaoning, China

Nationality: China

Education and Research

9/2005-Present Ph.D. student, Institute of Neurobiochemistry, Otto-von-Guericke-University of Magdeburg, Germany. Supported by Deutsche Forschungsgemeinschaft (Graduiertenkolleg 1167 für ‘‘Zell-Zell-Kommunikation in Nerven- und Immunsystem‘‘).

9/2000-8/2005

R&D member, Biostar Genechip Research Institute, BioStar Genechip Inc. Shanghai, China.

Development of new biochip technology

-Establishment of Oligo Genechip platform.

-Development in new labeling system in microarray.

-Establishment of new kind of genechip.

Application of genechip in medicine

-Genotyping of Human papillomavirus (HPV) and study on the correlation of HPV with tumorigenesis of cervix and ovarian cancer.

-Development of Glucose-6-Phosphate Dehydrogenase GeneChip and detection of G6PD mutations in Chinese.

-Development of Mediteranean Anemia GeneChip and detection of Mediteranean Anemia mutations in Chinese.

-Detection and genotyping of Avian influenza virus.

-Genechip and forensic Application.

-Genotyping of ABO and HLA.

SNPs Detection and analysis of some candidate genes

-Study on SNPs of several cytokines and receptors, and the correlation of polymorphism with transplant rejection.

-SNPs of candidate genes in Stagnation of blood.

-SNPs of candidate genes in diabetes.

9/1997-7/2000 Zhejiang University, Hangzhou, China

Master of Science majored in **Biophysics.**

Thesis: Studies of Glucose-oxidase/Peroxidase Co-immobilization on nylon film.

9/1993-7/1997 Zhejiang University, Hangzhou, China

Bachelor of Science majored in **Biological Science and Technology**

Thesis: The Isolation, Purification and Characterazation of NADPH-cytochrome P_{450} Reductase.